AN ABSTRACT OF THE THESIS OF

Michael Rogers for the degree of Master of Arts in Interdisciplinary Studies in Anthropology, Anthropology, and Physics presented on 20 March 2001.

Title:

Detection of Burials at the Confederated Tribes of Siletz Indians Historic Period Cemetery, Oregon: A Comparison of Ground-Based Remote Sensing Methods

Abstract approved: _____

Barbara Roth

This project hypothesizes that the use of multiple ground-based remote sensing methods can collectively characterize the geophysical signatures of four marked human burials at the Confederated Tribes of Siletz Indians historic period cemetery. If the geophysical signatures of the marked burials can be characterized, these signatures may be used to located unmarked burials within the Siletz cemetery. To investigate this hypothesis, several research questions focused on the results from topographic, cesium gradiometer, and ground-penetrating radar surveys. A $15m \times 15m$ region of the cemetery containing four marked burials defines the survey region. The results of each survey were individually and collectively examined to identify the characteristic geophysical signatures of the four marked burials. The topographic and magnetic surveys identified geophysical anomalies spatially associ-

ated with the some of the marked burials. The ground-penetrating radar survey was the most productive by identifying geophysical anomalies spatially associated with all four marked burials. Even though signals from the burials appeared with mixed results, it proved difficult to characterize the geophysical signatures of the burials in the individual and collective geophysical data. Without a characterization of the geophysical signature of the marked burials, it is difficult to identify unmarked burials at the Siletz cemetery. Due to the success of the radar at "seeing" all four marked burials it may be possible to identify areas free of unmarked burials.

Detection of Burials at the Confederated Tribes of Siletz Indians Historic Period Cemetery, Oregon: A Comparison of Ground-Based Remote Sensing Methods

by

Michael Rogers

A THESIS

submitted to

Oregon State University

in partial fulfillment of
the requirements for the
degree of

Master of Arts in Interdisciplinary Studies

Completed 20 March 2001
Commencement June 2001

Master of Arts in Interdisciplinary Studies thesis of Michael Rogers presented on 20 March 2001

APPROVED:

Major Professor, representing Anthropology

Committee member, representing Anthropology

Committee member, representing Physics

Redacted for Privacy

Chair of the Department of Anthropology

Redacted for Privacy

Dean of the Graduate School

I understand that my thesis will become part of the permanent collection of Oregon State University libraries. My signature below authorizes release of my thesis to any reader upon request.

Redacted for Privacy

Michael Rogers, Author

ACKNOWLEDGMENTS

Many people helped make this thesis possible; please indulge me as I thank them all, and in an order that reflects nothing of my feelings of gratitude.

I would first like to thank Robert Kentta and the Confederate Tribes of Siletz Indians who supported my research at their cemetery. In doing so, we established a relationship of communication, mutual respect, and cooperation between a tribe and a multi-disciplinary research team in a way that happens far too often.

I also want to thank all of the people who donated their time and equipment, and made this thesis possible:

- Jim Bell, Linn-Benton Community College, introduced me to remote sensing fieldwork and allowed me to participate in his work at the Confederated Tribes of Siletz Indian historic period Cemetery.
- Robson Bonnichsen, Center for the Study of the First Americans-Oregon State University, for letting me use his transit and stadia rod; as well as giving me advice on my research design.
- Rowland French and Northwest Geophysical Association for letting me use their cesium gradiometer and assisting with the magnetic survey.
- Gerry Sandness and Battelle National Labs for letting me use their GPR unit.

- John Selker and Michael Neimtz, Department of Bioresource Engineering-Oregon State University, who taught me a bit more about conducting GPR surveys, and loaned me their $500MHz$ GPR antenna and cables.

This acknowledgement would not be complete without thanking those individuals who assisted me in conducting my surveys, analysis, and contributing to my research ideas:

- David Cebula, Department of Physics-Oregon State University, for spending numerous hours listening to my ideas and making helpful suggestions.

- Larry Conyers, Department of Anthropology-University of Denver, who donated his time to conduct preliminary GPR time-slices and made post-acquisition processing suggestions.

- Clark Davidson, James Mayer (formerly of Department of Anthropology-Oregon State University), and Jun Kinoshita (Department of Anthropology-Oregon State University) who assisted in establishing the grid. James also helped me conduct the GPR survey.

- Derrick Hilger, Travis Peery (Department of Physics-Oregon State University), and Rowland French (Northwest Geophysical Association) who assisted me in conducting the Cesium Gradiometer survey. Derrick also helped me conduct the topographic survey and spent hours listening to my writing ideas.

- Henri Jansen, Department of Physics-Oregon State University, who enthusiastically listened to my research ideas, volunteered to be a part of the project, and helped me understand the physics.

- Anna Keeton, (Department of Anthropology-Oregon State University) for giving me time to write, listening to my organizational ideas, and making me smile frequently.

- Sunil Khanna, (Department of Anthropology-Oregon State University) for helping me bridge the gap between the natural sciences and the social sciences.

- Barbara Roth, (Department of Anthropology-Oregon State University) for her writing feedback, her interest in archaeological geophysical methods, and helping me understand archaeological methods.

- Chris Southers, (School of Education-Oregon State University) who found my project interesting enough to agree to serve as my Graduate Council Representative.

- Bill & Iris, (Interzone Coffee Shop) for providing such tasty brew and giving me a frequent reason to take a break.

TABLE OF CONTENTS

TABLE OF CONTENTS (Continued)

LIST OF FIGURES

LIST OF FIGURES (Continued)

LIST OF TABLES

LIST OF APPENDICES

DEDICATION

This thesis is dedicated to my mother; who started this all by taking me to see the 1976 King Tut exhibit at the Metropolitan Museum of Art, New York City.

DETECTION OF BURIALS AT THE CONFEDERATED TRIBES OF SILETZ INDIANS HISTORIC PERIOD CEMETERY, OREGON: A COMPARISON OF GROUND-BASED REMOTE SENSING METHODS

1. INTRODUCTION

This thesis explores the use of ground-based remote sensing methods at the Confederate Tribes of Siletz Indians historic period cemetery. The hypothesis of this project is that the use of multiple ground-based remote sensing methods can aid in identifying the characteristic geophysical signatures of marked burials at the Siletz cemetery.

1.1. Project Purpose

The past two decades have seen an increase in the use of ground-based remote sensing methods in support of archaeological excavations. Surveys are frequently conducted prior to and during archaeological projects to help guide the excavation by identifying subsurface anomalies. Rarely are ground-based remote sensing surveys conducted without post-survey excavations. Occasionally sites are encountered where excavation is prohibited or limited, often due to logistics. Sites containing numerous trees or a site located on a steep slope or next to a river are examples of logistical difficulties in excavating. Excavation is prohibited or limited at other sites for cultural reasons. The Confederated Tribes of Siletz Indians historic period cemetery is an excellent example of a site where excavation is prohibited, but where

a functional need to understand the subsurface exists. The Siletz cemetery is similar in style to non-tribal Judeao-Christian cemeteries, but differs from many cemeteries due to the cemetery being managed by many tribes. Identifying unmarked burials or identifying regions free of unmarked burials is important to the Confederated Tribes of Siletz Indians, which re-gained tribal status in 1977 [22]. Excavations for new burials routinely encounter unmarked burials, and efficient management of the multi-tribe cemetery requires knowledge of where new burials can be placed without disturbing older burials.

This project used a ground-penetrating radar, a cesium gradiometer, and a transit & stadia rod in an attempt to identify the characteristic geophysical signatures of marked burials. These particular devices were selected because they have the potential for identifying the geophysical characteristics of a burial, and they were accessible without cost to the project. I developed seven research questions, based on the accessibility of these devices, to investigate the hypothesis that the use of multiple ground-based remote sensing methods can aid in identifying the characteristic geophysical signatures of marked burials at the Siletz cemetery. These seven research questions are:

1. Can the geophysical signature of four marked historic period human burials be identified using a topographic survey?
2. Can the geophysical signature of four marked historic period human burials be identified using a cesium gradiometer?
3. Can the geophysical signature of four marked historic period human burials be identified using a ground-penetrating radar?
4. Can the geophysical signature of four marked historic period human burials be characterized in enough detail to aid in the identification of unmarked burials within the Confederated Tribes of Siletz Indians historic period cemetery using a topographic survey?
5. Can the geophysical signature of four marked historic period human burials be characterized in enough detail to aid in the identification of unmarked burials within the Confederated Tribes of Siletz Indians historic period cemetery using a cesium gradiometer?
6. Can the geophysical signature of four marked historic period human burials be characterized in enough detail to aid in the identification of unmarked burials within the Confederated Tribes of Siletz Indians historic period cemetery using a ground-penetrating radar?
7. Can a combined analysis of the topographic, cesium gradiometer, and ground-penetrating radar surveys be used to characterize the geophysical signature of four marked historic period human burials in enough detail to aid in the identification of unmarked burials within the Confederated Tribes of Siletz Indians historic period cemetery?

To address these research questions, the data from each ground-based remote sensing device was separately and collectively examined to identify characteristic geophysical signatures of four marked burials residing in the cemetery. If characteristic geophysical signatures of the marked burials are identified, these signatures may aid in the identification of unmarked burials within the cemetery. This project directly benefits the Confederated Tribes of Siletz Indians, and builds upon a cooperative relationship between the Confederated Tribes of Siletz Indians and the scientific community. This project also contributes to understanding how burials

appear in ground-based remote sensing data, and explores methods that archaeologists can use at sites where excavation is restricted or prohibited. To foster an open dialog with scientists, Robert Kentta, of the Confederated Tribes of Siletz Indians Department of Siletz Culture & History, has agreed to let all of the data from this project be recorded on a CD-ROM [23]. Ground-based remote sensing methods often produce large amounts of data that are difficult to store on transportable media. By creating a CD-ROM, the data are preserved for the Confederated Tribes of Siletz Indians and allow other researchers to examine the raw and analyzed data. Access to the raw data can aid researchers in understanding their own data, and can also be incorporated into educational settings where data gathering by students is not possible.

1.2. Description of the Confederated Tribes of Siletz Indians Historic Period Cemetery

The Siletz cemetery is in the Coast Range mountains approximately 15 miles northeast of Newport, Oregon (Figure 1.1). The cemetery sits on top of layers of sediments and basalts which were sea floor before being uplifted due to plate tectonic motion to form the Coast Range (for more information on the geologic history of Oregon's Coast Range consult Baldwin's [4], "Geology of Oregon" and Alt & Hyndman's [2], "Roadside Geology of Oregon"). A more in-depth discussion of the Coast Range is not included in this thesis because excavation is prohibited at the site. Usually, excavation provides information about the site stratigraphy and

an understanding of the geomorphology. Additionally, a literature review failed to identify information about soils at the site. Understanding the subsurface soils and geology can provide additional data to aid in the interpretation of the archaeological geophysical data, but knowledge of the subsurface geology is not required for all projects. In part, the intent of this project is to explore methods of identifying archaeological geophysical signatures without complete knowledge of the subsurface soils.

FIGURE 1.1. Geographic location of Siletz, Oregon

The Siletz cemetery is adjacent to the Confederated Tribes of Siletz Indians Headquarters on Government Hill in the city of Siletz, Oregon. The Siletz headquarters can be reached from US-20 by turning North onto OR-229 (Siletz Highway). After travelling for approximately 7.4 miles, turn right onto East Logsden Road. Travel east for 0.2 miles and turn right onto Bagley Street. Head south for 0.1 miles and turn right onto East Swan Avenue. The tribal headquarters is located at 201 East Swan Avenue (See Figure 1.2 for a legal description of the cemetery location).

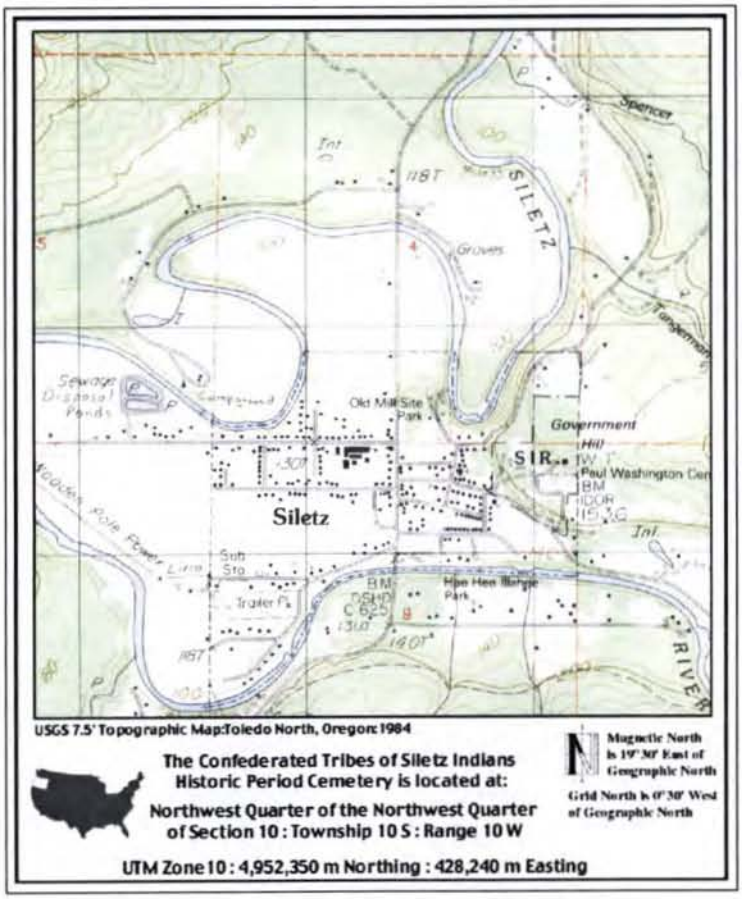

FIGURE 1.2. Location of the Confederated Tribes of Siletz Indians Historic Period Cemetery

The cemetery is approximately $300m \times 200m$ in size with a one-lane gravel road running through the cemetery. The Confederated Tribes of Siletz Indians includes 27 bands [22] and the cemetery has 500-600 marked burials [5]. The majority of marked burials have their long axis oriented east-west, and the burials are organized primarily by family, band, and then where space provides. The predominent methods of marking burials are headstones, tombstones, and monuments. Along with these markers, burials may also display flower arrangements, flags, fences, and benches. Marked burials are found in groupings with "empty" space between groupings. The empty space is identified by the lack of marked burials, but that does not mean that burials are absent in these regions.

1.3. History of the cemetery

This thesis is made more complete by the following contribution on the history of the Siletz Tribal cemetery by Robert Kentta. Mr. Kentta's knowledge of the history and words speak more directly than any words that I might write. I am pleased to include his discussion of the history of the cemetery in this thesis.

> History of the Confederated Tribes of Siletz Indians' Paul Washington Cemetery, Government Hill, Siletz, Oregon.
>
> The Coast (or Siletz) Reservation was established by Executive Order of President Franklin Pierce November 9, 1855. Many aboriginal Tribes and Bands throughout western Oregon and parts of extreme northern California had signed treaties agreeing to cede vast tracts of tribal lands to the United States. In most of these treaties, the tribes reserved the right to remain within their home territory until their permanent reservation was selected under the direction of the President. The 1855 Executive

Order then marked the creation of the body of people that would become known as the Confederated Tribes of Siletz Indians, a process that was started with the confederation of various Tribes and Bands under each of the treaties.

The area now known as the city of Siletz was to become the headquarters for the 1.1 million acre reservation. An U.S. Army Blockhouse was among the first structures to be built at Siletz, and a low hill over-looking the valley was selected as the permanent site for this main fortification against Indian attack on the Siletz Indian Agent and his employees. The Siletz Agency was established in 1856/57 under military rule, and the Siletz Blockhouse had close interaction with the three forts that were built on the perimeter of the Coast Reservation (Forts Yamhill, Umpqua, and especially Hoskins). The Agent's house, offices, boarding school, hospital and other Agency buildings naturally were erected near the Blockhouse, so the low hill eventually became known as "Government Hill".

It is not clear exactly when the cemetery immediately to the south of the Siletz Agency was established. Most of the very early reservation era tribal cemeteries were established near each of the many villages that individual bands established up and down the Siletz River and in other parts of the large reservation. It's possible that there were early burials of U.S. Army personnel and Siletz Agency employees that started the Government Hill cemetery, but the earliest known burials to be placed there were tribal members in the 1860's. Family and village cemeteries, however, were used most frequently until probably the 1920's.

In the late 1800's, the Catholic Church was allowed to build a church at the east end of the cemetery on Government Hill. Around 1900, there were many homesteader families that began moving into areas of the Siletz Reservation that had been opened to settlement. About 1912, town lots were sold out of the Agency Farm to establish what's now the City of Siletz. All of these events brought more non-Indians into the community. The Catholic Church had a small portion of the cemetery consecrated near the church in which both Indians and some non-Indians were buried. Before 1920, the Catholic Church structure was sledded down the hill to its present location.

During WWI, two Siletz boys from the Washington family were killed in Europe. The first killed was Paul Washington. The Cemetery was then dedicated in his honor. As Siletz families lost control of their allotment parcels, they lost access to their family cemeteries and the Government

Hill cemetery (Paul Washington Cemetery) became increasingly used and known as, "the Siletz Tribal cemetery".

In 1954, federal recognition of the Confederated Tribes of Siletz was terminated under the Western Oregon Termination Act. By 1956, the last remaining Siletz Reservation lands were deeded or sold by the BIA. The Government Hill property was turned over to the City of Siletz by the Tribe. The Paul Washington Cemetery continued to be the main cemetery for Siletz Tribal families.

In the early 1970's the Confederated Tribes of Siletz Indians re-organized as a group and sought restoration of the federal recognition as a tribe that was lost through the Termination Act. In 1977 the Tribe was restored. In 1980 the residents of the City of Siletz (by a narrow margin) voted to return ownership of Government Hill to the Tribe, to be included in the Siletz Reservation Act, restoring some scattered parcels of land to the tribe.

There had been no record of burial locations kept over the 120 + years of using the cemetery. The consecrated Catholic cemetery area was perhaps the most vague and confusing of all. Around 1978, the first attempt to map the Paul Washington Cemetery was made. There were efforts to locate and mark older unmarked graves at that time. Many were easily discernable as an oval sunken feature. In some cases fragments of crumbled stone markers, wooden crosses and metal markers indicated actual locations. In many instances though (particularly in the older sections of the cemetery), it was becoming not uncommon to encounter evidence of earlier graves while digging a new one. Prodding the ground before digging was sometimes an accurate finding aid, but many older burials still went undetected before digging commenced.

In the 1990's plans were made to re-map the cemetery and also use some modern technology to assist us in finding unmarked graves. Richard Ross from OSU was hired as our mapper and Jim Bell from Linn-Benton Community College was contracted to use both Ground Penetrating Radar and a Magnetometer to try to locate unknown graves. Michael Rogers became involved in the project at this time also, and eventually did his own additional survey work to check and re-check findings within some control plots. The survey results seem to indicate over 100 unmarked grave locations that we can now avoid. Disturbance of older graves is very upsetting to all tribal members and an added burden to bereaved family members who are not only upset about the disturbance of an

existing burial, but then have to re-select a location for their recently passed loved one's resting place.

The contributions of Mr. Rogers, Mr. Bell, and Mr. Ross have added a great deal of planning ability and peacefulness to management of the Paul Washington Cemetery.

Robert Kentta, Cultural Resources Director [24]

1.4. History of the Ground-Based Remote Sensing Surveys at the Cemetery

In 1996 James Bell, of Pacific Geophysical Surveys, was contracted by the Confederated Tribes of Siletz Indians to conduct ground-penetrating radar and magnetic surveys at the Siletz cemetery. The intent of these surveys was the location of unmarked burials within the cemetery. I served as a survey assistant for most of the three-week project. The project used a Geophysical Survey Systems, Inc SIR-2® ground-penetrating radar to survey portions of the cemetery and an Geometrics, Inc. G-856 proton magnetometer to survey other sections. Fifty to seventy percent of the cemetery was surveyed using these two devices. The cemetery was divided into smaller survey regions whose size and orientation was selected based on local features. Transect spacing varied between prospection surveying (no set transect spacing or transect lines) and 3 feet. All data were recorded by hand while in the field. No post-acquisition processing was conducted. Bell's project report includes a basemap of the cemetery with hand drawn X's marking the location of probable unmarked burials [5].

The hypothesis and research questions of this thesis were generated while assisting James Bell. During the course of Bell's surveys we used radar or magnetics, and did not use both devices over the same region. This is not surprising due to the time and money restrictions commonly present during a contract project. While we were working, I kept wondering what the data would look like if we surveyed the same region with both devices. During the course of the project, Bell and I noticed depressions throughout the entire cemetery that had the possiblity of being associated with burials. The presence of these depressions inspired me to include a topographic survey in my research design.

While working at the cemetery with James Bell, I had the opportunity to collect radar and magnetic data over one portion of the cemetery. These feasability surveys indicated possible success of in-depth studies into the use of multiple ground-based remote sensing surveys at the Siletz cemetery. These feasibility surveys used a transpect spacing of 3 feet ($1m$), and identified that $1m$ transect spacing was too large an interval. These factors helped form the research design used for this thesis.

1.5. Description of the Survey Region

A $15m \times 15m$ survey region oriented on grid north was established using a Leopold® transit, stadia rod, and survey tapes. A temporary benchmark placed by James Bell during the 1997 survey [5] of the cemetery was used as a starting point for placement of the survey grid. The temporary benchmark is $7m$ south of the south-east corner of the survey grid, and is identified by grid position ($515m$,

993m). The transit was positioned and levelled over the temporary benchmark, and aligned on magnetic north. An adjustment of 20° 10′ degrees west of magnetic north aligned the transit on grid north. A fiberglass survey tape was stretched 22m from south to north starting at the temporary benchmark. The transit operator gave hand and voice signals to align the survey tape along grid north. Once aligned, a steel spike marked grid position (515m, 1015m). A distance of 22m was chosen to roughly correspond to the 1997 survey. Unfortunately, the 1997 survey is not oriented on grid north, or one of the standard orientations. Instead the 1997 survey region was oriented on a gravel road that meanders its way through the cemetery. The 1998 survey could have been aligned with the 1997 survey, but orienting the survey region on grid north retains a consistency with other surveys conducted by the 1998 survey team. An angle of 3° 10′ between the 1997 and 1998 survey grids is sufficiently small to facilitate comparison between the two surveys.

While the survey tape was stretched between grid positions (515m, 993m) and (515m, 1015m) a steel spike was driven into the ground at grid position (515m, 1000m) to identify the southeast corner of the survey region. With the transit positioned at the temporary benchmark, a shot was taken to a damaged benchmark residing within the survey region. I was unable to obtain information about this damaged benchmark and assigned this benchmark an arbitrary elevation of 50m. If future investigations provide more information about this damaged benchmark,

my data can be converted to actual elevation and positions [1]. Surveying data was recorded on a pre-printed survey form (Figure 1.3).

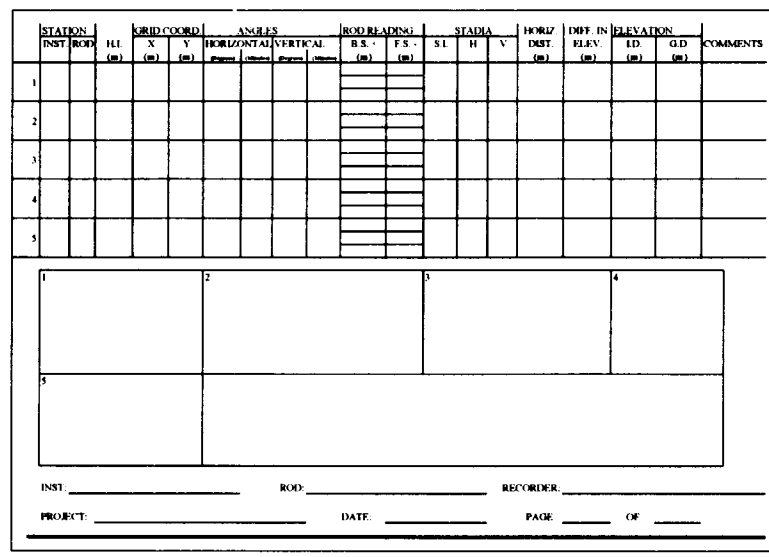

FIGURE 1.3. Survey Region Form

Using standard surveying techniques, the remaining corners defining the survey region were marked through the placement of steel spikes. A final steel spike was placed at grid position ($500m$, $993m$) to ensure that my survey region was properly tied into the 1997 Bell surveys. With the absence of errors, the plot of the traverse data should close to form a rectangle (Figure 1.4). Due to errors in both

[1]Out of respect for the people and the families of the people buried within my survey region I am omitting specific information about the location of my survey region and I have assigned numbers to identify the marked burials. All of the necessary information about the burials and the survey region location are recorded in my field notes. Permission to access this information must be obtained from the Confederated Tribes of Siletz Indians.

angles and distances, traverses seldom close. This error is called the *error of closure* [28]. Surveying often involves unknown distances and angles, but establishing an archaeological survey grid usually involves identifying the corners of a rectangle. The survey grid at the Siletz Cemetery is rectangular in shape. This shape allowed for angles to be set with minimal error during the traverse that established the survey grid. The final survey reading, taken from turning point five, TP5, to the temporary benchmark served to identify the error of closure (Figure 1.4). There was no observable angular error in the final reading and a distance error of -0.10m. Due to the small size of the error of closure and the desired accuracy for the intended surveys, no corrections to the traverse that established the grid are necessary.

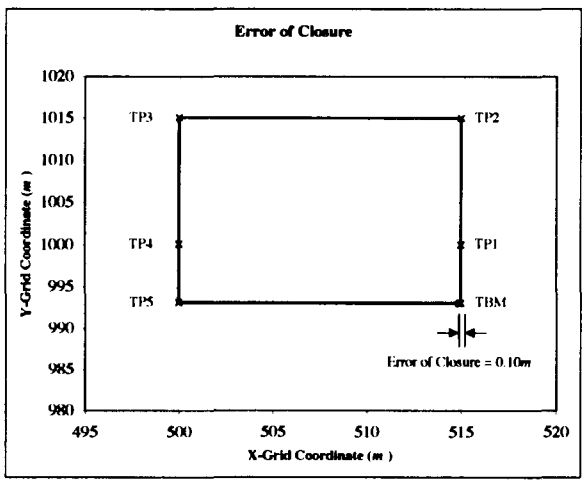

FIGURE 1.4. Plot of traverse data, identifying error of closure = 0.10m

2. THEORETICAL FOUNDATION

Harry Burns, "You know, I have a theory that hieroglyphics are just an ancient comic strip about a character named Sphinxy."
- When Harry Met Sally [13]

2.1. Contextual Archaeology

Any study of burials must concern itself with placing the graves into a larger cultural, environmental, geological, geographic, and temporal framework. Burials exhibit a wide spectrum of characteristics. Understanding the factors that create the burial characteristics is essential to understanding the burial itself. This approach to understanding sites is referred to as contextual archaeology. Contextual archaeology demands that sites and artifacts be placed in their larger context; only then can a true understanding and interpretation of material culture be obtained [33].

Contextual archaeology provides a theoretical framework to help guide ground-based remote sensing methods at cemeteries. Cemeteries are, by their very design, influenced by cultural factors. Graves can be oriented horizontally or vertically, with or without a coffin, using an iron coffin or a wooden coffin, with or without grave goods, and many other regional variations. As an example, the method of burial at a Catholic cemetery in New York may differ from the method of burial at a Catholic cemetery in Italy. The environment in which the grave resides can also influence how the person is buried. It might be difficult to create a deep burial pit in cold climates [9], and a handy bog might be used to dispose of a criminal [17]. The

geological environment can influence the distinctiveness of the boundary between the burial pit and surrounding soils. Burial back fill is often homogenized and aerated when compared to the surrounding soil [25], but burials in sandy soils might lack a clear burial pit boundary. Time is also a factor to consider when studying burials. Burial customs change, and a single burial will change over time. Coffins collapse, back fill settles, vegetation grows, organic materials decompose, and many other changes can take place. Not only do cultural, environmental, geological, geographic, and temporal events directly create the geophysical grave signatures, they also affect each other. This complexity is exactly what the contextual archaeological framework attempts to manage.

2.2. Contextual Archaeology and Geophysical Data

Contextual elements are often identified through literature review, historic records, and excavation. Ground-based remote sensing methods provide another means for identifying contextual elements. These methods record different properties of the materials being examined. Topographic surveying records changes in elevation and magnetic surveying records magnetic properties of objects. The properties recorded by geophysical methods are added to the list of contextual elements identified through other means.

Identifying and interpreting geophysical data can be made easier by recording a range of contextual elements. If a buried pipe is known to be iron, then an interpretation of a large amplitude, linear magnetic anomaly as a buried pipe is

more likely correct, but a correct interpretation of the anomaly can also be made without fore knowledge of a buried iron pipe.

Geophysical surveys add to the list of contextual elements, but historic records describing burials at the Siletz cemetery are sparse and difficult to locate. A lack of historic records combined with the inability to test excavate makes it difficult to identify non-geophysical elements of the marked burials. Lack of this information makes interpretation of the geophysical data more challenging, but the geophysical elements of the burials may be sufficient for this study.

2.3. Geophysical Elements Anticipated at the Siletz Cemetery

A topographic survey using a small sampling size can identify depressions associated with the settling of a burial. The size, shape, and depth of the depression depends upon the orientation of the burial, use of a coffin, and the length of time since the burial [25]. A topographic survey can also identify mounds associated with burials [14]. Most sites have topographic variations not associated with burials. This makes the interpretation of topographic data difficult, but the topographic data is a powerful tool when used in conjunction with other ground-based remote sensing methods. The use of multiple lines of evidence leads to an increase in confidence when interpreting the data within the contextual archaeology framework.

Ground-penetrating radar responds to differences between the electromagnetic properties of materials. A ground-penetrating radar wave striking an interface between materials with similar relative dielectric permittivities will transmit through

the interface with a small portion of the incident wave being reflected. As the difference in the relative dielectric permittivity increases, the amplitude of the reflected wave increases. Metal objects entirely reflect the incident wave [20]. Due to the size of the ground-penetrating radar wavelength, the ability to detect smaller objects is limited. Most non-metal grave goods, and the bones of the buried individual are too small to detect [11]. Ground-penetrating radar surveys might be able to detect the boundary between the burial pit and the surrounding soil, larger grave goods, metal grave components and goods, and variations in the back filled soil [25].

Magnetic gradient surveys record changes in the magnitude of the Earth's local magnetic field. Cesium gradiometers are sensitive to $0.01nT$ magnetic field changes [29]. To put this sensitivity into some context, the Earth's magnetic field is approximately 50,000 nanotesla at 45 degree northern latitudes [18]. If the coffin or grave goods contain any iron objects, such as nails, hinges, handles, pins, jewelry, and iron weapons, a magnetic gradient survey will record the effect that these items have on the Earth's local magnetic field. The back filled soil and the organic components can also influence the Earth's local magnetic field. Change in the soil chemistry due to the introduction of organic matter can lead to a difference in foliage growth over the grave [25]. The variance in vegetation along with the aeration and homogenization of the back fill soil can lead to a difference in water retention when compared to the surrounding soils [25]. The concentration of water in a material and the process of mixing soils changes the magnetic susceptibility of the material. These changes will show up as an increase or decrease in the Earth's local magnetic

field [29]. A difficulty in interpreting magnetic data is the existence of naturally occurring magnetic objects and magnetic fluctuations. Lightning strikes can magnetize the soil, trees that fall over due to moist soil are very similar in nature to burial pits, and naturally magnetic rocks can look deceptively like iron grave goods.

The difficulty in using ground-based remote sensing methods lies in the interpretation of the data. It is often difficult to distinguish between culturally generated signals and geologic signals. The hypothesis of this project is that the use of multiple ground-based remote sensing methods can aid in identifying the characteristic geophysical traits of marked burials at the Confederated Tribes of Siletz Indians historic period tribal cemetery. The ultimate goal of the Confederated Tribes of Siletz Indians is the identification of unmarked burials. Prior to addressing this issue the effectiveness of using a topographic survey, a ground-penetrating radar survey, and a cesium gradiometer survey to identify marked burials must be established. If these survey methods can, individually or collectively, establish characteristic geophysical traits of marked burials, then these methods can be used to assist the Confederated Tribes of Siletz Indians in avoiding the disturbance of unmarked burials when selecting locations for new burials.

3. TOPOGRAPHIC SURVEY

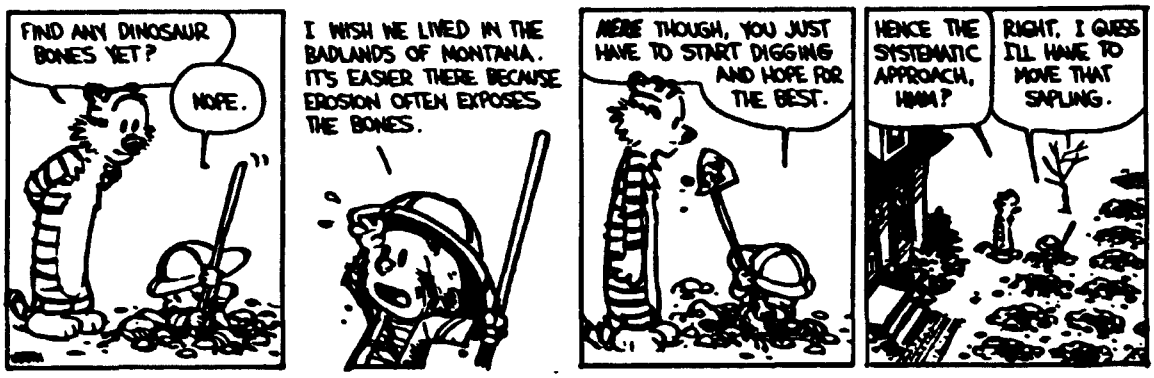

3.1. Introduction

Geologic and topographic surveying are among the oldest techniques in the archaeologist's tool kit. Approximately two thousand years ago, Eratosthenes measured the circumference of the earth using nothing more than a stick and the shadow cast by the sun. He achieved a result with an error less than 5% when compared to the current accepted value [35]. In a bind, an archaeologist could get by with sticks and shadows, but the modern archaeological tool kit is filled with an assortment of old and new survey tools. The Brunton compass, global positioning systems, electronic distance measuring devices, the laser transit, a transit and stadia rod, and a total station are some of the devices commonly seen at an archaeological site.

Archaeologists and archaeological-geophysicists often conduct topographic surveys to record site features and changes in elevation to create a basemap of the

site, and the surveying interval varies based on the needs at each site. In addition to topographic surveys, archaeologists also use surveying equipment to record the provenience of archaeological features and artifacts. During an archaeological geophysical investigation a high resolution topographic survey (two meters or less sampling interval) not only records the site topography in enough detail to identify contextual elements, but also provides information required to correct ground-penetrating radar for changes in elevation.

Because burial mounds are not used at the Siletz cemetery, I will limit my discussion to burial pits that are placed beneath the ground surface. The process of burying an individual often begins by removing soil from the ground to create a burial pit. Depending upon cultural practices, this burial pit may be lined with stone, cement, wood, or some other liner. Next, the body is placed into a burial container or directly into the burial pit. If the body is placed into a burial container, the burial container is eventually placed into the burial pit. At this point in the interment, the burial pit may be backfilled with the removed soil or capped with stone, cement, wood, or some other cap. The final process of burying an individual often entails covering the burial with soil.

Over time, depending upon how the interment was performed, elements of the burial will settle. The soil will slowly compact, coffins and burial pit liners collapse, and the body decomposes. Each of these processes can be seen at ground level, in the form of a depression in the ground or a mound above the ground. Depth (or height) and size depend upon various elements of a burial. A high resolution topographic

survey measures these elements by recording elevation changes, and depressions or mounds due to a burial may be seen in a plot of the topographic data [25]. Based on the context, the depression or mound may be easily interpreted as a burial, but they can also be related to other processes. The plot of the topographic data may be difficult to interpret by itself, but this plot provides collaborative information with other ground-based remote sensing surveys.

3.2. Survey Method

The topographic survey for this project took 6 hours to conduct on 3 October 1998 using a Leopold® transit and stadia rod (Figure 3.1). The temperature was 60°F with partial cloud cover. Derrick Hilger [1] assisted me with the survey. The metal stakes marking the corners of the survey region were located and the transit was set up over the metal stake marking grid position ($500m$, $993m$). The transit was placed $7m$ away from the survey region to facilitate topographic surveying. If the transit was located closer to the survey region, the stadia rod marks could not be clearly seen through the transit's telescope.

Two Keyson® fiberglass surveyor ropes were stretched between grid positions ($500m$, $1000m$) to ($515m$, $1000m$) and ($500m$, $1015m$) to ($515m$, $1015m$) to identify the baseline and a parallel line to control transect spacing. To identify the $0.5m$ spaced survey transects, 10-$30m$ long, Komelon®Corporation fiberglass survey tapes

---

[1]Department of Physics, Oregon State University, Corvallis, Oregon

FIGURE 3.1. The topographic survey crew. Derrick Hilger and Michael Rogers are pictured with the transit and stadia rod.

were positioned at x = $500m$, $501m$, $502m$,..., $509m$ marking the first, third, fifth ..., and nineteenth transects. All ten tapes started at grid position y=$1000m$ and stretched to y=$1015m$. Every other transect, instead of every transect, was marked using a survey tape, to minimize the number of times that the survey tapes needed to be moved (Figure 3.2). The position of the survey transect between the meter spaced survey tapes was easily identified by looking at the survey tapes to either side of the transect [10].

Elevation readings were taken every $0.5m$ along each survey transect. Approximately every hour, Derrick and I alternated between working the transit and working the stadia rod; switching jobs kept us alert during the monotonous data collection process. The transit operator recorded the elevation readings on a preprinted

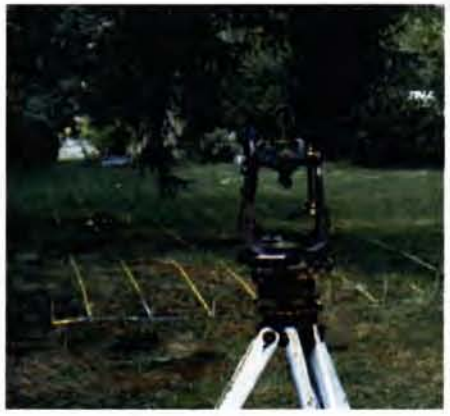

(a) The transit overlooking the survey region.

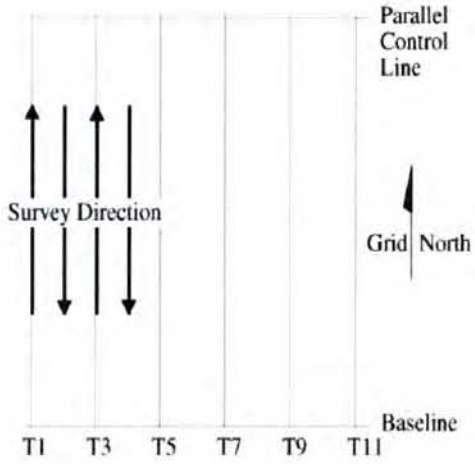

(b) Diagram of the survey method.

FIGURE 3.2. Description of the topographic survey method. A baseline (an east-west running line) and a parallel control line provide the means for accurate horizontal position data.

form (Figure 3.3). The horizontal position of the corners of the four headstones of the marked burials residing within the survey region were recorded during the topographic survey. After surveying the nineteenth transect, the survey tapes were moved to identify the remaining transects. In this fashion the entire site was surveyed.

3.3. Data

With an elevation reading taken every $0.5m$, 961 readings were acquired for the $15m \times 15m$ survey region. The minimum elevation equals $49.74m$ and the

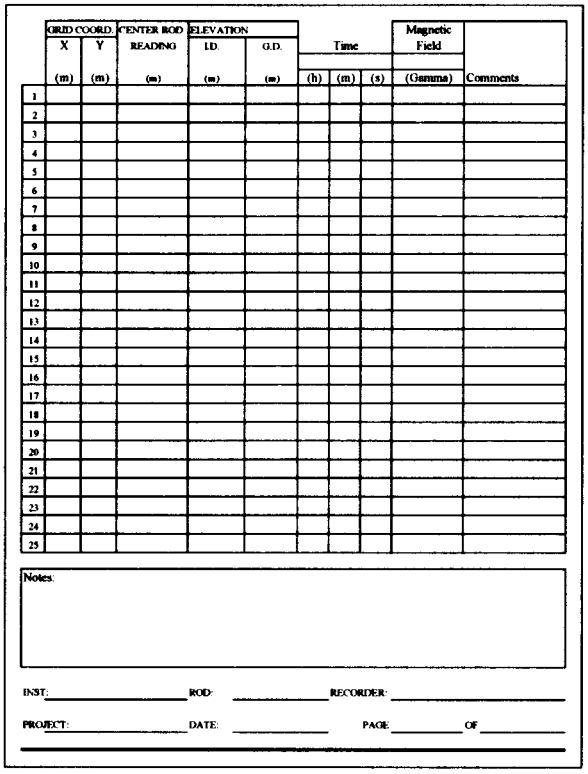

FIGURE 3.3. Topographic survey form. These forms were created using Microsoft Excel®and printed on "Rite in the Rain"®waterproof paper.

maximum elevation equals $50.172m$ with an average elevation of $49.944m$ using an arbitrary elevation of $50m$ for the primary datum. Setting up the transit and grid took approximately one hour, and it took five hours to acquire the elevation readings.

Back in the laboratory, the elevation data recorded on the survey forms were hand-entered into a computer database. Once the data were entered and checked for accuracy, mapping software was used to graphically examine the data (See Appendix C for the raw data). The topographic survey at the Siletz cemetery was conducted using a transit and stadia rod due to a total station not being available. It is useful to note that the process of hand-recording data and manual data entry would be

eliminated by the use of a total station, resulting in quicker and more accurate data transfer from the field to the analysis computer.

3.4. Analysis

The first stage of the topographic data analysis is a visual inspection of the data. This visual inspection looks for data entry errors and potential outlying data points. One outlying data point, located at grid position ($503m$, $1008.5m$), was identified and removed from the data set. Upon completion of the visual inspection, the data was plotted using Golden Software Inc., Surfer®.

The first stage of graphically analyzing the topographic data involves the creation of a contour plot. To find the best way to graphically represent the data in a contour plot, I tried Linear Kriging, Nearest Neighbor, Minimum Curvature, and Shepards Method contouring algorithms. For each of these contouring algorithms, I explored the difference between the following contour intervals: $0.002m$, $0.02m$, and $0.01m$. After examining each of the contour plots, which all looked comparable, I selected Linear Kriging with a contour interval of $0.01m$ as clear, readable representation of the topographic data. The data identifying the horizontal position of the corners of the four headstones was plotted on a separate map layer. The headstone map layer was laid on top of the topographic plot using Surfer®. Overlaying the headstone map on the topographic map facilitates the identification of topographic changes in association with the marked graves (Figure 3.4).

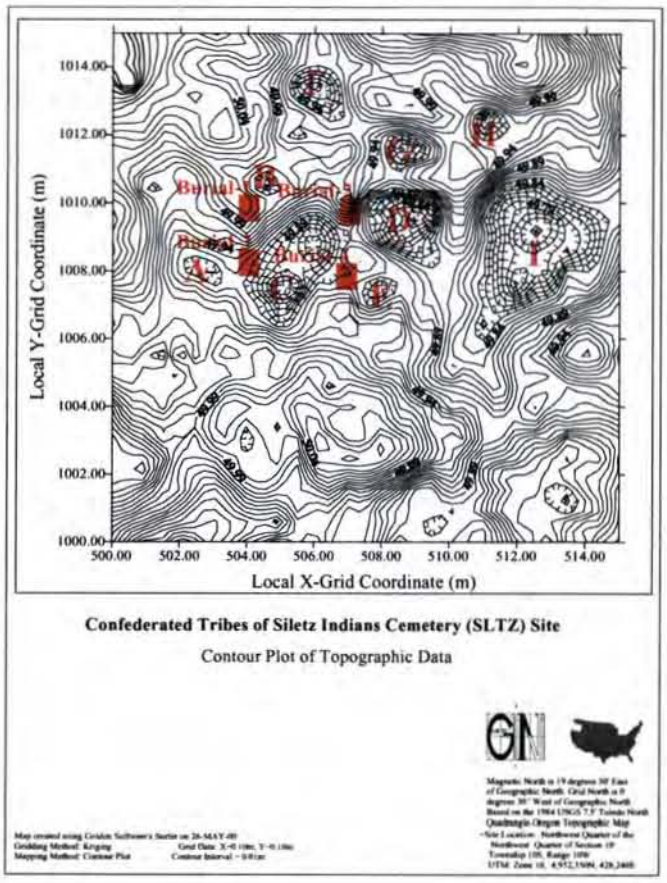

FIGURE 3.4. Contour plot of the topographic data using a $0.01m$ contour interval.

Depressions in the vicinity of the marked burials, labelled Burial-1 through Burial-4, are apparent upon visual inspection of the contour plot. Nine depressions are identified and labelled A-I. These depressions are spatially large enough to be candidates for burials. Additional depressions present near the edge of the survey region will not be studied because only part of the depressions appear in the survey region.

Depressions A,B,C, D, and E are contenders for depressions associated with the marked burials due to their spatial assocation with the headstones marking the

burials. Depressions F, G, H, and I are candidates for unmarked burials, but may be geologic in nature. It is informative to characterize each depression individually.

- Depression-A is oval in shape with dimensions $0.75m \times 1.5m$ and an approximate depth of $4cm$.

- Depression-B has a circular shape with an approximate diameter of $1m$, and a depth of $4cm$. Depression-B's position $1m$ north of Burial-1 suggests a possible correlation with Burial-1. During a survey on August 3rd, 1997 this headstone did not reside within the survey region, but was in place on August 17th, 1997 and subsequent surveys. This headstone was moved into place sometime between 3 August 1997 and 17 August 1997 by an unknown individual for an unknown reason. The most likely explanation is that one of the grounds keepers noticed the marker out of place and returned the marker to the proper general location. Depression-B is shallow and smaller than expected for an adult who is buried horizontally, but only part of the burial may have started to collapse. Of course, it is always possible that Depression-B is geologic in nature.

- Depression-C is rectangular in shape with two depressions lying next to each other at the bottom of the main depression. The long axis of the rectangle shape is oriented southeast to northeast, and is approximately $2m \times 3.5m$ in size. The two depressions lying within the larger depression are both circular in shape with an approximate diameter of $1m$. Depression-C is approximately

$5cm$ to $8cm$ deep. This depression is large enough to correspond with a burial, but its orientation does not agree with the practice at the cemetery of an east-west long axis burial alignment.

- Depression-D is roughly rectangular in shape with dimensions $1.5m \times 2.5m$ and an approximate depth of $15cm$. Depression-D is the strongest candidate for a depression in association with a burial due to its size, orientation, and location near the headstone marking Burial-2.

- Depression-E is roughly circular in shape with a diameter of $1.5m$ and a depth of $5cm$. Depression-E is located just south and east of the headstone marking Burial-4, and Depression-E may be associated with this burial.

- Depression-F is oval in shape with approximate dimensions $1.5m \times 2.0m$ and a depth of $6cm$.

- Depression-G is also oval in shape with dimensions $1.5m \times 2.0m$ and an approximate depth of $8cm$.

- Depression-H has a circular shape with a $1.0m$ diameter and an approximate depth of $4cm$.

- Depression-I is the largest and deepest depression in the survey region and has an unusual shape. Depression-I has a long axis, $6m$ long, running southwest to northeast at approximately the same orientation as Depression-C.

Depression-I has a width that varies from $2m$ to $5m$, and has an approximate depth of $20cm$.

It is important to note that my description of the shape, size, depth, and orientation of the depressions is based entirely on the contour plot. The contour plot is only a representation of the site based on the topographic data that was acquired every $50cm$ across the survey region. For a topographic survey, $50cm$ is a fairly small sampling interval and produces a contour plot that describes the broad features of the depressions. Subtle detail, features smaller than $50cm$, are not recorded using a sampling interval of $50cm$. Figure 3.5 is a visual example of how the shape and size of a depression can be altered by topographic features on a scale less than $50cm$. Figure 3.5 compares the effects of creating a contour plot with and without the outlying elevation point at grid position ($503m$, $1008.5m$). The data point that was omitted from the data set is not a product of a data entry error, but rather an outlying data point that appears in my field notes. When including this data point in the contour plot, a series of diamond shaped contour lines appear. If I were to interpret this contour feature without knowledge of site topography, I would conclude that a small, $6cm$ high, pyramid shaped object sits at grid position ($503m$, $1008.5m$). No such pyramid exists, but a small, localized high region may exist at this grid position. The pyramid shape in the contour plot is an artifact of the mapping software extrapolating from the elevation reading at grid position ($503m$, $1008.5m$) to the next elevation readings $50cm$ away.

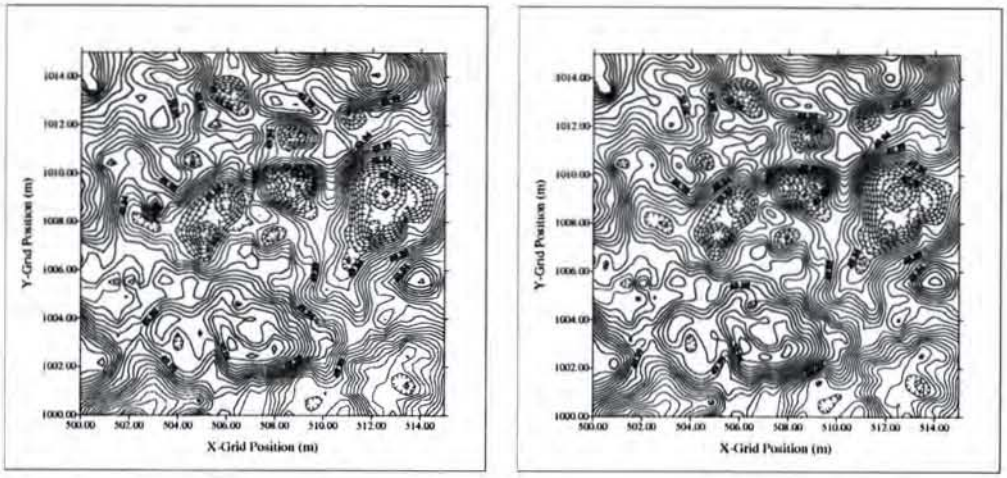

(a) With anomalous data point

(b) Without anomalous data point

FIGURE 3.5. A comparison of contour plots with and without the anomalous elevation reading at grid position ($503m$, $1008.5m$)

Another graphical way of viewing topographic data is the production of an image plot. When producing an image plot, the mapping software assigns color or grayscale values to the maximum and minimum elevation, then produces an even gradient of colors or grays transitioning between the maximum and minimum elevations [21]. White often represents the maximum elevation and black represents the minimum elevation. An image plot is often an effective way of looking at topographic data due to the blending of small details into a smoother image. Because the topographic data is already a sample of the survey region, the blending in the image plot removes some of the potentially incorrect estimates made by the contouring algorithm. One of the most striking aspects of the image plot of the Siletz

topographic data is the apparent association of the four headstones with depressions B-E (Figure 3.6).

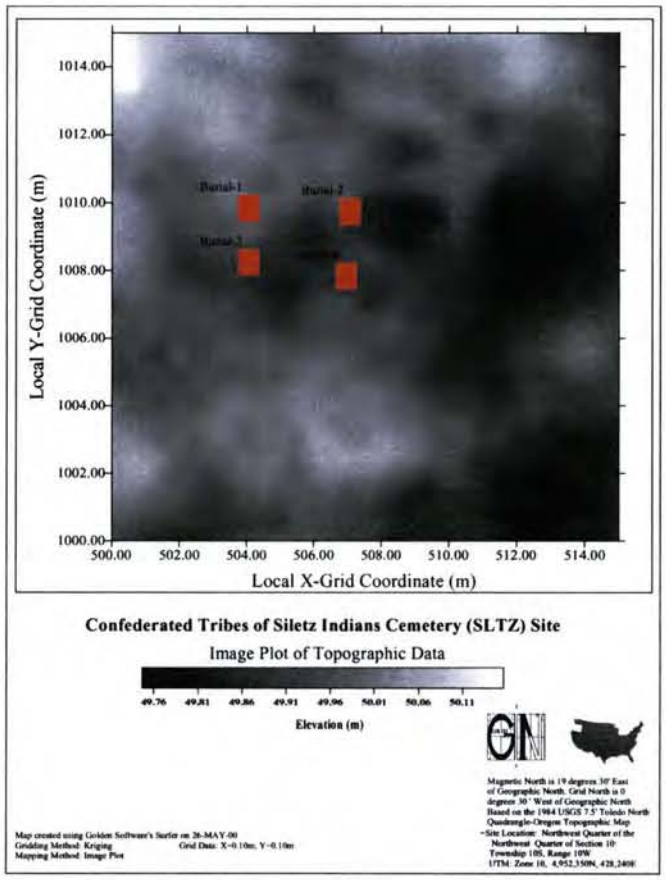

FIGURE 3.6. Image plot of the topographic data using Surfer's® grayscale palette

Another effective way of viewing the topographic data is the creation of a 3-D topographic plot. A contour plot is the most effective way to obtain quantitative information about the topography, but a 3-D plot helps to visualize what the site actually looks like. Using Surfer® I created Figure 3.7 by experimenting with different elevation scales, orientation angles, and inclination angles. I selected my

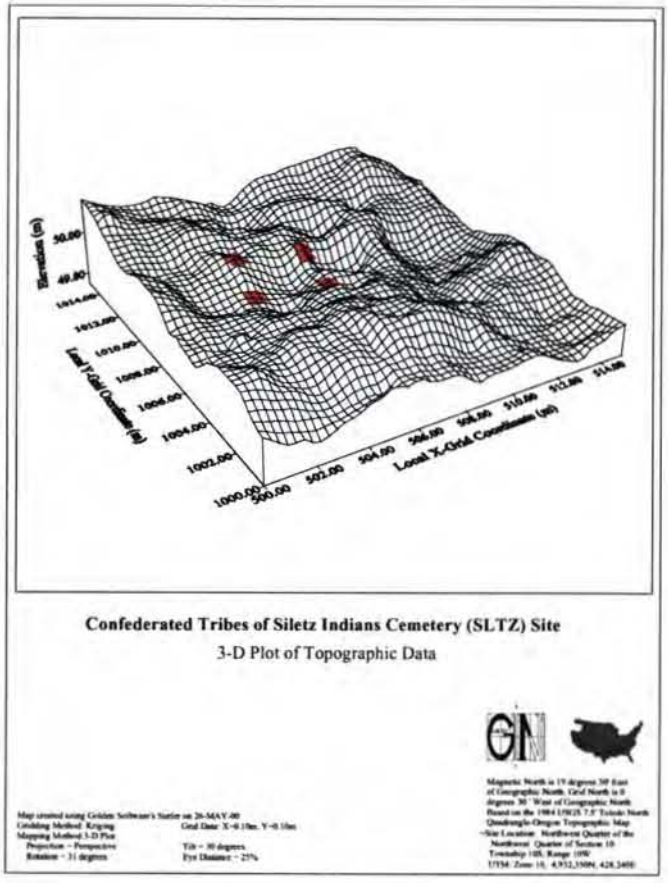

FIGURE 3.7. 3-D surface plot of the topographic data

final values based on what I thought best represented the data. I then used the overlay feature in Surfer® to place the position of the headstones on top of the 3-D topographic plot.

3.5. Conclusions

My first research question is, "Can the geophysical signature of four marked historic period human burials be identified using a topographic survey?" Based on an examination of the contour plot and image plot it appears that depressions

B,D,E, and F are associated with the four headstones. Depression-D is the only depression that has a clear spatial association with a headstone (Burial-2). Depressions B,E, and F are offset horizontally from the position of the headstones. This offset may be due to movement of the burials or movement of the headstones. The headstone marking Burial-1 appearing during the course of this research suggests that the headstones being out of position is the likely explanation for the offset of the depressions. It is not surprising that the answer to research question number one is *yes.* The entire intent of a topographic survey is to record changes in elevation, but the more subtle point is the methodology required to examine topographic changes due to burials. A sampling interval of $50cm$ or less seems necessary, and the use of multiple plotting methods and overlays are required to fully analyze the data.

The more difficult question is my fourth research question, "Can the geophysical signature of four marked historic period human burials be characterized in enough detail to aid in the identification of unmarked burials within the Confederated Tribes of Siletz Indians historic period cemetery using a topographic survey?" Based on my analysis of the topographic data, I think that it is difficult to characterize the topographic signature of the four marked burials. Depressions B-E look different from each other. I do not think that I would be able to identify depressions B-E as burials without having the position of the headstones overlaid on the topographic plots. That said, I do notice a pattern emerge when examining the image plot. Each depression's shape differs from the others, but examination of the spatial position of all of the depressions suggests that they are associated with burials.

Depressions G, D, and E form a north-south running line with the depressions lying parallel to each other. Depressions C and F also form a north-south running line. If burials are placed side by side, then this is the type of pattern of depressions that I would expect to emerge.

My research questions were concerned with identifying the characteristic traits of the individual marked burials, but it appears that an examination of the spatial distribution of depressions may aid in the identification of unmarked burials. In retrospect, this conclusion is not unexpected. I could have easily incorporated an additional research question, examining the spatial distribution of depressions, at the beginning of my project. I was focused on the properties of the individual burials, and was not thinking about the larger spatial distributions.

4. CESIUM GRADIOMETER SURVEY

The most exciting phrase to hear in science,
the one that heralds new discoveries,
is not 'Eureka!' (I found it!)
but 'That's funny ...
- Isaac Asimov [3]

4.1. Introduction

Scientists have been studying the magnetic properties of materials for several centuries, but the first archaeological magnetic survey did not occur until 1957 [31]. The lack of sensitivity in the earlier devices can be blamed for the delay in conducting magnetic surveys at archaeological sites. The proton precession magnetometer, invented in 1954, was the first device sensitive enough to detect the small amplitude magnetic anomalies commonly created by human modification of the landscape [31]. The proton magnetometer can measure the magnitude of the Earth's local magnetic field to an accuracy of $1.0nT$ [29]. Although the proton magnetometer takes several seconds to record a single reading [10], this device was used with a wide range of success at numerous archaeology sites. Faster, smaller, more power efficient, and more accurate magnetometers have emerged since the development of the proton magnetometer[1]. The fluxgate gradiometer and the cesium gradiometer are now commonly used at archaeological sites. Both devices are accurate to $0.1nT$

[1]Clark [10] and Scollar [29] have excellent descriptions of the history of magnetic archaeological geophysics.

or less [29], and take a reading in a fraction of a second [29]. The rapid speed of these devices allows them to be used in continuous mode (at a normal walking pace). The sensitivity of these devices is sufficient to detect a wide range of human activity. Burning, firing clay, creating iron material goods, and disturbing the soils —all have the potential of leaving a magnetic geophysical signature, and the act of burying an individual can incorporate one or all of these activities.

As stated previously, I will restrict my discussion to interments placed beneath the ground surface. The process of creating a burial pit involves the removal of soils to form the pit. Often, organic soils (A-Horizon) and inorganic soils (B-Horizon) [19] will be removed. The process of removing these soils and then using them to backfill the burial pit will mix the organic and inorganic soils. This mixing creates a new soil with magnetic properties different than the undisturbed soils. Organic soils tend to be more magnetic then inorganic soils [10]. The mixed backfill will have a blend of the magnetic properties of the original soils. The backfilled pit may also retain water differently than the undisturbed soils [25]. In essence, just digging a pit and backfilling it has the potential of creating a magnetic anomaly. I use the word, "potential" to stress that soil types, environmental condition, and human modification of the landscape can differ vastly from site to site.

The burial pit and its soils may be one source of magnetic influence on the Earth's local magnetic field, but cultural elements of the burial can provide additional influence. Introducing the body, clothing, wood, and other non-iron grave goods alters the iron content of the burial with respect to the surrounding

undisturbed soils. Depending upon the site specific conditions, the difference in iron content in the burial materials and the undisturbed soil will create a small magnetic anomaly in the vicinity of the burial. Iron grave goods and iron coffin components will have a larger effect on the Earth's magnetic field, and will generate a larger, more localized anomaly. The size, shape, and amplitude of a magnetic anomaly can aid in interpreting the anomaly as being associated with a burial.

4.2. Experimental Apparatus

The magnetic survey at the Siletz cemetery was conducted using a Geometrics, Inc. G-858 MagMapper^{TM} cesium gradiometer. This magnetic gradiometer consists of a control unit, two magnetometers, batteries, cables, magnetometer staff, and a carry harness. The batteries, worn on a waist belt, power the control unit and both magnetometers. The control unit is also attached to the waist belt, and contains the magnetometer controls, a display screen, and a keypad for adjusting control settings. A cable runs from the battery pack to the control unit. Shoulder straps attached to the waist belt help support the weight of the batteries and control unit. Two cables run from the control unit to each magnetometer. The magnetometers are mounted on the magnetometer staff. The magnetometers can be mounted in horizontal mode (a magnetometer on each end of the horizontal staff) or in vertical mode (the magnetometers mounted one above the other on a rod which is then attached to the magnetometer staff). When the magnetometers are mounted in vertical mode, a weight is attached to the opposite end of the magnetometer staff to

balance the weight of the two magnetometers. The magnetometer staff is supported by a shoulder strap (Figure 4.1).

FIGURE 4.1. Photograph of the Geometrics, Inc. G-858 MagMapper^{TM} cesium gradiometer configured in vertical mode. Notice that I am wearing clothing and shoes that reduce the magnetic contamination from the gradiometer operator.

Each cesium magnetometer, individually, records the magnitude of the Earth's local magnetic field to an accuracy of 0.01 nanotesla via an optical pumping method [29]. This method allows each cesium magnetometer to take a reading every

0.1 seconds. The rapid speed of taking a reading allows the cesium gradiometer to be used in continuous mode where the gradiometer can be carried at walking speeds. With the cesium magnetometers in vertical mode, the values of the Earth's local magnetic field from each magnetometer along with the difference in the magnetic field between the two cesium magnetometers are recorded by the control unit.

4.3. Survey Method

The magnetic survey for this project took 3 hours to conducted on 25 March 1999. The temperature hovered around 55°F with overcast skies. Rowland French [2], Derrick Hilger and Travis Peery [3] participated in the survey. The metal stakes marking the corners of the survey region were located and removed. Bamboo skewers were put in place of the metal stakes to reduce magnetic contamination. Similar to the topographic survey, Keyson® fiberglass surveyor ropes stretched between grid positions ($500m$, $1000m$) to ($515m$, $1000m$) and ($500m$, $1015m$) to ($515m$, $1015m$) identified the baseline and a parallel line to control transect spacing. Ten Komelon®Corporation $30m$ fiberglass survey tapes were positioned at x = $500m$ to $509m$ marking the first, third, fifth ..., and nineteenth transects. Bamboo skewers were placed vertically into the ground at one meter intervals along the odd numbered

---

[2]Northwest Geological Association, Corvallis, Oregon

[3]Department of Physics, Oregon State University, Corvallis, Oregon

survey tapes marking the transects to aid in the identification of the gradiometer surface position marks.

Although the survey region starts with grid coordinate ($500m$, $1000m$), the survey ropes and tapes were started $4m$ to $5m$ beyond the edge of the survey area. Instead of the "lower left hand corner," or the southwest corner, being marked by ($0m$, $0m$), the survey tapes read ($4m$, $5m$). All of the survey tapes were displaced to ensure that the metal components at the ends of the tapes were far enough away from the survey region to prevent magnetic contamination. The east-west running tapes and the north-south running tapes were offset different amounts to reduce confusion when working with the offset survey tapes. In retrospect, using $4m$ and $5m$ offsets is not the best method. Using different offsets introduces (instead of reduces) confusion when moving survey tapes and correcting for the offset. Using entirely non-magnetic survey tapes or a standard offset are better methods. Approximately one hour after arriving at the site the survey tapes were in place, and the survey region was clear of possible magnetic contaminates.

After magnetically decontaminating myself, by shedding my blue jeans and boots and donning running pants and sandals that were free of metal, I strapped on the gradiometer. The cesium magnetometers were vertically affixed to the support pole at a distance of $0.50m$. The shoulder carry strap was adjusted until the bottom magnetometer was suspended approximately $0.50m$ above the ground. The gradiometer was placed into continuous sampling, mapped survey mode [15] with a reading taken every 0.1 second. The first transect was surveyed, from south to

north, starting at grid coordinates ($500m$, $1000m$) and surveying to ($500m$ $1015m$). The $0.50m$ spaced transects were surveyed from grid south to grid north. Each transect took approximately one minute to survey. This corresponds to approximately 570 data points per $15.0m$ long transect. The surface position button was pushed when the magnetometers were over the meter marks identified along each transect. Pushing the surface position button records the position of the gradiometer along the transect. Post-acquisition processing software uses these surface position marks to extrapolate the position of the readings of the magnetic field between the surface position marks. Knowing when the magnetometers are directly over the meter marks is a source of error. Under recent development are devices that have a global positioning system incorporated into the control unit to facilitate recording the surface position marks. It is hopeful that future global positioning systems with an accuracy and sampling speed sufficient to record the precise position of each reading will be available at an accessible price. Having such a fast, accurate global position system will eliminate the need for extrapolation of data point position by post-acquisition processing software.

A distinct advantage of using a gradiometer over a single magnetometer is the removal of natural fluctuations in the Earth's magnetic field. Some common fluctuations are:

1. The 11-year sunspot activity cycle [35]

2. The 24-hour solar diurnal variation due to solar winds [30]

3. The few minutes to a few days solar sunspot magnetic storms [35]

The two magnetometers configured in gradient mode measure the same magnitude for these fluctuations. The gradient is obtained by subtracting the value recorded by one magnetometer from the other magnetometer and dividing by their separation distance. Fluctuations in the Earth's magnetic field are subtracted out, and only the local magnetic effects remain [29].

4.4. Data

With a transect spacing of $0.5m$, 31 transects were surveyed using the gradiometer. Each cesium magnetometer recorded a total of 17,689 data points. Table 4.1 presents the range of the magnetic data obtained at the Siletz cemetery.

TABLE 4.1. Range of the local Earth's magnetic field data.

	Magnitude of the Local Earth's Magnetic Field		
	Minimum	*Maximum*	*Average*
Top Magnetometer (nT)	53386.76	53565.55	53477.2478
Bottom Magnetometer (nT)	53246.71	53734.29	53478.2821
Vertical Gradient ($nT/0.5m$)	-411.414	440.367	-2.0685744

TABLE 4.2. Results of applying Microsoft Excel's® descriptive statistics analysis tool package to the magnetic gradient data

Mean	-1.981222115
Standard Error	0.217519561
Median	-1.414
Mode	0.047
Standard Deviation	28.93010155
Sample Variance	836.9507757
Kurtosis	57.36671076
Skewness	0.104838302
Range	851.781
Minimum	-411.414
Maximum	440.367
Sum	-35045.838
Count	17689

Assuming burial dimensions of $1m \times 2m$, each burial is represented by approximately 230 magnetic data points. Statistically, these data should be sufficient to identify magnetic signatures associated with a burial. Because the magnetic gradient contains the least amount of external interference, I will focus my discussion on these data. A visual inspection of the individual data points is not practical with such a large data set. The use of descriptive statistics is a common strategy to work with large data sets [32]. This initial statistical examination of the data will give me an idea of what the data set looks like. Microsoft Excel's® descriptive statistics package was used to examine the magnetic gradient data (Table 4.2).

The mean, median, and the mode are all clustered around 0 $nT/0.5m$. This alignment of these measures of central tendency indicates that the data is normally distributed around 0 $nT/0.5m$. This result is not surprising. Without any local

effects, the magnetic gradient would read 0 $nT/0.5m$ for all data points. It is anticipated that the magnetic effect of human modification on the landscape will produce a small magnetic anomaly. In some cases both geologic and cultural magnetic signatures can produce large magnetic signatures. Depending upon the type of activity at a specific site, numerous, large magnitude magnetic anomalies may be found. This first descriptive statistical glimpse at the Siletz magnetic data indicates numerous small magnetic anomalies and a few large ones.

Along with "getting a feel for the data," it is also important to check the data for possible spatial positioning errors. The gradiometer control unit extrapolates the position of the readings based on the surface position marks recorded by the operator. It is important to check that the surface position marks were recorded correctly, and that the control unit extrapolated correctly. To examine the spatial distribution of the data points, I plotted the X and Y grid positions of the data in an XY-Scatter plot using Microsoft Excel® (Figure 4.2).

Due to the large number of data points, the individual symbols in the XY-Scatter plot blend together to form straight lines. The majority of the data looks complete and accurate, but it is evident that a surface position mark is missing along the X=501.5m survey transect due to the missing symbols from Y=1014m to Y=1015m. The symbols missing from the end of the transect does not imply that this is where the missing surface position mark resides. Further analysis is required to identify the location of this missing mark. One method of locating the position of the missing mark is to examine the number of data points between each meter

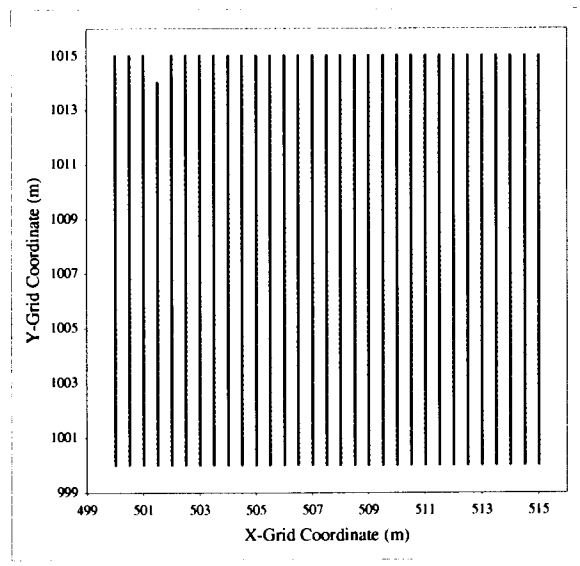

FIGURE 4.2. XY-Scatter plot examining the spatial distribution of the data points along the X=501.5m transect.

interval. I expect to find twice as many data points in the meter interval where the surface position mark is missing. Microsoft Excel® was used to count the number of data points in each meter interval along the X=501.5m transect. Excel® was also used to plot the data from this transect using a Line plot (Figure 4.3).

The average number of readings per meter interval for 15 surface position marks is 34. The interval from 1000m to 1001m, along the X=501.5m transect, contains 57 readings. This is nearly double the average number of readings expected. This suggests that the missing surface position mark resides at Y=1001m. The plot of the reading number versus position along the X=501.5m transect (Figure 4.3) confirms that Y=1001m is the location of the missing mark. If all of the surface position marks are recorded accurately and the control unit evenly distributes the reading between marks, a plot of the reading number versus position should produce

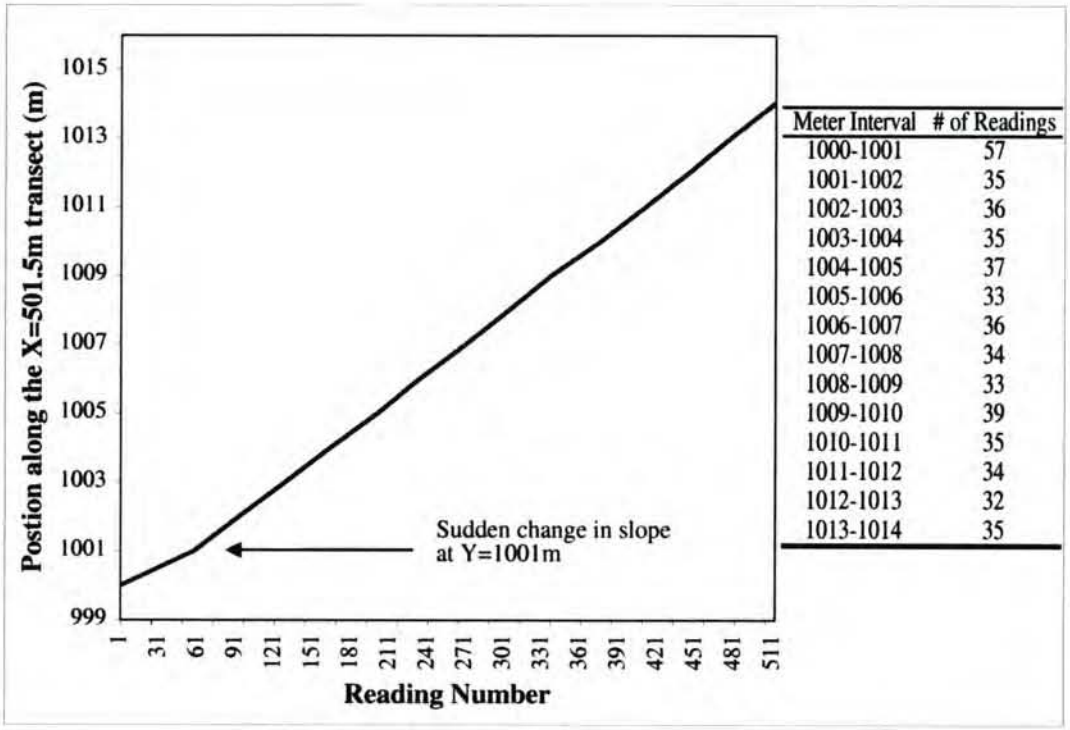

Meter Interval	# of Readings
1000-1001	57
1001-1002	35
1002-1003	36
1003-1004	35
1004-1005	37
1005-1006	33
1006-1007	36
1007-1008	34
1008-1009	33
1009-1010	39
1010-1011	35
1011-1012	34
1012-1013	32
1013-1014	35

FIGURE 4.3. Line plot examining the spatial distribution of the data points along the X=501.5m transect.

a straight line. The line in Figure 4.3 changes slope at Y=1001m. This change in slope is created by the missing surface position mark.

It is not easy to correct for this missing surface position mark. I could try and redistribute the data points, but this action could introduce anomalies into the data. The better method is to discard the readings from Y=1000m to Y=1001m and label the first surface position mark Y=1002m. In this fashion, I can remove the offending data, but keep as much of the accurate data as possible. Even with correcting for the missing surface position mark in this fashion, it will be important to use a critical eye when examining the data from this portion of the survey region.

4.5. Analysis

It is important to recognize that using descriptive statistics to examine human modification of the landscape is tricky business. If Table 4.2 described student scores on an ANTH110 exam, I would discard the high and low outlying points prior to selecting my grading curve. When examining magnetic data from an archaeology site, these outlying points are probably of interest. When using descriptive statistics to examine archaeological geophysical data it is important to focus on the basic tenets of statistics, and ensure that these tenets are used to maximize understanding of the data.

Along with using descriptive statistics, it is useful to graphically examine the data. Descriptive statistics identify properties of the data, but discard spatial distribution information. An image plot, similar to the one produced using the topographic data (Figure 3.6), presents the spatial distribution of the magnetic data. Figure 4.4 is a grayscale image plot, using Surfer's® preloaded grayscale palette and the Kriging algorithm, of the vertical magnetic gradient between the top and bottom magnetometers respectively. The most striking feature of Figure 4.4 is the large magnetic anomaly near the headstone marking the position of Burial-1. Also evident in the image plot are small changes to the vertical gradient throughout the survey region. Distinct patterns to these changes are not evident.

Surfer's® grayscale palette assigns an evenly distributed grayscale gradient to the data, but this even distribution may not be the best way to display them. To

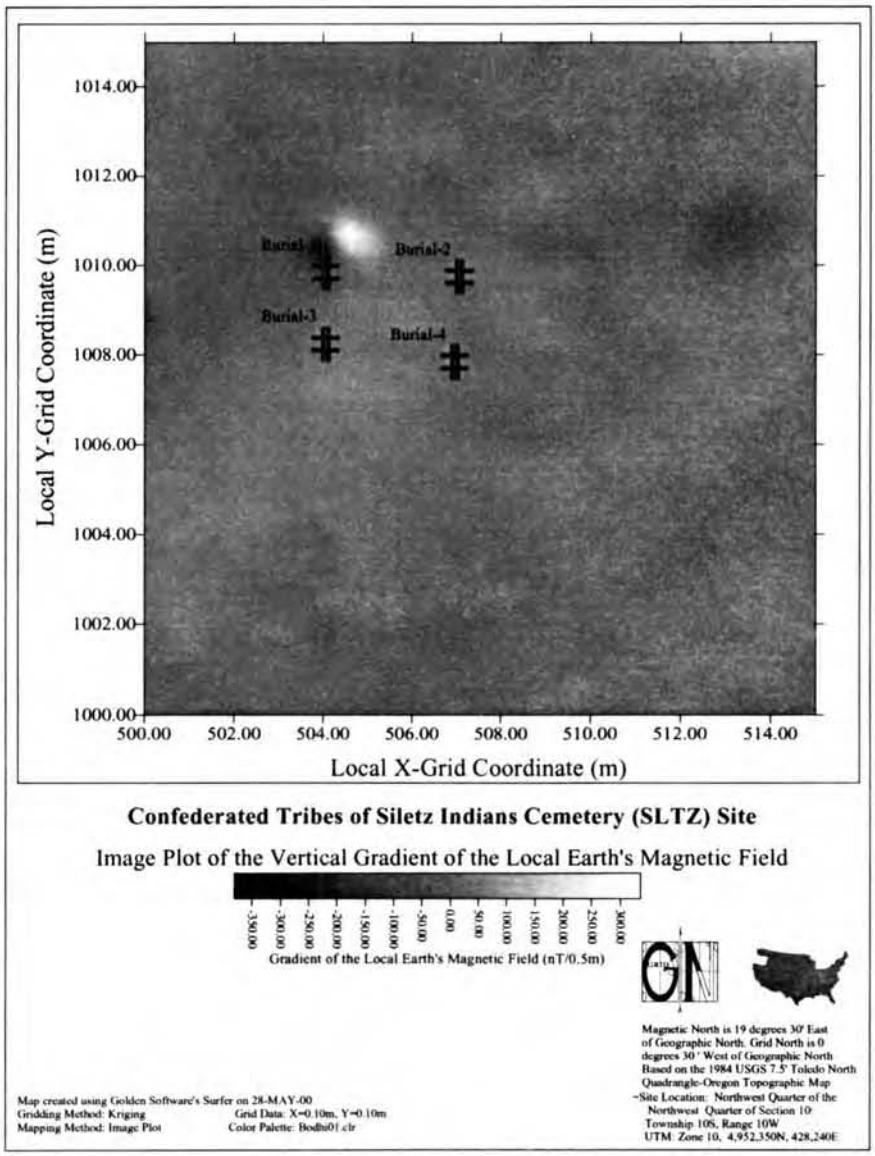

FIGURE 4.4. Grayscale image plot of the vertical magnetic gradient using Surfer's® grayscale color palette and Kriging algorithm.

find the best graphical method I selected Surfer's® preloaded *Rainbow* color palette to explore the benefit to using color instead of a grayscale. Figure 4.5 is the results of using Surfer's® rainbow palette and plotting the vertical gradient data in a plan view image plot.

When examining Figure 4.5, I find it easier to see patterns in the data due to the use of color; other researchers may prefer greyscale or some other color palette. The large magnitude magnetic anomaly near the headstone marking the position of Burial-1 is still evident in the color image plot, and additional magnetic anomalies appear in the vicinity of the headstones. Another spatially large anomaly is seen centered on grid coordinate ($513m$, $1011m$).

Surfer's® *Rainbow* color palette assigns color in an even distribution similar to the way that Surfer® evenly distributes its grayscale palette. Adding color may help some individuals better view the data, but using a preloaded color palette may not be the best display method. To determine the best method of assigning color to the magnetic gradient data, Microsoft Excel® was used to create histograms. Selecting a bin size when plotting the data using a histogram is a method similar to selecting the color interval for the plan view image plot. The quantitative information obtained is an advantage to using a histogram, and aids in the identification of useful intervals for assigning color. With a maximum gradient of $440.367nT/0.5m$ and a minimum gradient of -$411.414nT/0.5m$ to ensure an adequate view at the distribution of the data, I selected a bin size of 5 $nT/0.5m$ (Table 4.3, Figure 4.6).

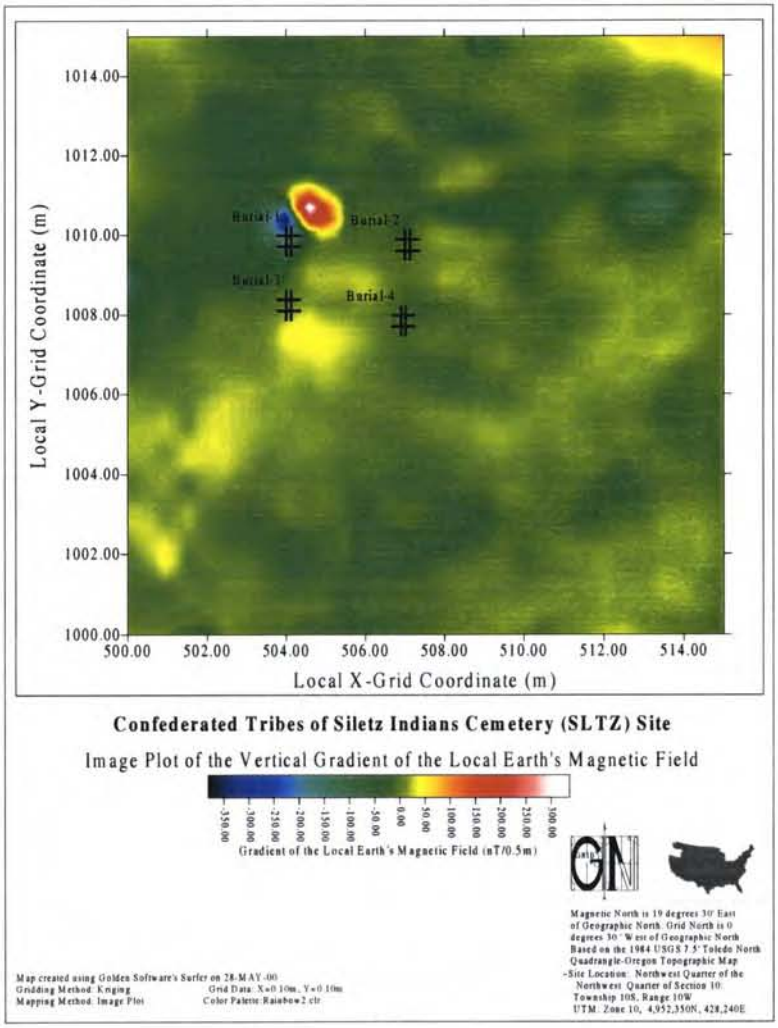

FIGURE 4.5. Color image plot of the vertical magnetic gradient using Surfer's® Rainbow color palette.

TABLE 4.3. Histogram of magnetic data using a bin size of $5nT/0.5m$

Range of Magnetic Gradient $nT/0.5m$	Percent of Data Points
-100 to 100	99
-50 to 50	98
-40 to 40	96
-30 to 30	91
-20 to 20	76
-10 to 10	48
-5 to 5	30

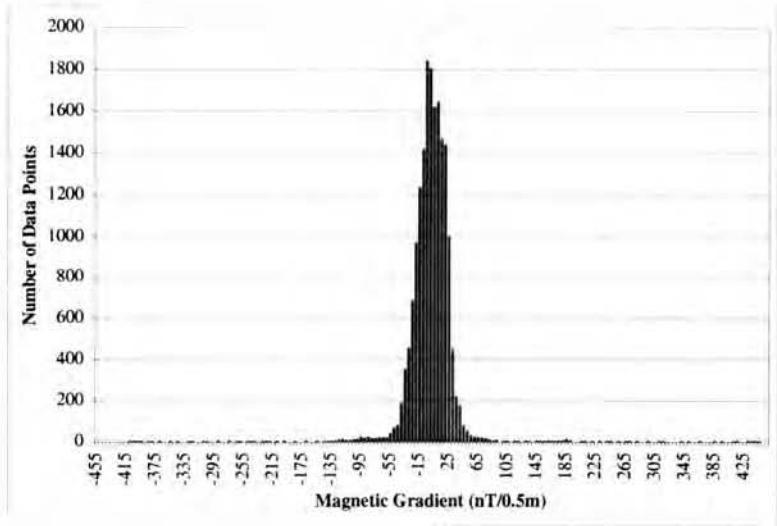

FIGURE 4.6. Histogram of the vertical gradient data using a bin size of $5nT/0.5m$

Table 4.3 indicates that 99% of the data points fall between $-100nT/0.5m$ and $100nT/0.5m$. To obtain a better graphical view of the data it is useful to zoom-in on the $-100nT/0.5m$ and $100nT/0.5m$ range, and plot a new histogram (Figure 4.7).

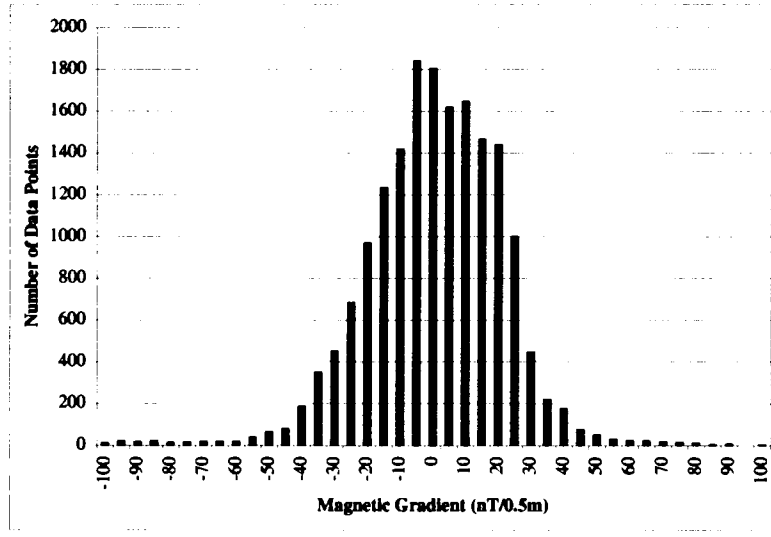

FIGURE 4.7. Histogram of the vertical gradient data from -$100nT/0.5m$ to $100nT/0.5m$ using a bin size of $5nT/0.5m$

The next goal is to select appropriate intervals to divide the colors in an image plot of the gradient data. One complication is that Surfer® uses a percentage scale instead of gradient values when assigning colors. It is necessary to decide what color intervals to use and then convert these intervals to a percentage.

With these percentages, I could create my own color palette in Surfer®. Because 99% of the data points fall between -100$nT/0.5m$ and 100$nT/0.5m$, two obvious intervals are -411.414$nT/0.5m$ to -100.000$nT/0.5m$ and 100$nT/0.5m$ to 440.367$nT/0.5m$. Based on the distribution of data points presented in Table 4.3, I selected the intervals for assigning color (Table 4.4).

TABLE 4.4. Vertical gradient color intervals converted to percentages to facilitate assigning color intervals in Surfer®

Magnetic Gradient Interval $nT/0.5m$	Percentage
-411.414	0
-100.000	37
-50.000	42
-30.000	45
-15.000	47
0.000	48
15.000	50
30.000	52
50.000	54
100.000	60
440.367	100

Using the percentages in Table 4.4, I created my own color palette. Figure 4.8 is the image plot of the vertical gradient that is a result of applying this color palette. By selecting contrasting colors and generating discrete transitions between colors, the spatial distribution of the data takes form. Clearly seeing positive and negative magnetic anomalies is an advantage to using my color palette. Seeing clear patterns indicative of human activity is the most desirable result from plotting the magnetic

data using these methods, but the use of my color palette does not highlight any features not already evident on other plotting methods.

4.6. Conclusions

My second research question is, "Can the geophysical signature of four marked historic period human burials be identified using a cesium gradiometer?" Two of the marked burials have magnetic anomalies spatially associated with them, but these anomalies are not well defined. It is not clear if these anomalies are created by the burials.

My fifth research question is, "Can the geophysical signature of four marked historic period human burials be characterized in enough detail to aid in the identification of unmarked burials within the Confederated Tribes of Siletz Indians historic period cemetery using a cesium gradiometer?" With an inability to answer my second research question I must say that the answer to this question is *no*. There are no clear magnetic anomalies associated with the four marked burials.

It seems strange that the burial pits of the marked burials do not have a magnetic signature. Not being able to conduct test excavations severely limits my ability to understand the results of the magnetic survey. The poor results of the magnetic survey may also be isolated to the small portion of the cemetery chosen for this project. Other burials at the cemetery may have more identifiable magnetic signatures.

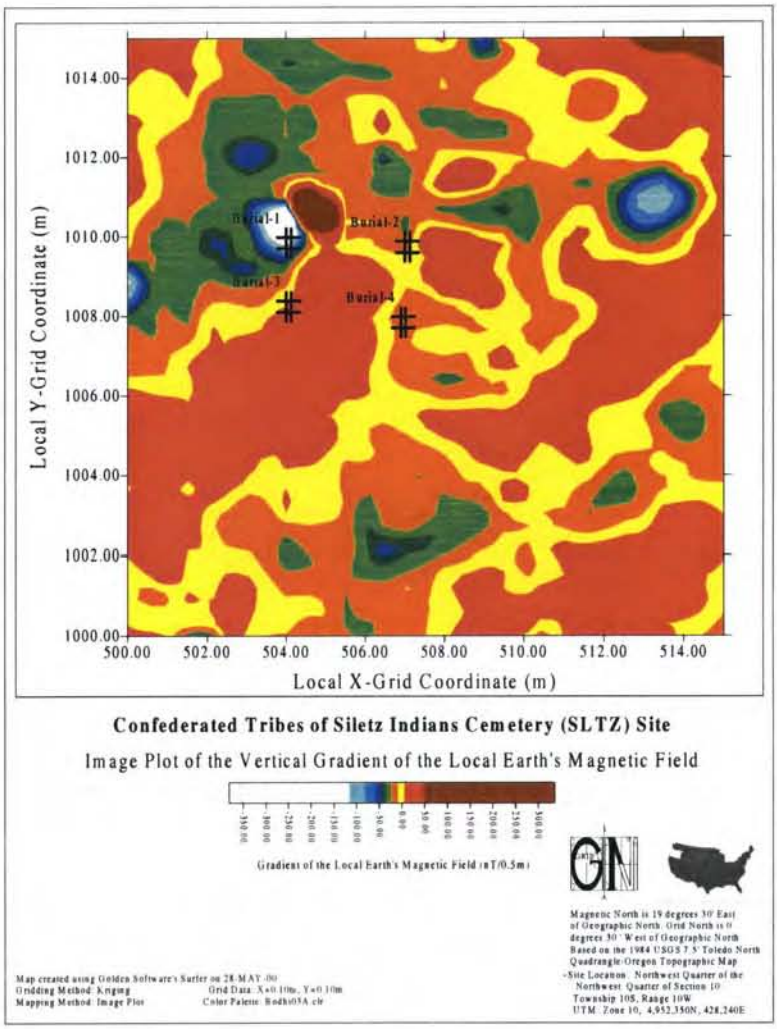

FIGURE 4.8. Color image plot of the vertical gradient using my color intervals

5. GROUND-PENETRATING RADAR SURVEY

God runs electromagnetics by wave theory
on Monday, Wednesday, and Friday,
and the Devil runs them by quantum theory
on Tuesday, Thursday, and Saturday.
- William Bragg [8]

5.1. Introduction

The past decade has witnessed an impressive increase in the processing power of desktop and laptop computers, and the use of GPR on archaeological projects has also increased dramatically. Increased computer processing and more efficient power usage has made field use of GPR more viable. Large amounts of data can be gathered, digitally stored, initially processed while still in the field, and transported to the laboratory for in-depth analysis.

Even with this processing power, the success of a GPR survey to identify subsurface features is very dependent upon the material that the radar signal is travelling through. When the soils at a site are conducive to propagating a radar wave, a GPR survey can yield information about the three-dimensional spatial position of stratigraphic layers and subsurface features. Because a GPR survey records the reflection of the radar wave from a subsurface object, it is often difficult to know precisely what object created the reflection. Many different objects can have the same reflection. To correctly interpreting the data all of the following are helpful: results from other GPR surveys, computer modelling, knowledge of the site,

knowledge of possible features, and experience. Ground-penetrating radar is sensitive to the relative dielectric permittivity of materials and the radar wave reflects back to the antenna upon striking an interface between materials with different relative dielectric permittivities [11]. When dug, a burial pit has distinct walls and a floor. The walls and floor create interfaces between the undisturbed soils and the material in the burial pit. If the relative dielectric permittivity of the undisturbed soil is different from the relative dielectric permittivity of the materials in the burial, the radar wave will reflect from this interface. The amplitude of the reflected wave will be larger if the difference between the two relative dielectric permittivities is larger. Objects within the burial also create interfaces between different materials, and these objects may reflect the radar wave. The larger the interface and the larger the difference in relative dielectric permittivities, the more likely it is that the radar wave will be reflected. The depth into the soil and the size of the interfaces that can be detected are dependent upon the frequency of the antenna being used. The higher the frequency, the shallower the penetration, but smaller objects can be detected.

5.2. Experimental Apparatus

The primary components of a standard GPR device are the control unit, the transmitting antenna, the receiving antenna, the antenna cable, the display, and the power supply. External data storage devices, keyboards, survey wheels, and thermal printers are additional devices often used with the standard GPR device.

A Geophysical Survey Systems, Inc. SIR-2 GPR with a $500MHz$ antenna was used to conduct the GPR surveys at the Siletz cemetery.

The SIR-2® transmits 8,000 to 64,000 radar pulses per second into the ground [16]. Due to the enormous number of pulses being transmitted in such a short time, the control unit must sample the reflected wave data. The SIR-2® control unit allows the user to set the samples per scan to 128, 256, 512, 1024, or 2048. The higher the number the more data points per pulse (often called scan or trace), but the larger the data file. For archaeological applications where the features of interest lie $2m$-$3m$ beneath the surface 512 samples per scan is often sufficient [11], and this setting was used during my surveys of the cemetery. Another adjustable parameter that is linked to the samples per scan setting is the range (or time window). For my survey I set the range to $100ns$. All reflected waves received after $100ns$ were discarded. By increasing the range, radar signals from deeper into the ground will be recorded, but the trade off is less resolution due to the samples per scan setting. For example, if the samples per scan is set to 512 and the range is $64ns$ then eight data points will be recorded every nanosecond. If the range is changed from $64ns$ to $128ns$ and the samples per scan remains at 512, then only four data points are recorded for every nanosecond. It is advantageous to set the range to an appropriate value for a particular study area to maximize the amount of data recorded per nanosecond and keep the data files a manageable size.

There are two more adjustable parameters that are essential to keeping data files manageable. The bits per sample can be set to 8 or 16. The benefit of selecting

16 bits per sample is better resolution of smaller objects, but this setting doubles the file size. When each $20m$ long transect can produce files 1-2 Megabytes in size using a setting of 8 bits per sample, careful consideration must be given to the appropriate bits per sample setting. With recent development of large (greater than 60 Gigabytes) and inexpensive harddrives, it will be easier to record 16 bits per sample in the field. Eight bits per sample were used during the Siletz survey. The user can also set the scans per second to 16, 24, 32, 48, or 64. This setting is used when the GPR survey is conducted in continuous mode. Again, because of the enormous number of pulses per second, the control unit must also sample the number of scans recorded. The scans per seconds is a horizontal sampling of the data, where the samples per scan is a vertical sampling of the data. The scans per second is set based on the speed that the radar antenna is pulled along the survey transect. The faster the antenna is pulled the larger the scans per second need to be in order to record sufficient data. Because I was pulling the antenna by hand at a walking pace, I used 32 scans per second.

When the antenna is pulled slowly, multiple pulses can be *stacked* to improve the signal-to-noise ratio. If the stack is set to 4, then the average of 4 consecutive scans is computed. The amplitude of a reflection from a subsurface feature will average to a value approximately equal to the amplitude of the reflection, but noise will average to a smaller value or zero. Scan stacking allows for better identification of low amplitude reflections. Not only can stacking help in identifying low amplitude reflections, stacking also helps reduce the file size. A disadvantage to stacking is the

requirement that the antenna be moved slowly. Walking speed is often slow enough to facilitate stacking. Because stacking can be performed as a post-acquisition process, I chose not to stack pulses while conducting the survey.

Additional filters are available that can be applied during or after the survey. Low Pass and High Pass Vertical Frequency filters, Horizontal Smoothing, and Horizontal Background Filters assist in removing unwanted noise from the data. I used GSSI's 500D stored settings which automatically set the filters (see Appendix E for a list of GSSI's 500D settings).

A final, important setting is the gain. As the radar wave travels deeper into the ground, the amplitude of the wave decreases. This decrease is due to reflections from interfaces and attenuation due to travelling through different media. Under ideal conditions, identical objects at the same depth in the same material generate reflected signals with the same amplitude. Now move one of the identical objects deeper into the ground and the deeper object will have a smaller reflection amplitude due to the radar wave travelling though more soil. If this object is moved even deeper into the ground the reflection amplitude may get so small that it cannot be identified. By applying gains to the signal the amplitude of the reflection from the deeper object is "boosted" to facilitate better identification. Gain adjustments can be made at varying depths and with varying intensity. During my surveys I chose to let the SIR-2® control unit automatically set the gains.

After reviewing the possible SIR-2® settings, I hope that it is evident that using a GPR is far more complicated than conducting a topographic or gradiometer

survey. An experienced GPR operator can adjust all of the settings to maximize the success of a GPR survey at any given site. Even with experience it is difficult to understand all of the complexity of the subsurface materials at a particular site. The challenge of setting up the GPR at a site such as the Siletz cemetery is increased due to the restriction on excavation to obtain information about the soils and stratigraphic layers.

5.3. Survey Method

The GPR survey took 7 hours to conducted on 26 May 1998 using the Geophysical Survey Systems, Inc., SIR-2® with a $500MHz$ antenna. The temperature was between 50°F and 60°F. James Mayer [1] helped conduct the survey. Similar to the topographic and magnetometer surveys, Keyson® fiberglass surveyor ropes stretched between grid positions ($500m$, $1000m$) to ($515m$, $1000m$) and ($500m$, $1015m$) to ($515m$, $1015m$) identified the baseline and a parallel line to control transect spacing. Two Plumb fiberglass survey tapes were positioned at X = $500m$ and X = $501m$ marking the first and third transects. Bamboo skewers were placed horizontally on the ground at $1.0m$ intervals along the survey tapes marking the transects to aid in the identification of the antenna surface position (Figure 5.1).

Starting with the antenna at grid position ($500m$, $1000m$) the antenna operator pushed the antenna handle button to open the data file and begin recording,

---

[1]Department of Anthropology, Oregon State University, Corvallis, Oregon

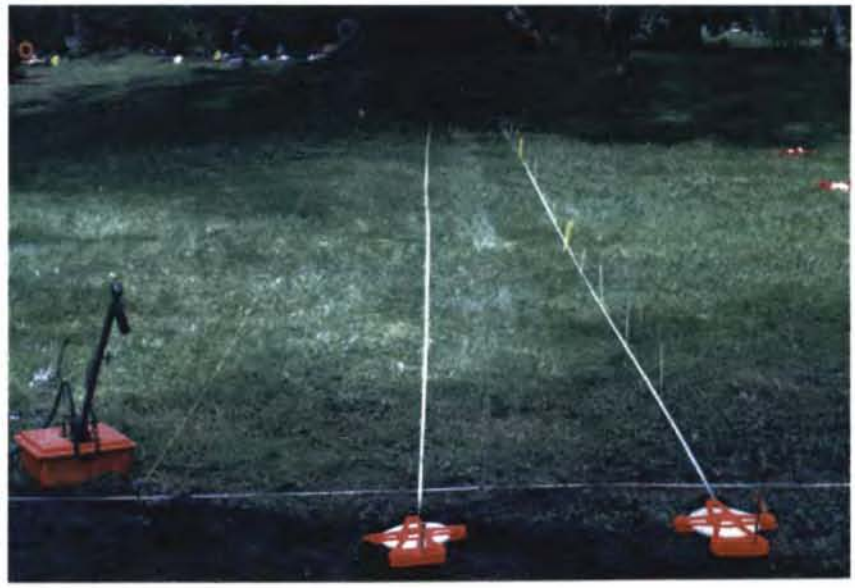

FIGURE 5.1. GPR survey method. Bamboo skewers used to identify every meter along transects can be seen in this photograph.

and then pushed the antenna handle button again to create the first tick mark. The antenna was pulled from south to north along transect one, marking the antenna surface position every meter by watching for the bamboo skewers and pushing the antenna handle button. Each time the antenna handle button is pushed, a tick mark is recorded in the data file that corresponds the antenna's surface position to the appropriate data trace. At the end of the transect, the antenna operator pushed and held the antenna handle button until the control unit operator informed the antenna operator that the data file was successfully closed and saved. An undesirable feature of the SIR-2® is its remote saving procedure. If the antenna operator pushes and holds the antenna handle button for less than three seconds, the data file is paused. If the antenna handle button is pushed and held for more than three

seconds the data file is closed and saved. When the data file is successfully saved the control unit emits a distinct sequence of tones, but the antenna operator is often out of hearing range of the control unit. The pausing option creates an environment that requires the antenna operator and the control unit operator to continually and carefully communicate with each other to ensure that the data files are being saved properly.

To decrease the survey time, transects were surveyed in a bi-directional pattern, surveying from south to north on odd-numbered transects, then north to south on even-numbered transects. While surveying the even-numbered transects, the antenna operator used the survey tapes on either side of the antenna to identify the location of the transect. After surveying three transects the survey tapes were moved and the process repeated. In this fashion 31 north-south oriented transects were surveyed.

Upon completion of the north-south oriented survey the surveyor ropes identifying the baseline and the parallel control line were moved. The surveyor ropes were stretched between grid positions ($500m$, $1000m$) to ($500m$, $1015m$) and ($515m$, $1000m$) to ($515m$, $1015m$) identifying the meridian and a parallel control line. Using the same survey method 31 east-west oriented transects were surveyed.

While the survey was being conducted the control unit operator monitored the display screen to ensure that the radar was functioning properly and identified any interesting anomalies that required further study while at the site. The control

unit operator also recorded the file name, the transect, the survey direction, and any surface features (such as tree roots, holes, bushes, etc.) for each transect (Figure 5.2).

FIGURE 5.2. The GPR control unit operator. James Mayer is pictured in the "mobile command unit."

5.4. Data

While conducting the GPR survey, the data from each transect was recorded to the SIR-2® control unit harddrive. The SIR-2® control unit automatically names the files using a sequential file naming system (file1.dzt, file2.dzt,...). The N-S oriented GPR survey produced 31 files and the E-W oriented survey produced an additional 31 files. Each of these files is approximately $1MB$ in size. These files

contain the GSSI header information, the trace position of the surface marks, and the amplitude and two-way travel time of the radar reflections.

Upon completion of the survey, the data were transferred from the SIR-2® control unit to an analysis computer. This transfer can be conducted while in the field (if you have a portable computer) or in the laboratory. The transfer of data was a labor intensive process with the model of SIR-2® that I used. This version of the SIR-2® uses an older 486 computer processor that relies upon older data transfer technology. I had to dig around to find an analysis computer that contained a 486 processor running MS-Dos v. 6.2. The transfer can be conducted using a bi-directional parallel port or the serial port. I could not find an appropriate computer with a bi-directional port, and had to sit through the painstakingly slow process of transferring approximately $60 Megabytes$ of data through a serial port. Fortunately, GSSI has upgraded their GPR control units to use more modern transfer protocols and faster ports. Unfortunately, the older devices are still in use (Figure 5.3).

Once the data was transferred from the control unit to the analysis computer it was copied onto a Zip disk, and then archived on a laboratory computer and burned to a CD-ROM. The data was renamed from the GSSI format of FILE*.dzt to SLTZ*.dzt. In this manner the files can be recognized as originating from the Siletz (SLTZ) site, and prevent erasure by accidently copying data from subsequent surveys over top of these files.

FIGURE 5.3. Transferring data from the GPR control unit.

5.5. Analysis Method 1 : Visual Inspection of the GPR Profiles

The most fundamental way to analyze GPR data is to examine the raw data from a single transect in profile view, where the X-axis is the scan number and the Y-axis is the two-way travel time (in nanoseconds). Raw data are often difficult to interpret due to changes in walking speed and noise. By recording a surface position mark every meter along a transect, software can be used to adjust for variations in walking speed. This process is often referred to as "rubbersheeting," where the data between surface position marks are stretched or compacted to create equal intervals between surface position marks. Jeff Lucius's program GPR_DISP was used to rubbersheet the data and display them in profile view. After rubbersheeting, the X-axis is displayed as the horizontal distance along the transect (in meters) and

the Y-axis is the two-way travel time (in nanoseconds). The rubbersheeted GPR profiles are presented in Appendix F.

Common reflections seen in GPR profiles are hyperbola, planar, and clutter. Hyperbola shaped reflections are generated from point objects such as pipes, large rocks, voids, and tunnels. If the antenna transmitted a very narrow radar signal, than the reflection from a buried point object would appear as a point reflection. Instead, due to the design of radar antennas, the antenna transmits a radar signal in an asymmetric cone shape. As the antenna is pulled along a survey transect, the cone shape of the radar signal will contact a buried object before the antenna is directly over the object. Because the first part of the radar signal to contact the object travels diagonally from the antenna to the object the signal recorded appears deeper than the actual object. As the antenna gets closer to being over the object the time it takes the radar signal to reach the object decreases, with the shortest time occurring when the antenna is directly over the object. As the antenna is pulled beyond the object the "tailend" of the radar cone will continue to bounce off of the object with increasing travel time. The resulting reflection has the shape of a hyperbola (Figure 5.4).

Planar reflections are created by planar features such as stratigraphic layers, flat buried objects, and flat compacted surfaces. A planar reflection is created when the radar signal bounces from the linear feature in the ground. As an example, consider an ideal case of a buried concrete pad that is parallel to the ground surface. As the antenna is pulled along the surface, the distance between the antenna and

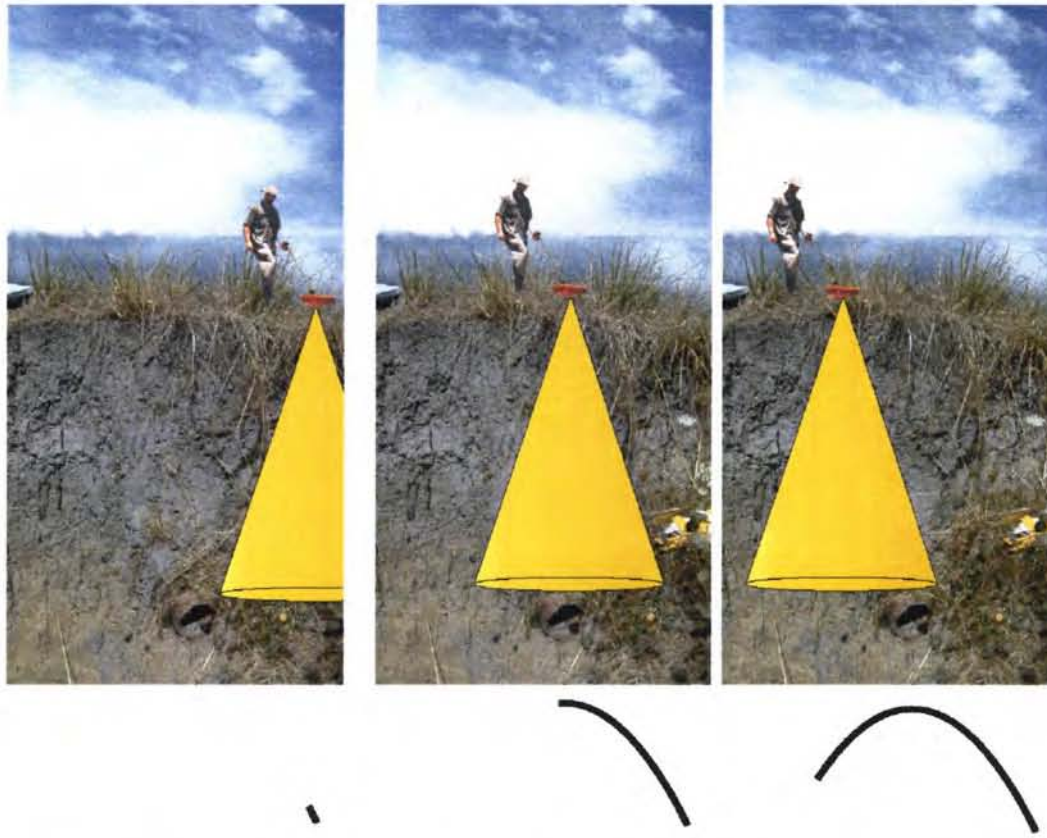

(a) Leading edge of radar cone reflects from object

(b) Center of radar cone reflects from object

(c) Tail edge of radar cone reflects from object

FIGURE 5.4. Creation of a hyperbola shaped signal from subsurface point-like objects due to the conical shape of the radar signal

the buried concrete pad does not change. Each radar pulse that reflects from the concrete pad will have the same approximate two-way travel time and appear as a planar reflection in the radar profile. Due to the asymmetrical cone shape of the radar signal, the planar reflection will appear as a wide strip instead of a thin line. The width of the planar reflection is related to the size of the radar cone.

Clutter reflections are produced due to variations in the soils. These small variations create numerous reflections that may be important pieces of information depending upon the study being conducted. Figure 5.5 contains examples of common GPR reflections.

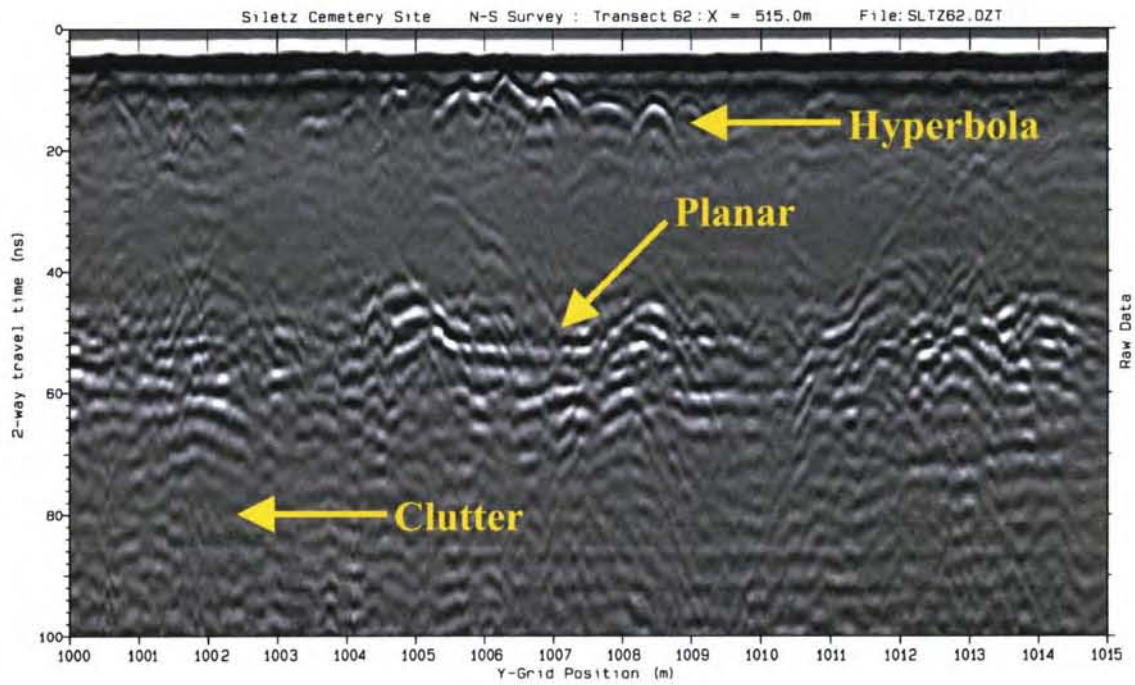

FIGURE 5.5. Examples of common GPR reflections

Visual inspection of the GPR profiles gathered at the Siletz cemetery identifies all three types of commonly seen reflections. There are clutter reflections throughout all of the profiles with two regions of increased "activity" from $0ns$-$20ns$

and $40ns$-$60ns$. Both of these regions appear to have a larger number of clutter reflections and hyperbola reflections when compared to the other regions in the profiles. There are also numerous $1m$-$3m$ long planar reflections throughout the profiles. Due to the absence of longer planar reflections, there is no clearly defined stratigraphic layers, but the $40ns$-$60ns$ region has a suggestive number of planar features that may correspond to a stratigraphic layer.

One of the difficulties in interpreting GPR data is not knowing the reflector depth, in meters, beneath the surface. The GPR control unit records the two-way travel time of the radar wave. To convert this two-way travel time to depth it is necessary to have knowledge of the velocity of the radar wave in the different subsurface materials [2]. At a site where excavation is prohibited, obtaining this knowledge is difficult. Due to the restrictive nature of working at a cemetery, my analysis is restricted to working with two-way travel time. It is anticipated that the burial pit floors at the cemetery are $2m$-$3m$ beneath the surface, but it is not clear what two-way travel times correspond with these depths. This complicates positive identification of the burial pit floors of the four marked burials within the study area.

A burial should create a planar or partially hyperbola shaped reflection due to its rectangular or pit shape. Objects within the burial pit that are large enough to

---

[2]Conyers and Goodman's book, Ground-Penetrating Radar: An Introduction for Archaeologists contains an excellent chapter on methods of converting two-way travel time into depth below surface.

reflect radar waves should create hyperbola shaped reflections [11]. Large amplitude planar reflections at an approximate depth of $50ns$ in the vicinity of the marked burials are apparent in the profiles. These reflections are evident (Figure 5.6), but are difficult to characterize as burials.

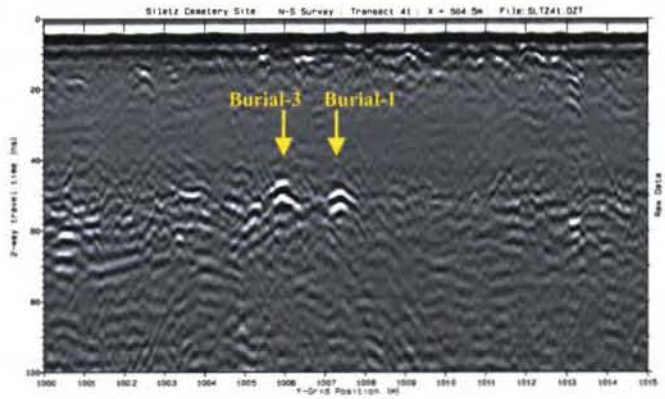

(a) GPR signals from Burial-1 and Burial-3

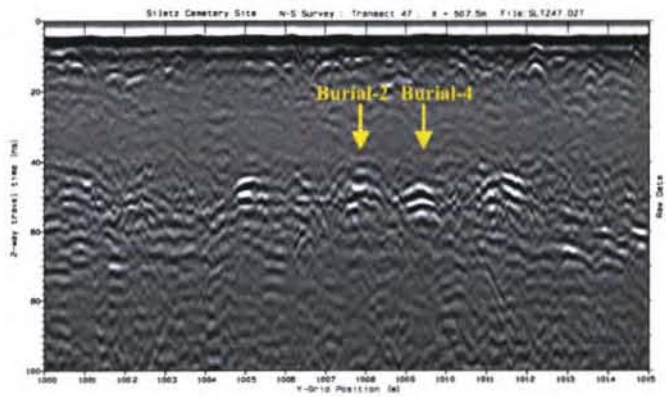

(b) GPR signals from Burial-2 and Burial-4

FIGURE 5.6. GPR signals from the four marked burials

Examination of the radar profiles identifies numerous reflections that have similar shape and amplitude to the reflections that appear spatially associated with the horizontal position of the marked burials. These other reflections may or may not be burials due to the difficulty in characterizing the GPR signature of the marked burials. It is clear that there are reflectors located beneath the surface. If I did not know that these positions corresponded with marked burials, however, I would simply identify these reflectors as GPR anomalies.

5.6. Analysis Method 2 : GPR Time Slices

Examining the data in profile view is only one method of examining the data. It is also possible to use software to assemble the individual profiles into a three-dimensional data set. This three-dimensional data set can be examined in profile view or plan view. Plan view plots have the advantage of presenting the horizontal association of the data, and are often referred to as time, amplitude, or depth slices. To create time slices of the Siletz GPR data I used a beta version of the program GPR_Process [3]

GPR_Process is a windows interface to a series of C++ programs that generate the required files to create time slices. Because the survey was conducted using a bi-directional survey, the first step is to "flip" every other profile to have

---

[3]Development team: L. Conyers, J. Lucius, M. West. For additional information please contact Lawrence B. Conyers, Dept. of Anthropology, University of Denver, 2130 S. Race Street, Denver, CO 80208, 303-871-2684 (phone), 303-871-2740 (fax), lconyers@du.edu

all of the profiles align correctly (note: when printing out the rubbersheeted GPR profiles included in Appendix F, the profiles were aligned by flipping every other profile). Along with aligning the profiles it is necessary to create XYZ files that tell GPR_Process information about the survey grid. With information about the grid, GPR-Process then reads each data file and extracts the scan position of the surface position marks and creates a *.MEDT file. GPR_Process examines these *.MEDT files to see if the number of surface position marks agree with the size of the grid. It is very easy to miss hitting the surface position mark when conducting the survey. If any errors are located GPR_Process notifies the user and allows the user to add in the missing mark. The *.MEDT file contains the mark number, the trace number, and the number of traces between the previous mark and the mark in question. If the walking pace while pulling the antenna was fairly constant, it is often easy to spot the missing mark by examining the number of traces between marks. The missing mark is where the number of traces between marks is double that of all the other marks. The next step introduces error, but is required to create time sliced plots. Based on the average number of traces between marks, a trace is selected to represent the missing mark. The position of the missing mark is certainly wrong and will incorrectly plot the position of the reflections surrounding this missing mark during the rubbersheeting process. This method is less than ideal; the ideal is to not miss any marks while in the field, but this is the only way to correct such a mistake. When I conducted the GPR survey I did not know that the first push of the surface position button started recording data and that a second push of the

button was required to record the first surface position mark. Every one of Siletz GPR files was missing the first surface position mark. Fortunately I discovered my mistake and easily identified the location of the missing marks, but the process of hand-entering marks into 62 files was labor intensive.

Once all of the *.MEDT files are corrected for missing marks, GPR_Process creates the final *.MRK files that will be used to create the time slices. There are several settings necessary to create time slices. The **#-of-cells** setting instructs GPR_Process as to how many horizontal data points to include in the time slice. The product of a time slice is a *.DAT file that contains X, Y, and Amplitude information that can be imported into mapping software. During the Siletz survey the antenna was continuously pulled along a transect, then moved over $0.5m$ to the next transect. The sampling interval in one direction is $0.5m$, but much smaller in the other direction. The #-of-cells setting allows the sampling interval in the X and Y directions to be defined. It is possible to extrapolate additional data points between the $0.5m$ transects. GPR_Process compares reflections across transects, and extrapolating a few points between transects produces data for smoother plotting.

Setting the **Box-Size** tells GPR_Process how to average the reflection amplitudes across transects. The Box-Size is related to the #-of-cells size in generating good plots. A Box-Size is also set in the Z direction. This setting tells GPR_Process how "thick" to make the time slice. My profiles go from $0ns$ to $100ns$ along the Z-axis. If I set the Z-Box-Size to $10ns$, GPR_Process will produce 10 time slices where each slice is a $10ns$ thick average of the reflection amplitudes. A final important

setting tells GPR_Process whether or not to remove background noise. Background noise appears as horizontal bands in the data. These horizontal bands can obscure important data, but removing the background noise also removes any horizontal reflections in the data. It is usually advantageous to look at the data with and without the background removed.

After examining the results of different slice parameters (see Appendix G) the following settings were used to create time slices of the E-W GPR data: #-of-cells = (15,15,10), and box-size=($0.25m$, $0.75m$, $10ns$). Figure 5.7 is the $50ns$ to $60ns$ time slice that contains the probable burial reflections identified when examining the GPR profiles.

Visual inspection of the $50ns$ to $60ns$ time slice identifies a strong GPR reflection spatially associated with marked Burial-4, and no GPR reflections associated with the other three marked burials. The presence of reflections in the GPR profiles for all four marked burials and the absence of reflections in the time slice for three of the burials is curious. The absence of reflections in the time slice may have to do with the averaging processes involved in creating the time slice. More in-depth post-acquisition processing may assist in producing a time slice that identifies the GPR reflections from all four marked burials. Such post-acquisition processing is time consuming and beyond the scope of this thesis.

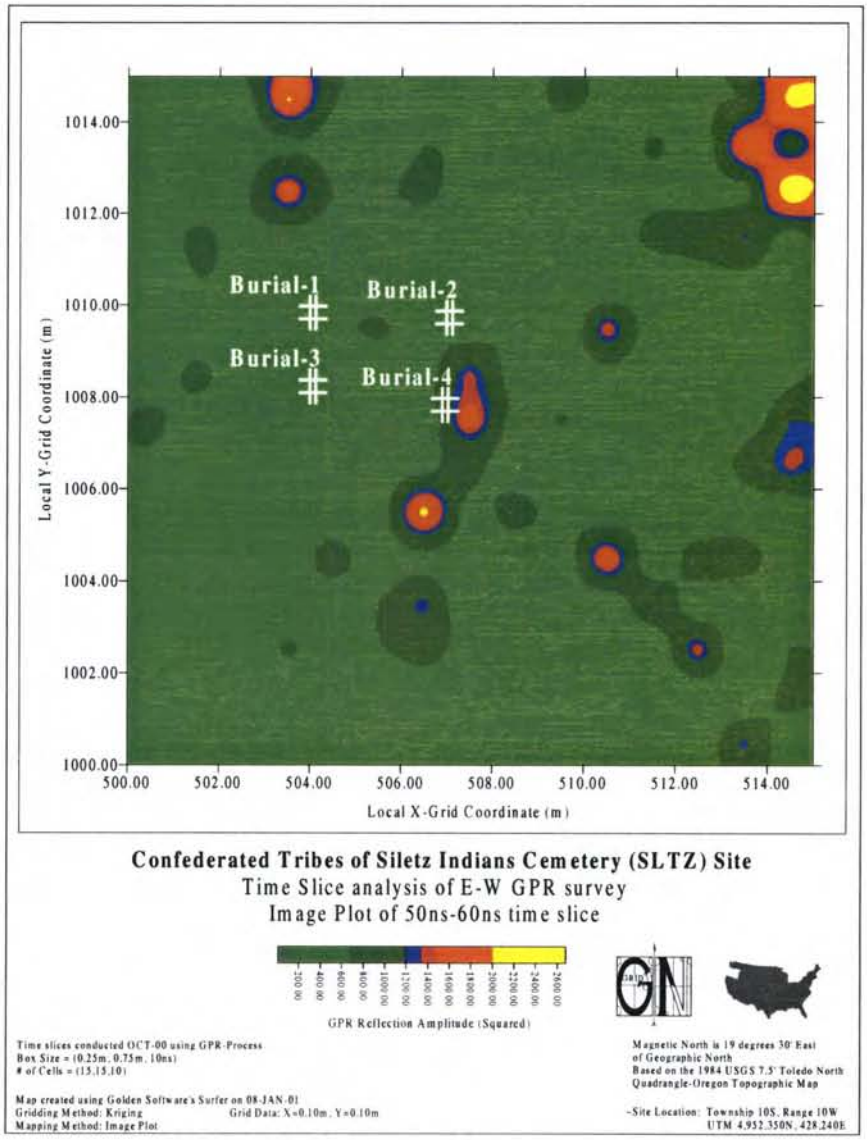

FIGURE 5.7. $50ns$ to $60ns$ time slice of marked burials

5.7. Conclusions

My third research question is, "Can the geophysical signature of four marked historic period human burials be identified using a ground-penetrating radar?" An examination of the radar profiles identified radar reflections approximately $50ns$ deep that appear spatially associated with the position of the four marked burials. The plan view time slice from $50ns$ to $60ns$ identified a GPR reflection spatially associated with marked Burial-4, but failed to identify reflections from the other three marked burials. A GPR survey seems capable of identifying burials at the Siletz Cemetery. Post-acquisition processing seems necessary to fully analyze the data and identify the reflections from burials in the plan view time slices.

My sixth research question is, "Can the geophysical signature of four marked historic period human burials be characterized in enough detail to aid in the identification of unmarked burials within the Siletz cemetery using a ground-penetrating radar?" Based upon my examination of the radar profiles and time slices I am unable to characterize the reflections that are spatially associated with the marked burials. Although I am unable to characterize the radar signatures of the marked burials, this does not mean that a characteristic signature does not exist. Analyzing radar data is a complex process. Additional filtering, stacking, and gain adjustments might identify a characteristic signature of the marked burials. This additional post-acquisition processing is time consuming, requires the appropriate processing software, and is beyond the scope of this thesis. I would like to note

that one of the strengths of conducting non-invasive ground-based remote sensing surveys is that the data can always be examined later in more detail.

Even though I am unable to characterize the radar signature of the marked burials, the GPR survey was able to identify anomalous regions associated with the marked burials. An additional study that could be conducted is similar to my discovery of the potential for a spatial distribution study of the topographic data. If a larger portion of the cemetery was surveyed using GPR a spatial distribution analysis of the anomalies might yield information as to the spatial distribution of burials, and patterns might emerge that can be characterized in sufficient detail to locate unmarked burials.

6. COMPARISON OF METHODS

I'm astounded by people who want to 'know' the universe
when it's hard enough to find your way around Chinatown.
-Woody Allen (1935-) [1]

6.1. Introduction

An individual analysis of the data recorded by each survey method produced some positive and some negative results in identifying the geophysical signatures of the four marked burials. The hypothesis of this project is that the use of multiple ground-based remote sensing methods can aid in identifying the characteristic geophysical signatures of marked burials at the Siletz cemetery. Chapters 3, 4, and 5 demonstrate that the geophysical signatures of particular burials can be seen by one or more of the methods, but it is difficult to characterize the geophysical signatures of the burials using any single method. My final research question is, "Can a combined analysis of the topographic, cesium gradiometer, and ground-penetrating radar surveys be used to characterize the geophysical signature of four marked historic period human burials in enough detail to aid in the identification of unmarked burials within the Confederated Tribes of Siletz Indians historic period cemetery?" By overlaying the plots produced in previous chapters I can explore the data in more detail to see if additional information can be obtained through the collective analysis of the data.

6.2. Comparison of Topographic and Cesium Gradiometer Surveys

Without any further data analysis, I used Surfer® to overlay the topographic contour plot on the gradiometer image plot. Visual inspection of Figure 6.1 identifies some spatially associated magnetic anomalies with topographic depressions B, D, E, F, and G. Other than the large dipole magnetic anomaly near the headstone marking Burial-1, the magnetic anomalies spatially associated with depressions D, E, F, and G are small in amplitude. The source of the large dipole anomaly near Burial-1 may be a buried metal object or the magnetic properties of the headstone itself.

There are two additional magnetic anomalies that may be associated with depressions H and I. These anomalies appear northeast of depressions H and I at an approximate angle of 20 degrees. This angle is the same as the direction of the Earth's magnetic field. These two anomalies may be the result of the Earth's magnetic field inducing a magnetic field in subsurface objects. Because the gradiometer survey records the value of the magnetic field one-meter above the ground, a magnetic anomaly can appear displaced from the source. This may be the case with the magnetic anomalies northeast of depressions H and I.

There also appear to be numerous places where the magnetic data "follows" the topographic contours. In some places it is remarkable how the magnetic data seems to flow along a contour line. Recall that the changes in elevation are on the order of centimeters and not large geologic features, and yet there seems to

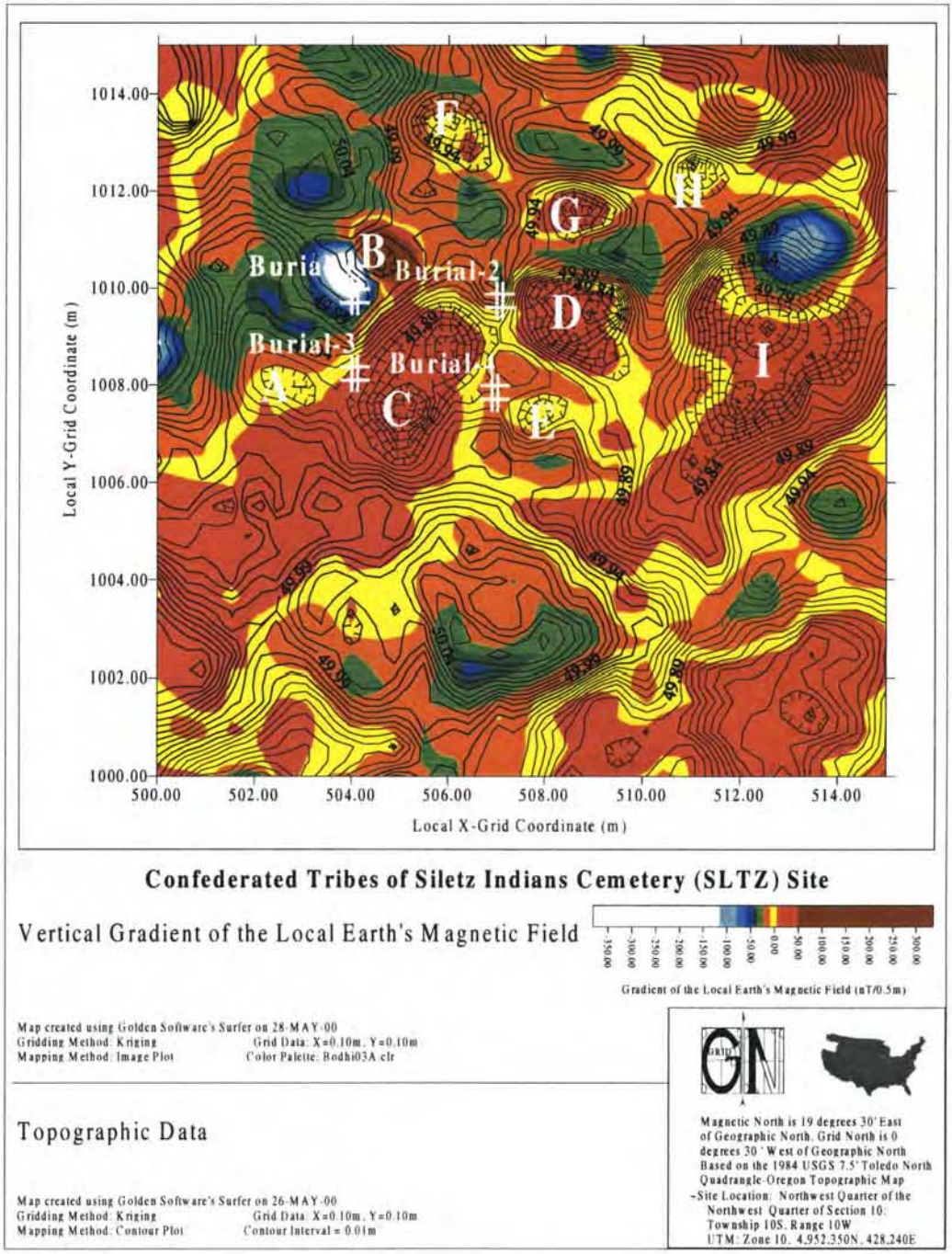

FIGURE 6.1. Overlay of the topographic data and gradiometer data

be a spatial association of the magnetic data and the contours. I did not expect this association. Without an in-depth analysis of the soils, their role in this effect is not clear. Another explanation may be found in studying the distance of the sensors from the ground surface. If the distance of the sensors from the ground surface changes due to changes in elevation the magnetometers will record a change in the magnetic field. An examination of the spatial association between changes in topography and the magnetic field data makes an excellent topic for future studies.

A comparison of the topographic data with the magnetic data does not provide any further insight into the characteristics of the marked burials. This comparison does identify general spatial associations between the magnetic data and changes in topography.

6.3. Comparison of Topographic and Ground Penetrating Radar Surveys

In a fashion identical to that in the previous section, Surfer® was used to overlay a plot of the topographic data on a plot of the GPR $50ns$ to $60ns$ timeslice (Figure 6.2).

In contrast to the number of magnetic anomalies spatially associated with depressions, there appear to be only spatial associations between radar reflections and depressions F and E. There also appears to be a lack of spatial association with radar reflections and changes in topography. A comparison of the topographic data to the GPR data seems unproductive in arriving at a better characterization of the geophysical signature of the marked burials. This is not a surprising result.

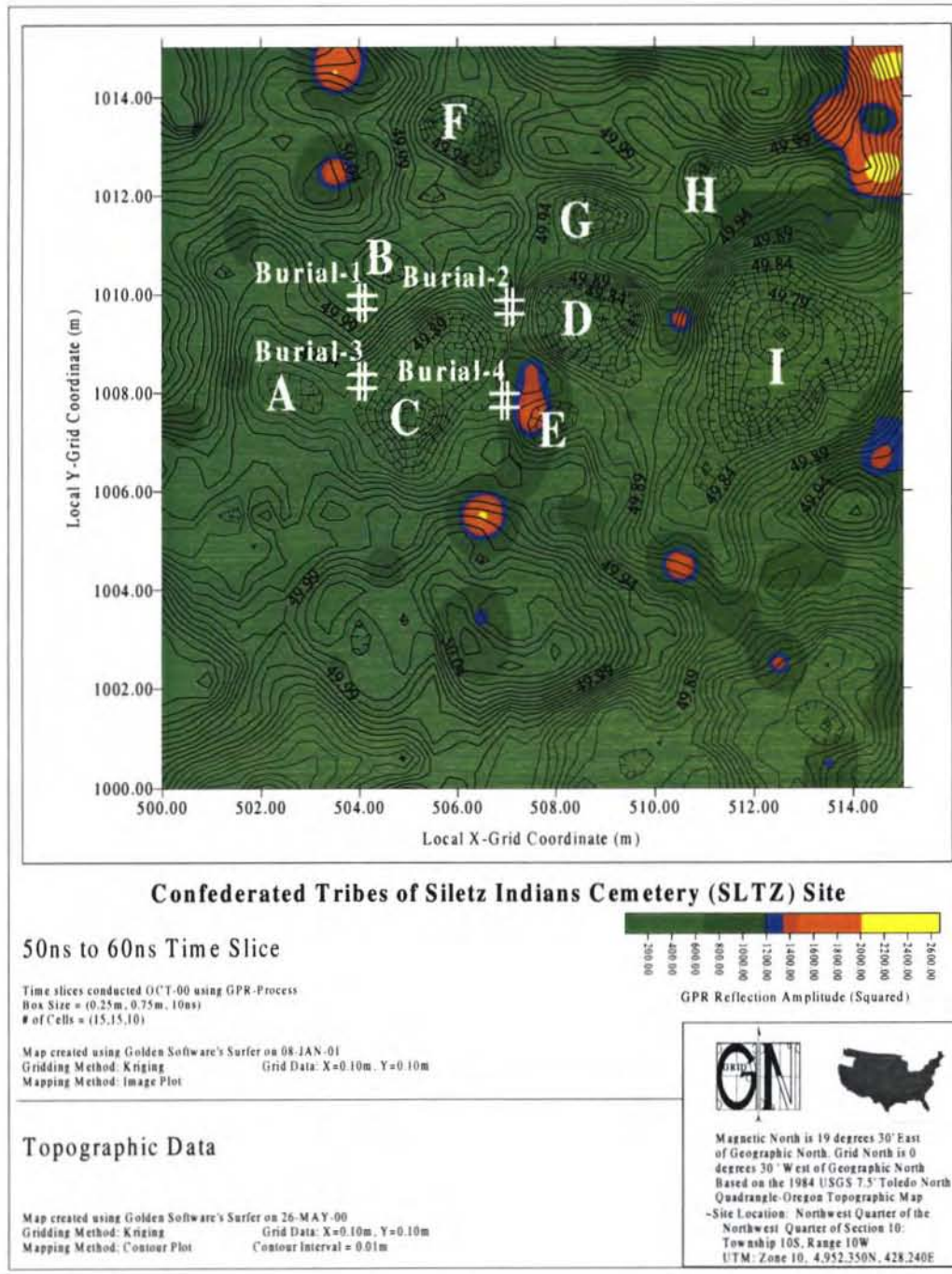

FIGURE 6.2. Overlay of the topographic data and GPR data

The GPR timeslice represents the amplitude of reflections from objects beneath the surface. The topographic shape of the stratigraphic layers and location of subsurface objects is most likely different than the topography of the ground surface.

An important reason to compare the topography of the surface with the GPR timeslice is to note any errors that might arise from changes in the topography at the surface. The changes in topography at the Siletz cemetery are so small as to not be of concern, but at some sites, such as burial mound sites, changes in topography can seriously alter the GPR data.

6.4. Comparison of Cesium Gradiometer and Ground Penetrating Radar Surveys

To compare the magnetic data with the GPR data it was necessary to create a contour plot of the magnetic data. The contour plot was created using the same grid file that was used to create the image plot (Figure 4.8). A contour interval of 10 $nT/0.5m$ produced a good representation of the magnetic data, and Surfer® was used to overlay the magnetic contour plot on the GPR time slice (Figure 6.3).

A visual inspection of the magnetic and GPR data identifies the extreme difference in these two data sets. There appears to be no spatial association between magnetic anomalies and GPR anomalies. This result is surprising. Metal objects generate large magnetic anomalies and are strong GPR reflectors. The lack of spatial association of magnetic and GPR anomalies may have two explanations. If some or all of the magnetic anomalies are created by subsurface metal, these metal objects

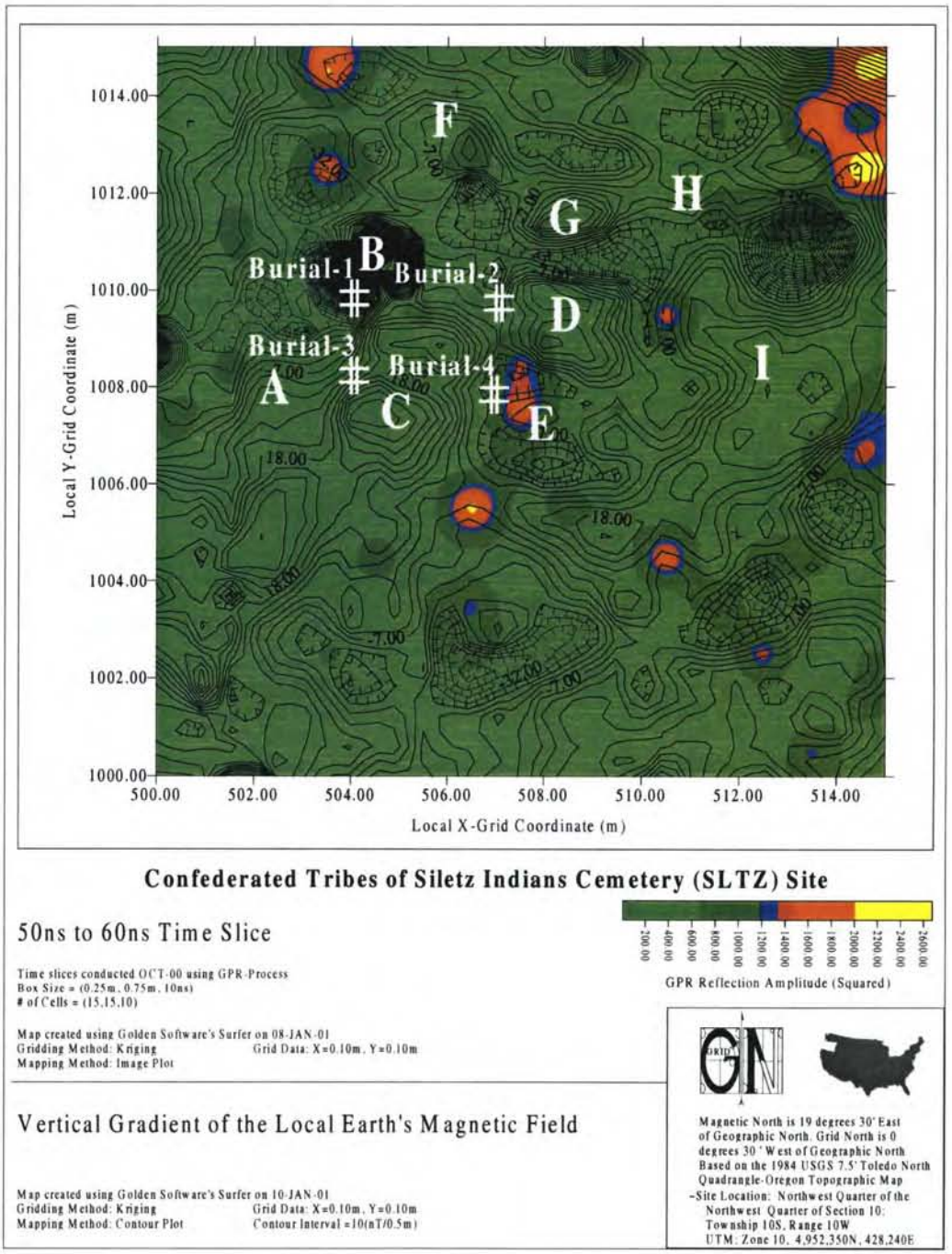

FIGURE 6.3. Overlay of the magnetic data and GPR data

may be small and undetectable by the GPR. Another possibility is that the magnetic anomalies are created by objects that are not strong GPR reflectors. Without the ability to excavate, it is difficult to explore the reason for the differences between the magnetic and GPR data.

6.5. Comparison of All Three Methods

A comparison of all three methods can be achieved by using Surfer® to lay the magnetic contour on the GPR time slice and then laying the topographic contour on the combined magnetic and GPR plot. This method produces a final plot that is complicated. Data in the top overlay may block information in the middle or bottom plots. A better way to compare the three methods is to use an RGB (also referred to as color compositing) imaging method commonly used in astronomy. To produce color images using a charged-coupled device (CCD) that only records grey-scale images, astronomers take three separate images of the same object. The first image is taken by letting the light pass through a red filter prior to being recorded by the CCD. The second image is taken with a green filter, and the final image is taken using a blue filter, thus the name RGB (Red-Green-Blue). The image taken with the red filter has recorded the red information. Areas of the object being photographed that are red will show up as white areas in the image and areas of the object that do not contain red will show up as black. Figure 6.4 is an example of RGB images taken of the familiar Apple Computer, Inc. logo. Examination of

the colored bands in the apple identifies the role that the colored filters have when taking the pictures.

(a) Grayscale picture using a red filter

(b) Grayscale picture using a green filter

(c) Grayscale picture using a blue filter

FIGURE 6.4. RGB grayscale images of the familiar Apple Computer, Inc. logo

Using the National Institute of Health's program NIH-Image, the RGB images were stacked and converted to a single 8-bit color image (Figure 6.5). NIH-Image mixes the color recorded in each grayscale image in a fashion similar to mixing paints. This mixing should result in a decent color representation of the object with the quality of the filters and photographs playing a role in the quality of the color image.

Color compositing is common to astronomy, but application to archaeological-geophysical survey data is new. My literature review identified only a

FIGURE 6.5. 8-bit color image of Apple Computer, Inc. logo from grayscale RGB images.

single reference to the application of color compositing to archaeological-geophysical data. Kenneth Kvamme's web site [26] discusses the use of color compositing to analyze the data from the Whistling Elk site, and provided the inspiration for the use of color compositing in this thesis.

The RGB method can be used to "mix" the results of my three survey methods. Instead of using filters to record the color information from an object, I created a grayscale color palette using white to identify large amplitude signals and black to indicate low amplitude signals with varying shades of grey in between. Because the magnetic data has positive and negative anomalies I chose $0nT/0.5m$ to be black and the extreme plus and minus values to be white. For the GPR data, white

corresponds to large amplitude reflection signals and black to low amplitude reflections. For the topographic data I am interested in depressions and will assign white to low elevations and black to high elevations.

If a low elevation is spatially associated with a large amplitude magnetic and radar signal NIH-Image will be mixing white(all red)+white(all green)+white(all blue) and result in white. NIH-Image assumes that the first image loaded was taken using a red filter, the next image with a green filter, and the final image with a blue filter. I am arbitrarily assigning the topographic data to the red filter, the gradiometer to the green filter, and the GPR to the blue filter. The resulting image indicates regions where all three methods have high amplitude signals spatially associated, where two methods are associated, and where all three methods have low signals spatially associated. The RGB to 8-bit color process is just a means to mix the results of all three survey methods and arbitrarily assign color to the resulting image.

To make it easier to interpret the color composite image of the three data sets, I created a color template that gives all possible combinations of mixing white, grey, and black (Figure 6.8). As expected, white represents the case when a depression, large amplitude magnetic anomaly, and a large amplitude GPR reflection are all spatially associated. When all three signals have medium amplitudes the result is grey, and when all three signals have low amplitudes the result is black. Because I arbitrarily placed the topographic data in the red sequence of creating an RGB image, red appears when there is a depression and low magnetic and radar signals.

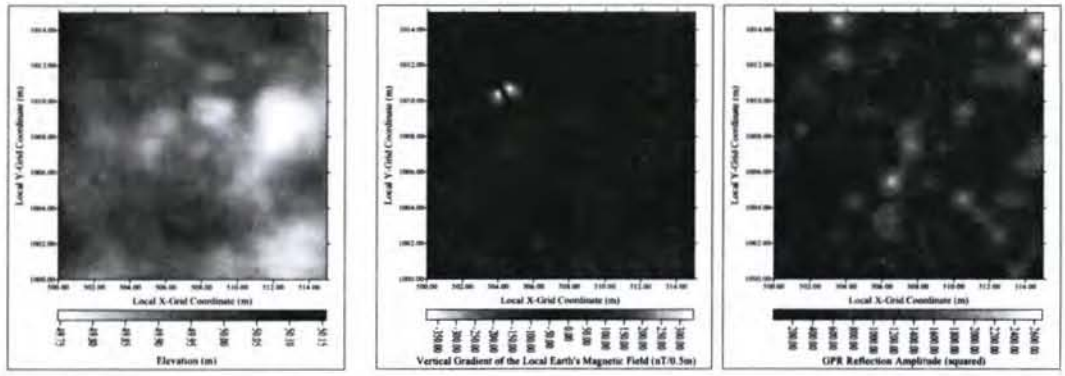

(a) Topographic data ("Red")

(b) Magnetic data ("Green")

(c) GPR data ("Blue")

FIGURE 6.6. RGB grayscale images of the results of all three survey methods

Green appears when only the magnetic signal is high, and blue appears when only a high GPR signal appears. Shades of these colors represent mixing of the different signals to different degrees.

Due to the low success of identifying characteristic geophysical traits of the burials when comparing the results of two survey methods, I did not expect any startling results from my RGB method of analyzing the results of all three survey methods. A visual inspection of Figure 6.7 identifies expected results. The large dipole magnetic anomaly appears green. This means that only the magnetic signal has a large amplitude at this geographic position within the survey region. Many of the GPR reflections show up as blue. This is expected due to the lack of spatial association with the topographic and magnetic data.

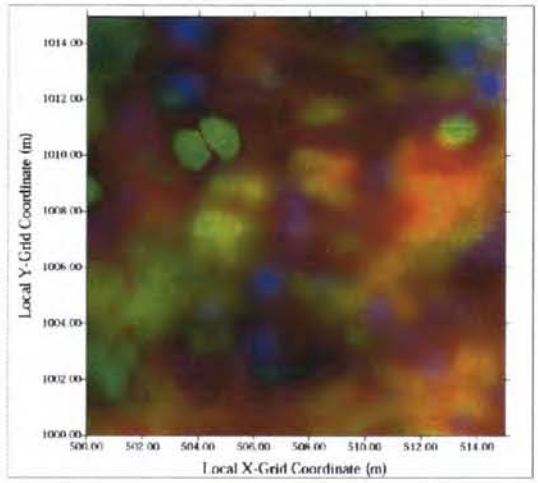

FIGURE 6.7. 8-bit color image from the RGB grayscale images of the survey data.

FIGURE 6.8. Color scale to assist in interpreting the color composite image of all three data sets.

A distinct advantage to this type of analysis is being able to identify which type of data has a larger value in a certain geographic position. When examining the topographic and magnetic data in section 6.2, I noticed spatial association of the two data sets, but it was difficult to identify where the topographic data had a large signal compared to the magnetic data. Because the color composite image is a mixture of amplitudes, it is easy to identify which surveys have larger signals in different geographic positions. Light green areas indicate large magnetic signals, medium topographic signals, and low amplitude GPR reflections. Orange areas indicate depressions, medium magnetic signals, and low amplitude GPR reflections. Instead of seeing a simple spatial association of the magnetic data and the topographic data, the color composite image yields insight into which signal "dominates."

A serious disadvantage to the RGB analysis method is the method's dependance on color. The use of color provides additional variation to aid in interpretation of the data, but it is not always possible to produce color images. Grayscale photocopies of color images are often more difficult to interpret than the color image, and using descriptive terms such as green, orange, and red lose meaning when color is lost. As an analysis tool the advantages of color compositing outweigh the disadvantages.

6.6. Conclusions

My final research question is, "Can a combined analysis of the topographic, cesium gradiometer, and ground-penetrating radar surveys be used to characterize the geophysical signature of four marked historic period human burials in enough detail to aid in the identification of unmarked burials within the Confederated Tribes of Siletz Indians historic period cemetery?" The answer to this question is no. If the marked burials contained common characteristic geophysical traits in two or all three survey methods, then the burials would show up in the color composite image with a distinct color. If a distinct color appeared, this color could form part of the characteristic traits of the marked burials that could be used to identify unmarked burials.

7. CONCLUSIONS

Finish each day and be done with it. You have done what you could;
some blunders and absurdities have crept in;
forget them as soon as you can. Tomorrow is a new day;
you shall begin it serenely and with too high a spirit
to be encumbered with your old nonsense.
- Ralph Waldo Emerson [12]

The hypothesis addressed by this research is that the use of multiple ground-based remote sensing methods can aid in identifying characteristic geophysical signatures of marked burials at the Siletz cemetery. Seven research questions focusing on the use of topographic, magnetic, and GPR surveys helped guide an investigation of my hypothesis. After answering all seven research questions, the hypothesis proposed by this thesis is false, and this result is tied strongly to the limits and scope of the research conducted.

Although the answer to my hypothesis was false, this does not mean that this thesis lacks positive results. A main goal was the identification of characteristic geophysical traits of four marked burials that could be used to identify unmarked burials at the Siletz cemetery. Identifying characteristic traits proved elusive, but the surveys recorded elements of the marked burials with varying success. The topographic survey identified depressions in the vacinity of the four marked burials. Each of the depressions varied in size and shape; this variation is what made identification of characteristic traits difficult. The cesium gradiometer survey identified only one small magnetic anomaly in the vicinity of a marked burial. The GPR

survey was the most successful of the three methods employed by identifying the location of all four marked burials. Even though the marked burials were evident in the GPR profiles, these reflections were difficult to characterize. Creating plan view GPR time slices did not add to the information contained in the GPR profile plots.

Due to the lack of geophysical signals that could be characterized individually by each of the surveys, a comparision of the surveys failed to provide additional information to aid in characterizing the geophysical signatures of the marked burials. Even with the failures of this project, the process of gathering the data, conducting post-acquistion analysis, creating plots, developing comparative methods, and conducting the RGB image analysis method were all very instructive. The skills that I developed increase the value of this thesis.

An interesting aspect of this thesis is that writing it took place a few years after the data was acquired. I have been involved in several other ground-based remote sensing projects during this time. These projects have given me experience that allows me to retrospectively examine this thesis in a way that is not normally available to graduate students. Is the answer to my hypothesis really false, or just a product of limitations of my research design and analysis?

One limitation in my work at the Siletz cemetery lies in the small size of the research area. Studying a $15m \times 15m$ region limits the ability to study larger distribution patterns and geologic trends in the geophysical data. Based on all of my research projects I am curious as to the minimum dimensions of a study area required to obtain meaningful geophysical data. Somewhere between $40m \times 40m$

and $60m \times 60m$ seems appropriate for seeing larger trends. The larger the survey region, the easier it is to see larger trends. I feel that all of the analyses conducted in this thesis would have been more productive if the surveys had covered a larger survey region that included more marked burials and site features.

Not having historic information about the marked burials within my study area is another limitation. Having information about non-geophysical contextual elements of the marked burials may have aided interpretation of the data. I began my research while working as part of James Bell's project and chose my study area to incorporate my work with Bell's work without increasing the time it took to complete his contract work. Under different circumstances it may have been possible to search the historic records to locate a portion of the cemetery that contained detailed historic documents. Addressing my hypothesis in a portion of the cemetery that contained easily accessable historic records would have provided more information to aid in interpretating the data.

The restriction on excavation was a clear limitation at the beginning of this project. Ground truthing through excavation after conducting ground-based remote sensing surveys can confirm and clarify results. It is not always necessary to ground truth because the results of surveys at some sites are easy to interpret. Ground truthing is helpful when interpretation of the data is difficult. A different research design would choose a site where historic documents exist and excavation is allowed, but there still exists a functional need to conduct investigations at sites such as the Siletz cemetery. When developing my research design I made the choice to accept

the limitations that came from working at the Siletz cemetery. These limitations are offset by contributing to solutions to burial problems at the cemetery.

The contribution of this thesis to helping solve burial problems at the Siletz cemetery lies in identifying GPR as the best method of identifying burials. An additional contribution is identifying the difficulty in characterizing the marked burials. Instead of looking for unmarked burials using GPR, a better strategy is to use GPR to identify regions free of anomalies. Because all four marked burials in my study area produced GPR reflections evident in the GPR profiles it is likely that regions free of GPR reflections are also free of unmarked burials.

The results of this thesis are consistent with results from other similar studies [6, 7, 25, 27, 31]. Using ground-based remote sensing surveys to located burials is a hit-or-miss endeavor. Additional research needs to be conducted to understand what elements of burials consistantly show up in the "hit" column and what elements appear in the "miss" column. Compiling such a list may lead to better understanding of when surveys in search of burials will be successful.

BIBLIOGRAPHY

[1] Woody Allen. [http://www.starlingtech.com/quotes/], February 2000.

[2] David D. Alt and Donald W. Hyndman. *Roadside Geology of Oregon.* Mountain Press Publishing Company, 1978.

[3] Isaac Asimov. [http://www.starlingtech.com/quotes/], February 2000.

[4] Ewart M. Baldwin. *Geology of Oregon.* Kendall/Hunt Publishing Company, 1976.

[5] James W. Bell. Report of the Remote Sensor Survey at the Siletz Tribal Cemetery. Technical report, Pacific Geophysical Surveys, 1997.

[6] Bruce Bevan. A Geophysical Survey at the Plains Cemeteries. Technical report, Geosight. Submitted to William C. Dulin, 1986.

[7] Bruce Bevan. A Radar Search for Burials in Sandy Soil. Technical report, Geosight. Submitted to the National Park Service, Purchase Order PX-6115-7-0163, 1987.

[8] William Bragg. [http://www.starlingtech.com/quotes/], February 2000.

[9] Don Brothwell. *The Bog Man and the Archaeology of People.* British Museum Press and Harvard University Press, 1992.

[10] Anthony Clark. *Seeing Beneath the Soil: Prospecting Methods in Archeaology.* B.T. Batsford Ltd, London, 1990.

[11] Lawrence B. Conyers and Dean Goodman. *Ground-Penetrating Radar: An Introduction for Archaeologists.* AltaMire Press, 1997.

[12] Ralph Waldo Emerson. [http://www.quoteland.com/quotes/], February 2000.

[13] Nora Ephron. "When Harry Met Sally". Directed by Rob Reiner. Distributed by Columbia Pictures Corporation., 1989.

[14] Joseph Fenwick. A Study of Rathra: A Multivallate Enclosure in Co. Roscommon. Master's thesis, National University of Ireland, Galway, 1997.

[15] Geometrics, Inc., Sunnyvale, California. *G-858 MAGMAPPER Operation Manual # 25309-OM REV.x2*, 1995.

[16] Geophysical Survey Systems, Inc., North Salem, New Hampshire. *SIR®System-2 Operation Manual # MN72-140*, 1994.

[17] P.V. Glob. *The Bog People: Iron-Age Man Preserved.* Cornell University Press, 1970.

[18] Don H. Heimmer. *Near-Surface, High Resolution Geophysical Methods for Cultural Resource Management and Archaeological Investigation.* Geo-Recovery Systems, Golden, Colorado, 1992.

[19] Norman Herz and Ervan G. Garrison. *Geological Methods for Archaeology.* Oxford University Press, 1998.

[20] J.D. Jackson. *Classical Electrodynamics.* John Wiley, New York, 1977.

[21] Doug Keckler. *Surfer®for Windows Version 6 User's Guide.* Golden Software, Inc., Golden, CO, 1997.

[22] Robert Kentta. "Confederated Tribes of Siletz Indians: Identity". [http://ctsi.nsn.us/], June 1999.

[23] Robert Kentta [rkentta@ctsi.nsn.us]. "Approval for CD-ROM production". Private e-mail message to Michael Rogers, [rogersm@ucs.orst.edu], 03 April 2000.

[24] Robert Kentta [rkentta@ctsi.nsn.us]. "History of the Confederated Tribes of Siletz Indians' Paul Washington Cemetery, Government Hill, Siletz, Oregon.". Private e-mail message to Michael Rogers, [rogersm@ucs.orst.edu], 08 March 2001.

[25] Edward W. Killam. *The Detection of Human Remains.* Charles C Thomas, 1990.

[26] Kenneth L. Kvamme. Whistling Elk Subsurface Imaging Project: Combining Data Through Color Compositing
. [http://www.cast.uark.edu/ kkvamme/Whistle/Composite.htm], January 2001.

[27] James S. Mellet. Ground-Penetrating Radar Survey of Gethsemane Cemetery Little Ferry, New Jersey. Technical report, Subsurface Consulting Limited. Submitted to County of Bergen Division of Cultural and Historic Affairs, Hackensack, New Jersey, 1989.

[28] Francis H. Moffitt and Harry Bouchard. *Surveying, Ninth Edition.* Harper Collins, 1992.

[29] I. Scollar, A. Tabbagh, A. Hesse, and I. Herzog. *Archaeological Prospecting and Remote Sensing.* Cambridge University Press, 1990.

[30] P. V. Sharma. *Geophysical Methods in Geology: Second Edition.* Elsevier, 1987.

[31] Michael Strutt. *Rediscovering the Dead: Practical Applications of Remote Sensing in Historic Cemeteris.* Volumes in Historical Archaeology XXV. University of South Carolina, 1994.

[32] David Hurst Thomas. *Refiguring Anthropology: First Principles of Probablity & Statistics.* Waveland Press, Inc., 1986.

[33] Bruce G. Trigger. *A History of Archaeological Thought.* Cambridge University Press, 1989.

[34] Bill Watterson. *Attack of the Deranged Mutant Killer Monster Snow Goons.* Andrews and McMeel, 1992.

[35] Michael Zeilik. *Astronomy: The Evolving Universe.* John Wiley & Sons, Inc., 6th edition, 1991.

APPENDICES

Appendix A. Commonly Used Abbrieviations and Acronyms

B.M.	Bench Mark
B.S.	Back Sight
F.S.	Fore Sight
G.D.	Ground Datum
GPR	Ground-penetrating radar
H.I.	Height of the Instrument
I.D.	Instrument Datum
INST.	Survey Instrument
R.R.	Rod Reading
ROD	Stadia Rod
S.I.	Stadia Intercept
T.B.M.	Temporary Bench Mark
T.P.	Turning Point

Appendix B. Establishing the Grid Data Forms

	STATION INST	STATION ROD	H.I. (m)	GRID COORD. X (m)	GRID COORD. Y (m)	ANGLES HORIZONTAL (Degrees)	ANGLES HORIZONTAL (Minutes)	ANGLES VERTICAL (Degrees)	ANGLES VERTICAL (Minutes)	ROD READING B.S. + (m)	ROD READING F.S. - (m)	STADIA S.I.	STADIA H	STADIA V	HORIZ. DIST. (m)	DIFF. IN ELEV. (m)	ELEVATION I.D. (m)	ELEVATION G.D. (m)	COMMENTS
1	1	1	1.555	515.00	993.00	360	0				1.616 1.504 1.392	0.224			22.400	0.051	51.370	49.866	TBM to TP2
2	1	2	1.555	To obtain this data please obtain permission from the Confederated Tribes of Siletz Indians															
3	1	3	1.555	515.00	993.00	270	0				1.552 1.476 1.400	0.152			15.200	0.079	51.370	49.894	TBM to TP5
4	1	4	1.555	515.00	993.00	360	0				1.520 1.485 1.450	0.070			7.000	0.070	51.370	49.885	TBM to TP1
5	2	1	1.540	515.00	1000.00														TP1 to TBM

1	2	3	4

5 Backsite "Northing" on TBM

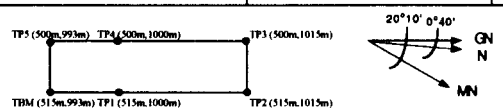

INST: M. Rogers ROD: C. Davidson RECORDER: M. Rogers

PROJECT: Siletz Cemetery DATE: 25 APR 98 PAGE 1 OF 4

	STATION INST	STATION ROD	H.I. (m)	GRID COORD. X (m)	GRID COORD. Y (m)	ANGLES HORIZONTAL (Degrees)	ANGLES HORIZONTAL (Minutes)	ANGLES VERTICAL (Degrees)	ANGLES VERTICAL (Minutes)	ROD READING B.S. + (m)	ROD READING F.S. - (m)	STADIA S.I.	STADIA H	STADIA V	HORIZ. DIST. (m)	DIFF. IN ELEV. (m)	ELEVATION I.D. (m)	ELEVATION G.D. (m)	COMMENTS
1	2	2	1.540	515.00	1000.00	0	0				1.632 1.556 1.480	0.152			15.200	-0.016	51.425	49.869	TP1 to TP2
2	3	1	1.480	515.00	1015.00	180	0												TP2 to TP1 Northing
3	3	2	1.480	515.00	1015.00	180	0				1.592 1.481 1.369	0.223			22.300	-0.001	51.296	49.815	TP2 to TBM
4	3	3	1.480	515.00	1015.00	270	0				1.280	0.000			0.000	0.200	51.296	50.016	TP2 to TP3
5	4	1	1.559	500.00	1015.00														TP3 to TP2 Northing

1	2	3	4

5

INST: C. Davidson ROD: J. Kinoshita RECORDER: M. Rogers

PROJECT: Siletz Cemetery DATE: 25 APR 98 PAGE 2 OF 4

	STATION			GRID COORD.		ANGLES				ROD READING		STADIA			HORIZ.	DIFF. IN	ELEVATION		
	INST.	ROD	H.I. (m)	X (m)	Y (m)	HORIZONTAL (Degrees)	HORIZONTAL (Minutes)	VERTICAL (Degrees)	VERTICAL (Minutes)	B.S. + (m)	F.S. - (m)	S.I.	H	V	DIST. (m)	ELEV. (m)	I.D. (m)	G.D. (m)	COMMENTS
1	4	2	1.559	500.00	1015.00						1.760	0.00			0.00	-0.201	51.575	49.815	TP3 to TBM
2	4	3	1.559	500.00	1015.00	180.00	0.00				1.650	0.00			0.00	-0.091	51.575	49.925	TP3 to TP4
3	5	1	1.248	500.00	1000.00														TP4 to TP3 Northing
4	5	2	1.430	500.00	1000.00	114.00	46.00				1.540	0.00			0.00	-0.110	51.355	49.815	TP4 to TBM
5	5	3	1.430	500.00	1000.00	180.00	0.00				1.579	0.00			0.00	-0.149	51.355	49.776	TP4 to TP5

1	2	3	4
5			

INST: M. Rogers ROD: C. Davidson RECORDER: M. Rogers

PROJECT: Siletz Cemetery DATE: 25 APR 98 PAGE 3 OF 4

	STATION			GRID COORD.		ANGLES				ROD READING		STADIA			HORIZ.	DIFF. IN	ELEVATION		
	INST.	ROD	H.I. (m)	X (m)	Y (m)	HORIZONTAL (Degrees)	HORIZONTAL (Minutes)	VERTICAL (Degrees)	VERTICAL (Minutes)	B.S. + (m)	F.S. - (m)	S.I.	H	V	DIST. (m)	ELEV. (m)	I.D. (m)	G.D. (m)	COMMENTS
1	6	1		500.00	993.00							0.00			0.00	0.000		0.000	TP5 to TP4 Northing
2	6	2		500.00	993.00	90.00	0.00				1.568 1.495 1.419	0.15			14.90	-1.495	51.310	49.815	TP5 to TBM
3																			
4																			
5																			

1 6	2	3	4
5			

INST: J. Kinoshita ROD: C. Davidson RECORDER: M. Rogers/J. Mayer

PROJECT: Siletz Cemetery DATE: 25 APR 98 PAGE 4 OF 4

Appendix C. Topographic Survey Raw Data

X-Grid Coordinate (m)	Y-Grid Coordinate (m)	Center Rod Reading (m)	Elevation (m)	X-Grid Coordinate (m)	Y-Grid Coordinate (m)	Center Rod Reading (m)	Elevation (m)	X-Grid Coordinate (m)	Y-Grid Coordinate (m)	Center Rod Reading (m)	Elevation (m)
500.00	1000.00	1.488	49.956	501.00	1000.00	1.56	49.880	502.00	1000.00	1.60	49.844
500.00	1000.50	1.472	49.972	501.00	1000.50	1.51	49.938	502.00	1000.50	1.54	49.904
500.00	1001.00	1.435	50.009	501.00	1001.00	1.47	49.974	502.00	1001.00	1.51	49.934
500.00	1001.50	1.398	50.046	501.00	1001.50	1.43	50.010	502.00	1001.50	1.47	49.978
500.00	1002.00	1.388	50.056	501.00	1002.00	1.37	50.071	502.00	1002.00	1.48	49.964
500.00	1002.50	1.394	50.050	501.00	1002.50	1.39	50.054	502.00	1002.50	1.47	49.974
500.00	1003.00	1.387	50.057	501.00	1003.00	1.43	50.018	502.00	1003.00	1.44	50.000
500.00	1003.50	1.406	50.038	501.00	1003.50	1.46	49.988	502.00	1003.50	1.46	49.982
500.00	1004.00	1.426	50.018	501.00	1004.00	1.48	49.966	502.00	1004.00	1.47	49.978
500.00	1004.50	1.474	49.970	501.00	1004.50	1.49	49.950	502.00	1004.50	1.49	49.952
500.00	1005.00	1.510	49.934	501.00	1005.00	1.50	49.948	502.00	1005.00	1.51	49.932
500.00	1005.50	1.498	49.946	501.00	1005.50	1.51	49.930	502.00	1005.50	1.45	49.994
500.00	1006.00	1.487	49.957	501.00	1006.00	1.48	49.964	502.00	1006.00	1.49	49.952
500.00	1006.50	1.464	49.980	501.00	1006.50	1.47	49.974	502.00	1006.50	1.50	49.944
500.00	1007.00	1.488	49.956	501.00	1007.00	1.47	49.974	502.00	1007.00	1.49	49.958
500.00	1007.50	1.439	50.005	501.00	1007.50	1.45	49.994	502.00	1007.50	1.51	49.934
500.00	1008.00	1.398	50.046	501.00	1008.00	1.45	49.998	502.00	1008.00	1.53	49.914
500.00	1008.50	1.380	50.064	501.00	1008.50	1.44	50.000	502.00	1008.50	1.53	49.914
500.00	1009.00	1.384	50.060	501.00	1009.00	1.42	50.022	502.00	1009.00	1.51	49.932
500.00	1009.50	1.376	50.068	501.00	1009.50	1.44	50.008	502.00	1009.50	1.50	49.946
500.00	1010.00	1.390	50.054	501.00	1010.00	1.45	49.996	502.00	1010.00	1.48	49.964
500.00	1010.50	1.410	50.034	501.00	1010.50	1.49	49.956	502.00	1010.50	1.47	49.974
500.00	1011.00	1.420	50.024	501.00	1011.00	1.45	49.998	502.00	1011.00	1.48	49.962
500.00	1011.50	1.425	50.019	501.00	1011.50	1.43	50.016	502.00	1011.50	1.44	50.002
500.00	1012.00	1.400	50.044	501.00	1012.00	1.39	50.050	502.00	1012.00	1.42	50.024
500.00	1012.50	1.372	50.072	501.00	1012.50	1.38	50.064	502.00	1012.50	1.40	50.040
500.00	1013.00	1.348	50.096	501.00	1013.00	1.38	50.064	502.00	1013.00	1.39	50.054
500.00	1013.50	1.325	50.119	501.00	1013.50	1.36	50.088	502.00	1013.50	1.38	50.064
500.00	1014.00	1.300	50.144	501.00	1014.00	1.34	50.104	502.00	1014.00	1.40	50.044
500.00	1014.50	1.294	50.150	501.00	1014.50	1.34	50.100	502.00	1014.50	1.39	50.058
500.00	1015.00	1.288	50.156	501.00	1015.00	1.34	50.100	502.00	1015.00	1.37	50.072
500.50	1000.00	1.528	49.916	501.50	1000.00	1.56	49.888	502.50	1000.00	1.58	49.864
500.50	1000.50	1.494	49.950	501.50	1000.50	1.54	49.908	502.50	1000.50	1.55	49.898
500.50	1001.00	1.442	50.002	501.50	1001.00	1.48	49.966	502.50	1001.00	1.54	49.906
500.50	1001.50	1.410	50.034	501.50	1001.50	1.46	49.982	502.50	1001.50	1.51	49.936
500.50	1002.00	1.392	50.052	501.50	1002.00	1.45	49.998	502.50	1002.00	1.50	49.948
500.50	1002.50	1.394	50.050	501.50	1002.50	1.42	50.026	502.50	1002.50	1.47	49.972
500.50	1003.00	1.406	50.038	501.50	1003.00	1.46	49.980	502.50	1003.00	1.47	49.970
500.50	1003.50	1.448	49.996	501.50	1003.50	1.47	49.976	502.50	1003.50	1.45	49.994
500.50	1004.00	1.476	49.968	501.50	1004.00	1.50	49.942	502.50	1004.00	1.48	49.968
500.50	1004.50	1.498	49.946	501.50	1004.50	1.50	49.944	502.50	1004.50	1.49	49.958
500.50	1005.00	1.520	49.924	501.50	1005.00	1.50	49.948	502.50	1005.00	1.47	49.978
500.50	1005.50	1.482	49.962	501.50	1005.50	1.53	49.918	502.50	1005.50	1.51	49.938
500.50	1006.00	1.498	49.946	501.50	1006.00	1.50	49.940	502.50	1006.00	1.50	49.946
500.50	1006.50	1.500	49.944	501.50	1006.50	1.49	49.956	502.50	1006.50	1.49	49.958
500.50	1007.00	1.468	49.976	501.50	1007.00	1.49	49.954	502.50	1007.00	1.49	49.954
500.50	1007.50	1.432	50.012	501.50	1007.50	1.49	49.958	502.50	1007.50	1.51	49.938
500.50	1008.00	1.430	50.014	501.50	1008.00	1.50	49.948	502.50	1008.00	1.54	49.900
500.50	1008.50	1.402	50.042	501.50	1008.50	1.48	49.960	502.50	1008.50	1.53	49.912
500.50	1009.00	1.426	50.018	501.50	1009.00	1.49	49.950	502.50	1009.00	1.50	49.944
500.50	1009.50	1.402	50.042	501.50	1009.50	1.48	49.964	502.50	1009.50	1.48	49.968
500.50	1010.00	1.398	50.046	501.50	1010.00	1.47	49.974	502.50	1010.00	1.47	49.972
500.50	1010.50	1.430	50.014	501.50	1010.50	1.47	49.972	502.50	1010.50	1.49	49.956
500.50	1011.00	1.434	50.010	501.50	1011.00	1.46	49.982	502.50	1011.00	1.46	49.982
500.50	1011.50	1.412	50.032	501.50	1011.50	1.44	50.002	502.50	1011.50	1.42	50.024
500.50	1012.00	1.400	50.044	501.50	1012.00	1.43	50.014	502.50	1012.00	1.40	50.044
500.50	1012.50	1.376	50.068	501.50	1012.50	1.41	50.038	502.50	1012.50	1.40	50.046
500.50	1013.00	1.362	50.082	501.50	1013.00	1.38	50.060	502.50	1013.00	1.38	50.066
500.50	1013.50	1.272	50.172	501.50	1013.50	1.37	50.074	502.50	1013.50	1.39	50.052
500.50	1014.00	1.310	50.134	501.50	1014.00	1.37	50.076	502.50	1014.00	1.40	50.042
500.50	1014.50	1.298	50.146	501.50	1014.50	1.36	50.088	502.50	1014.50	1.40	50.042
500.50	1015.00	1.320	50.124	501.50	1015.00	1.36	50.082	502.50	1015.00	1.38	50.068

X-Grid Coordinate (m)	Y-Grid Coordinate (m)	Center Rod Reading (m)	Elevation (m)	X-Grid Coordinate (m)	Y-Grid Coordinate (m)	Center Rod Reading (m)	Elevation (m)	X-Grid Coordinate (m)	Y-Grid Coordinate (m)	Center Rod Reading (m)	Elevation (m)
503.00	1000.00	1.55	49.894	504.00	1000.00	1.51	49.936	505.00	1000.00	1.46	49.984
503.00	1000.50	1.56	49.884	504.00	1000.50	1.54	49.902	505.00	1000.50	1.55	49.894
503.00	1001.00	1.54	49.900	504.00	1001.00	1.50	49.940	505.00	1001.00	1.50	49.940
503.00	1001.50	1.53	49.914	504.00	1001.50	1.47	49.976	505.00	1001.50	1.47	49.974
503.00	1002.00	1.50	49.942	504.00	1002.00	1.44	50.006	505.00	1002.00	1.45	49.998
503.00	1002.50	1.47	49.978	504.00	1002.50	1.44	50.006	505.00	1002.50	1.42	50.020
503.00	1003.00	1.43	50.012	504.00	1003.00	1.46	49.986	505.00	1003.00	1.43	50.014
503.00	1003.50	1.42	50.020	504.00	1003.50	1.45	49.998	505.00	1003.50	1.44	50.002
503.00	1004.00	1.44	50.006	504.00	1004.00	1.42	50.024	505.00	1004.00	1.43	50.016
503.00	1004.50	1.47	49.972	504.00	1004.50	1.45	49.996	505.00	1004.50	1.44	50.008
503.00	1005.00	1.48	49.960	504.00	1005.00	1.47	49.972	505.00	1005.00	1.48	49.962
503.00	1005.50	1.47	49.976	504.00	1005.50	1.47	49.976	505.00	1005.50	1.47	49.978
503.00	1006.00	1.48	49.960	504.00	1006.00	1.49	49.958	505.00	1006.00	1.50	49.942
503.00	1006.50	1.49	49.958	504.00	1006.50	1.52	49.920	505.00	1006.50	1.55	49.890
503.00	1007.00	1.50	49.944	504.00	1007.00	1.52	49.920	505.00	1007.00	1.58	49.868
503.00	1007.50	1.54	49.908	504.00	1007.50	1.54	49.906	505.00	1007.50	1.61	49.832
503.00	1008.00	1.55	49.896	504.00	1008.00	1.53	49.914	505.00	1008.00	1.57	49.872
503.00	1008.50	1.40	50.042	504.00	1008.50	1.52	49.924	505.00	1008.50	1.56	49.884
503.00	1009.00	1.48	49.960	504.00	1009.00	1.46	49.984	505.00	1009.00	1.55	49.896
503.00	1009.50	1.48	49.964	504.00	1009.50	1.44	50.004	505.00	1009.50	1.50	49.942
503.00	1010.00	1.45	49.990	504.00	1010.00	1.42	50.024	505.00	1010.00	1.46	49.982
503.00	1010.50	1.45	49.998	504.00	1010.50	1.46	49.988	505.00	1010.50	1.46	49.982
503.00	1011.00	1.43	50.014	504.00	1011.00	1.43	50.010	505.00	1011.00	1.45	49.996
503.00	1011.50	1.42	50.028	504.00	1011.50	1.41	50.034	505.00	1011.50	1.45	49.994
503.00	1012.00	1.37	50.072	504.00	1012.00	1.40	50.044	505.00	1012.00	1.47	49.970
503.00	1012.50	1.39	50.058	504.00	1012.50	1.42	50.022	505.00	1012.50	1.46	49.982
503.00	1013.00	1.39	50.056	504.00	1013.00	1.42	50.024	505.00	1013.00	1.47	49.974
503.00	1013.50	1.39	50.050	504.00	1013.50	1.43	50.012	505.00	1013.50	1.47	49.972
503.00	1014.00	1.43	50.016	504.00	1014.00	1.41	50.038	505.00	1014.00	1.45	49.994
503.00	1014.50	1.39	50.054	504.00	1014.50	1.38	50.066	505.00	1014.50	1.42	50.022
503.00	1015.00	1.36	50.086	504.00	1015.00	1.40	50.048	505.00	1015.00	1.47	49.974
503.50	1015.00	1.37	50.070	504.50	1015.00	1.43	50.014	505.50	1015.00	1.46	49.988
503.50	1014.50	1.39	50.052	504.50	1014.50	1.39	50.050	505.50	1014.50	1.47	49.972
503.50	1014.00	1.43	50.018	504.50	1014.00	1.41	50.030	505.50	1014.00	1.48	49.964
503.50	1013.50	1.40	50.042	504.50	1013.50	1.44	50.004	505.50	1013.50	1.53	49.916
503.50	1013.00	1.39	50.056	504.50	1013.00	1.41	50.034	505.50	1013.00	1.50	49.946
503.50	1012.50	1.38	50.064	504.50	1012.50	1.41	50.038	505.50	1012.50	1.46	49.984
503.50	1012.00	1.38	50.068	504.50	1012.00	1.43	50.014	505.50	1012.00	1.49	49.958
503.50	1011.50	1.41	50.034	504.50	1011.50	1.42	50.022	505.50	1011.50	1.44	50.002
503.50	1011.00	1.45	49.998	504.50	1011.00	1.46	49.982	505.50	1011.00	1.46	49.980
503.50	1010.50	1.42	50.028	504.50	1010.50	1.49	49.954	505.50	1010.50	1.44	50.000
503.50	1010.00	1.43	50.012	504.50	1010.00	1.45	49.998	505.50	1010.00	1.49	49.952
503.50	1009.50	1.46	49.980	504.50	1009.50	1.47	49.970	505.50	1009.50	1.54	49.900
503.50	1009.00	1.50	49.946	504.50	1009.00	1.51	49.932	505.50	1009.00	1.57	49.874
503.50	1008.50	1.51	49.936	504.50	1008.50	1.54	49.900	505.50	1008.50	1.57	49.872
503.50	1008.00	1.52	49.924	504.50	1008.00	1.55	49.894	505.50	1008.00	1.56	49.880
503.50	1007.50	1.53	49.918	504.50	1007.50	1.57	49.872	505.50	1007.50	1.60	49.844
503.50	1007.00	1.49	49.950	504.50	1007.00	1.54	49.908	505.50	1007.00	1.54	49.904
503.50	1006.50	1.49	49.954	504.50	1006.50	1.53	49.916	505.50	1006.50	1.53	49.918
503.50	1006.00	1.47	49.978	504.50	1006.00	1.47	49.976	505.50	1006.00	1.51	49.938
503.50	1005.50	1.45	49.990	504.50	1005.50	1.45	49.990	505.50	1005.50	1.46	49.986
503.50	1005.00	1.48	49.960	504.50	1005.00	1.46	49.986	505.50	1005.00	1.44	50.004
503.50	1004.50	1.44	50.006	504.50	1004.50	1.46	49.980	505.50	1004.50	1.42	50.020
503.50	1004.00	1.41	50.032	504.50	1004.00	1.43	50.014	505.50	1004.00	1.40	50.046
503.50	1003.50	1.42	50.022	504.50	1003.50	1.42	50.026	505.50	1003.50	1.41	50.038
503.50	1003.00	1.42	50.020	504.50	1003.00	1.43	50.012	505.50	1003.00	1.44	50.002
503.50	1002.50	1.45	49.994	504.50	1002.50	1.44	50.002	505.50	1002.50	1.46	49.984
503.50	1002.00	1.46	49.982	504.50	1002.00	1.43	50.010	505.50	1002.00	1.48	49.962
503.50	1001.50	1.51	49.934	504.50	1001.50	1.45	49.990	505.50	1001.50	1.46	49.980
503.50	1001.00	1.53	49.918	504.50	1001.00	1.50	49.944	505.50	1001.00	1.47	49.978
503.50	1000.50	1.55	49.896	504.50	1000.50	1.53	49.916	505.50	1000.50	1.49	49.958
503.50	1000.00	1.54	49.908	504.50	1000.00	1.49	49.952	505.50	1000.00	1.49	49.954

X-Grid Coordinate (m)	Y-Grid Coordinate (m)	Center Rod Reading (m)	Elevation (m)	X-Grid Coordinate (m)	Y-Grid Coordinate (m)	Center Rod Reading (m)	Elevation (m)	X-Grid Coordinate (m)	Y-Grid Coordinate (m)	Center Rod Reading (m)	Elevation (m)
506.00	1000.00	1.47	49.976	507.00	1000.00	1.51	49.93	508.00	1000.00	1.54	49.900
506.00	1000.50	1.50	49.946	507.00	1000.50	1.52	49.93	508.00	1000.50	1.53	49.914
506.00	1001.00	1.49	49.958	507.00	1001.00	1.51	49.93	508.00	1001.00	1.54	49.904
506.00	1001.50	1.46	49.980	507.00	1001.50	1.48	49.96	508.00	1001.50	1.50	49.946
506.00	1002.00	1.42	50.026	507.00	1002.00	1.42	50.02	508.00	1002.00	1.43	50.014
506.00	1002.50	1.39	50.054	507.00	1002.50	1.37	50.07	508.00	1002.50	1.38	50.062
506.00	1003.00	1.38	50.068	507.00	1003.00	1.42	50.03	508.00	1003.00	1.38	50.064
506.00	1003.50	1.38	50.062	507.00	1003.50	1.42	50.02	508.00	1003.50	1.41	50.034
506.00	1004.00	1.41	50.038	507.00	1004.00	1.41	50.03	508.00	1004.00	1.42	50.028
506.00	1004.50	1.42	50.026	507.00	1004.50	1.42	50.02	508.00	1004.50	1.44	50.008
506.00	1005.00	1.42	50.024	507.00	1005.00	1.45	49.99	508.00	1005.00	1.49	49.954
506.00	1005.50	1.45	49.990	507.00	1005.50	1.46	49.98	508.00	1005.50	1.52	49.928
506.00	1006.00	1.49	49.956	507.00	1006.00	1.50	49.95	508.00	1006.00	1.49	49.958
506.00	1006.50	1.50	49.940	507.00	1006.50	1.50	49.95	508.00	1006.50	1.50	49.948
506.00	1007.00	1.51	49.938	507.00	1007.00	1.48	49.96	508.00	1007.00	1.53	49.912
506.00	1007.50	1.52	49.922	507.00	1007.50	1.52	49.92	508.00	1007.50	1.58	49.868
506.00	1008.00	1.56	49.886	507.00	1008.00	1.54	49.91	508.00	1008.00	1.53	49.914
506.00	1008.50	1.59	49.852	507.00	1008.50	1.51	49.93	508.00	1008.50	1.54	49.906
506.00	1009.00	1.59	49.850	507.00	1009.00	1.54	49.91	508.00	1009.00	1.61	49.838
506.00	1009.50	1.56	49.884	507.00	1009.50	1.51	49.94	508.00	1009.50	1.59	49.856
506.00	1010.00	1.51	49.936	507.00	1010.00	1.43	50.01	508.00	1010.00	1.61	49.834
506.00	1010.50	1.48	49.962	507.00	1010.50	1.48	49.97	508.00	1010.50	1.52	49.924
506.00	1011.00	1.47	49.978	507.00	1011.00	1.47	49.97	508.00	1011.00	1.51	49.934
506.00	1011.50	1.45	49.994	507.00	1011.50	1.44	50.01	508.00	1011.50	1.52	49.928
506.00	1012.00	1.47	49.970	507.00	1012.00	1.47	49.97	508.00	1012.00	1.51	49.932
506.00	1012.50	1.48	49.964	507.00	1012.50	1.49	49.95	508.00	1012.50	1.46	49.986
506.00	1013.00	1.52	49.924	507.00	1013.00	1.48	49.97	508.00	1013.00	1.43	50.018
506.00	1013.50	1.55	49.898	507.00	1013.50	1.47	49.98	508.00	1013.50	1.45	49.992
506.00	1014.00	1.49	49.956	507.00	1014.00	1.48	49.97	508.00	1014.00	1.45	49.992
506.00	1014.50	1.50	49.948	507.00	1014.50	1.47	49.98	508.00	1014.50	1.42	50.026
506.00	1015.00	1.50	49.946	507.00	1015.00	1.44	50.01	508.00	1015.00	1.39	50.052
506.50	1015.00	1.48	49.960	507.50	1015.00	1.40	50.04	508.50	1015.00	1.40	50.048
506.50	1014.50	1.50	49.948	507.50	1014.50	1.43	50.01	508.50	1014.50	1.42	50.024
506.50	1014.00	1.48	49.960	507.50	1014.00	1.48	49.96	508.50	1014.00	1.45	49.994
506.50	1013.50	1.52	49.924	507.50	1013.50	1.45	50.00	508.50	1013.50	1.46	49.986
506.50	1013.00	1.53	49.918	507.50	1013.00	1.43	50.01	508.50	1013.00	1.43	50.010
506.50	1012.50	1.50	49.944	507.50	1012.50	1.47	49.98	508.50	1012.50	1.45	49.994
506.50	1012.00	1.48	49.964	507.50	1012.00	1.49	49.95	508.50	1012.00	1.54	49.904
506.50	1011.50	1.46	49.986	507.50	1011.50	1.48	49.96	508.50	1011.50	1.56	49.884
506.50	1011.00	1.45	49.994	507.50	1011.00	1.50	49.94	508.50	1011.00	1.53	49.916
506.50	1010.50	1.48	49.960	507.50	1010.50	1.50	49.95	508.50	1010.50	1.53	49.914
506.50	1010.00	1.49	49.950	507.50	1010.00	1.58	49.87	508.50	1010.00	1.63	49.814
506.50	1009.50	1.53	49.912	507.50	1009.50	1.57	49.88	508.50	1009.50	1.61	49.832
506.50	1009.00	1.56	49.884	507.50	1009.00	1.55	49.89	508.50	1009.00	1.64	49.802
506.50	1008.50	1.56	49.884	507.50	1008.50	1.51	49.93	508.50	1008.50	1.57	49.874
506.50	1008.00	1.54	49.908	507.50	1008.00	1.52	49.93	508.50	1008.00	1.53	49.912
506.50	1007.50	1.54	49.908	507.50	1007.50	1.55	49.89	508.50	1007.50	1.54	49.900
506.50	1007.00	1.49	49.950	507.50	1007.00	1.55	49.89	508.50	1007.00	1.51	49.932
506.50	1006.50	1.50	49.948	507.50	1006.50	1.49	49.95	508.50	1006.50	1.48	49.962
506.50	1006.00	1.49	49.958	507.50	1006.00	1.49	49.95	508.50	1006.00	1.49	49.954
506.50	1005.50	1.46	49.988	507.50	1005.50	1.48	49.96	508.50	1005.50	1.51	49.934
506.50	1005.00	1.44	50.006	507.50	1005.00	1.47	49.97	508.50	1005.00	1.48	49.962
506.50	1004.50	1.46	49.986	507.50	1004.50	1.43	50.01	508.50	1004.50	1.46	49.982
506.50	1004.00	1.40	50.040	507.50	1004.00	1.42	50.03	508.50	1004.00	1.45	49.990
506.50	1003.50	1.43	50.016	507.50	1003.50	1.41	50.03	508.50	1003.50	1.44	50.004
506.50	1003.00	1.38	50.060	507.50	1003.00	1.42	50.02	508.50	1003.00	1.40	50.046
506.50	1002.50	1.39	50.052	507.50	1002.50	1.38	50.06	508.50	1002.50	1.41	50.036
506.50	1002.00	1.40	50.040	507.50	1002.00	1.41	50.04	508.50	1002.00	1.46	49.986
506.50	1001.50	1.44	50.004	507.50	1001.50	1.47	49.97	508.50	1001.50	1.53	49.918
506.50	1001.00	1.48	49.966	507.50	1001.00	1.50	49.95	508.50	1001.00	1.56	49.888
506.50	1000.50	1.49	49.952	507.50	1000.50	1.51	49.94	508.50	1000.50	1.56	49.886
506.50	1000.00	1.51	49.938	507.50	1000.00	1.51	49.94	508.50	1000.00	1.59	49.854

X-Grid Coordinate (m)	Y-Grid Coordinate (m)	Center Rod Reading (m)	Elevation (m)	X-Grid Coordinate (m)	Y-Grid Coordinate (m)	Center Rod Reading (m)	Elevation (m)	X-Grid Coordinate (m)	Y-Grid Coordinate (m)	Center Rod Reading (m)	Elevation (m)
509.00	1000.00	1.56	49.880	510.00	1000.00	1.57	49.878	511.00	1000.00	1.55	49.894
509.00	1000.50	1.57	49.874	510.00	1000.50	1.57	49.872	511.00	1000.50	1.55	49.896
509.00	1001.00	1.57	49.878	510.00	1001.00	1.58	49.868	511.00	1001.00	1.59	49.854
509.00	1001.50	1.58	49.868	510.00	1001.50	1.54	49.906	511.00	1001.50	1.57	49.876
509.00	1002.00	1.50	49.944	510.00	1002.00	1.50	49.942	511.00	1002.00	1.59	49.856
509.00	1002.50	1.43	50.016	510.00	1002.50	1.49	49.958	511.00	1002.50	1.57	49.876
509.00	1003.00	1.43	50.018	510.00	1003.00	1.50	49.946	511.00	1003.00	1.54	49.906
509.00	1003.50	1.44	50.006	510.00	1003.50	1.47	49.972	511.00	1003.50	1.55	49.896
509.00	1004.00	1.46	49.980	510.00	1004.00	1.54	49.908	511.00	1004.00	1.54	49.904
509.00	1004.50	1.51	49.934	510.00	1004.50	1.54	49.906	511.00	1004.50	1.56	49.880
509.00	1005.00	1.54	49.908	510.00	1005.00	1.60	49.844	511.00	1005.00	1.60	49.848
509.00	1005.50	1.52	49.926	510.00	1005.50	1.59	49.856	511.00	1005.50	1.60	49.846
509.00	1006.00	1.52	49.924	510.00	1006.00	1.59	49.852	511.00	1006.00	1.62	49.826
509.00	1006.50	1.55	49.894	510.00	1006.50	1.58	49.868	511.00	1006.50	1.63	49.812
509.00	1007.00	1.55	49.890	510.00	1007.00	1.58	49.864	511.00	1007.00	1.61	49.832
509.00	1007.50	1.54	49.906	510.00	1007.50	1.57	49.876	511.00	1007.50	1.62	49.820
509.00	1008.00	1.55	49.890	510.00	1008.00	1.57	49.878	511.00	1008.00	1.61	49.836
509.00	1008.50	1.60	49.846	510.00	1008.50	1.57	49.876	511.00	1008.50	1.61	49.832
509.00	1009.00	1.61	49.834	510.00	1009.00	1.54	49.904	511.00	1009.00	1.60	49.846
509.00	1009.50	1.65	49.790	510.00	1009.50	1.54	49.906	511.00	1009.50	1.61	49.832
509.00	1010.00	1.61	49.834	510.00	1010.00	1.51	49.934	511.00	1010.00	1.58	49.864
509.00	1010.50	1.51	49.938	510.00	1010.50	1.48	49.966	511.00	1010.50	1.52	49.926
509.00	1011.00	1.49	49.952	510.00	1011.00	1.47	49.970	511.00	1011.00	1.47	49.972
509.00	1011.50	1.57	49.876	510.00	1011.50	1.47	49.976	511.00	1011.50	1.49	49.954
509.00	1012.00	1.51	49.930	510.00	1012.00	1.48	49.966	511.00	1012.00	1.51	49.930
509.00	1012.50	1.45	49.996	510.00	1012.50	1.46	49.988	511.00	1012.50	1.55	49.896
509.00	1013.00	1.43	50.012	510.00	1013.00	1.49	49.956	511.00	1013.00	1.47	49.974
509.00	1013.50	1.46	49.982	510.00	1013.50	1.47	49.972	511.00	1013.50	1.43	50.012
509.00	1014.00	1.45	49.994	510.00	1014.00	1.46	49.988	511.00	1014.00	1.44	50.008
509.00	1014.50	1.42	50.026	510.00	1014.50	1.44	50.008	511.00	1014.50	1.41	50.032
509.00	1015.00	1.38	50.066	510.00	1015.00	1.37	50.076	511.00	1015.00	1.36	50.082
509.50	1015.00	1.38	50.068	510.50	1015.00	1.37	50.076	511.50	1015.00	1.35	50.094
509.50	1014.50	1.44	50.002	510.50	1014.50	1.41	50.030	511.50	1014.50	1.40	50.042
509.50	1014.00	1.46	49.984	510.50	1014.00	1.43	50.014	511.50	1014.00	1.39	50.056
509.50	1013.50	1.48	49.966	510.50	1013.50	1.45	49.996	511.50	1013.50	1.42	50.026
509.50	1013.00	1.47	49.976	510.50	1013.00	1.47	49.972	511.50	1013.00	1.45	49.992
509.50	1012.50	1.44	50.006	510.50	1012.50	1.48	49.966	511.50	1012.50	1.52	49.926
509.50	1012.00	1.48	49.960	510.50	1012.00	1.49	49.956	511.50	1012.00	1.50	49.940
509.50	1011.50	1.53	49.914	510.50	1011.50	1.47	49.978	511.50	1011.50	1.49	49.952
509.50	1011.00	1.49	49.956	510.50	1011.00	1.47	49.972	511.50	1011.00	1.52	49.924
509.50	1010.50	1.49	49.958	510.50	1010.50	1.48	49.962	511.50	1010.50	1.61	49.832
509.50	1010.00	1.60	49.842	510.50	1010.00	1.51	49.934	511.50	1010.00	1.64	49.800
509.50	1009.50	1.63	49.816	510.50	1009.50	1.53	49.912	511.50	1009.50	1.65	49.794
509.50	1009.00	1.58	49.868	510.50	1009.00	1.55	49.898	511.50	1009.00	1.64	49.804
509.50	1008.50	1.59	49.858	510.50	1008.50	1.57	49.876	511.50	1008.50	1.65	49.790
509.50	1008.00	1.57	49.872	510.50	1008.00	1.59	49.850	511.50	1008.00	1.65	49.794
509.50	1007.50	1.57	49.876	510.50	1007.50	1.60	49.842	511.50	1007.50	1.64	49.802
509.50	1007.00	1.55	49.890	510.50	1007.00	1.58	49.868	511.50	1007.00	1.64	49.806
509.50	1006.50	1.54	49.906	510.50	1006.50	1.59	49.852	511.50	1006.50	1.61	49.838
509.50	1006.00	1.52	49.920	510.50	1006.00	1.60	49.840	511.50	1006.00	1.59	49.852
509.50	1005.50	1.55	49.898	510.50	1005.50	1.60	49.840	511.50	1005.50	1.57	49.878
509.50	1005.00	1.56	49.884	510.50	1005.00	1.57	49.876	511.50	1005.00	1.58	49.864
509.50	1004.50	1.54	49.908	510.50	1004.50	1.55	49.892	511.50	1004.50	1.60	49.846
509.50	1004.00	1.48	49.960	510.50	1004.00	1.53	49.918	511.50	1004.00	1.56	49.880
509.50	1003.50	1.49	49.954	510.50	1003.50	1.49	49.950	511.50	1003.50	1.53	49.914
509.50	1003.00	1.47	49.978	510.50	1003.00	1.48	49.962	511.50	1003.00	1.54	49.904
509.50	1002.50	1.47	49.978	510.50	1002.50	1.53	49.914	511.50	1002.50	1.57	49.872
509.50	1002.00	1.54	49.904	510.50	1002.00	1.54	49.908	511.50	1002.00	1.63	49.816
509.50	1001.50	1.57	49.872	510.50	1001.50	1.55	49.890	511.50	1001.50	1.60	49.846
509.50	1001.00	1.56	49.880	510.50	1001.00	1.57	49.874	511.50	1001.00	1.63	49.810
509.50	1000.50	1.58	49.862	510.50	1000.50	1.57	49.876	511.50	1000.50	1.58	49.860
509.50	1000.00	1.57	49.874	510.50	1000.00	1.55	49.890	511.50	1000.00	1.58	49.868

X-Grid Coordinate (m)	Y-Grid Coordinate (m)	Center Rod Reading (m)	Elevation (m)	X-Grid Coordinate (m)	Y-Grid Coordinate (m)	Center Rod Reading (m)	Elevation (m)	X-Grid Coordinate (m)	Y-Grid Coordinate (m)	Center Rod Reading (m)	Elevation (m)
512.00	1000.00	1.61	49.834	513.00	1000.00	1.66	49.786	514.00	1000.00	1.60	49.844
512.00	1000.50	1.64	49.806	513.00	1000.50	1.63	49.810	514.00	1000.50	1.59	49.856
512.00	1001.00	1.63	49.814	513.00	1001.00	1.64	49.806	514.00	1001.00	1.64	49.802
512.00	1001.50	1.63	49.814	513.00	1001.50	1.65	49.790	514.00	1001.50	1.62	49.824
512.00	1002.00	1.63	49.814	513.00	1002.00	1.64	49.806	514.00	1002.00	1.61	49.832
512.00	1002.50	1.59	49.858	513.00	1002.50	1.63	49.810	514.00	1002.50	1.63	49.818
512.00	1003.00	1.58	49.866	513.00	1003.00	1.58	49.862	514.00	1003.00	1.62	49.824
512.00	1003.50	1.55	49.896	513.00	1003.50	1.58	49.866	514.00	1003.50	1.57	49.874
512.00	1004.00	1.54	49.908	513.00	1004.00	1.54	49.908	514.00	1004.00	1.55	49.896
512.00	1004.50	1.54	49.904	513.00	1004.50	1.52	49.926	514.00	1004.50	1.53	49.910
512.00	1005.00	1.54	49.908	513.00	1005.00	1.54	49.904	514.00	1005.00	1.49	49.956
512.00	1005.50	1.54	49.908	513.00	1005.50	1.50	49.948	514.00	1005.50	1.45	49.992
512.00	1006.00	1.55	49.892	513.00	1006.00	1.52	49.920	514.00	1006.00	1.46	49.986
512.00	1006.50	1.58	49.860	513.00	1006.50	1.54	49.906	514.00	1006.50	1.49	49.950
512.00	1007.00	1.63	49.814	513.00	1007.00	1.59	49.852	514.00	1007.00	1.55	49.894
512.00	1007.50	1.70	49.748	513.00	1007.50	1.64	49.802	514.00	1007.50	1.61	49.832
512.00	1008.00	1.68	49.766	513.00	1008.00	1.67	49.776	514.00	1008.00	1.61	49.830
512.00	1008.50	1.66	49.782	513.00	1008.50	1.66	49.786	514.00	1008.50	1.64	49.802
512.00	1009.00	1.69	49.758	513.00	1009.00	1.68	49.764	514.00	1009.00	1.65	49.790
512.00	1009.50	1.67	49.776	513.00	1009.50	1.69	49.754	514.00	1009.50	1.64	49.800
512.00	1010.00	1.66	49.784	513.00	1010.00	1.63	49.812	514.00	1010.00	1.60	49.840
512.00	1010.50	1.61	49.832	513.00	1010.50	1.61	49.832	514.00	1010.50	1.58	49.866
512.00	1011.00	1.56	49.886	513.00	1011.00	1.57	49.876	514.00	1011.00	1.53	49.912
512.00	1011.50	1.52	49.928	513.00	1011.50	1.55	49.896	514.00	1011.50	1.55	49.896
512.00	1012.00	1.50	49.948	513.00	1012.00	1.53	49.918	514.00	1012.00	1.51	49.930
512.00	1012.50	1.49	49.954	513.00	1012.50	1.52	49.926	514.00	1012.50	1.49	49.954
512.00	1013.00	1.43	50.012	513.00	1013.00	1.45	49.992	514.00	1013.00	1.48	49.962
512.00	1013.50	1.39	50.058	513.00	1013.50	1.42	50.022	514.00	1013.50	1.49	49.958
512.00	1014.00	1.36	50.086	513.00	1014.00	1.40	50.046	514.00	1014.00	1.46	49.986
512.00	1014.50	1.37	50.070	513.00	1014.50	1.40	50.044	514.00	1014.50	1.47	49.972
512.00	1015.00	1.36	50.086	513.00	1015.00	1.43	50.018	514.00	1015.00	1.50	49.948
512.50	1015.00	1.36	50.084	513.50	1015.00	1.48	49.962	514.50	1015.00	1.55	49.898
512.50	1014.50	1.37	50.070	513.50	1014.50	1.43	50.016	514.50	1014.50	1.52	49.924
512.50	1014.00	1.37	50.074	513.50	1014.00	1.42	50.024	514.50	1014.00	1.52	49.928
512.50	1013.50	1.38	50.062	513.50	1013.50	1.45	49.996	514.50	1013.50	1.51	49.932
512.50	1013.00	1.46	49.982	513.50	1013.00	1.48	49.962	514.50	1013.00	1.52	49.926
512.50	1012.50	1.50	49.944	513.50	1012.50	1.51	49.936	514.50	1012.50	1.50	49.948
512.50	1012.00	1.50	49.942	513.50	1012.00	1.53	49.914	514.50	1012.00	1.52	49.924
512.50	1011.50	1.53	49.910	513.50	1011.50	1.53	49.912	514.50	1011.50	1.52	49.924
512.50	1011.00	1.56	49.884	513.50	1011.00	1.54	49.902	514.50	1011.00	1.55	49.898
512.50	1010.50	1.63	49.816	513.50	1010.50	1.57	49.870	514.50	1010.50	1.59	49.852
512.50	1010.00	1.65	49.792	513.50	1010.00	1.63	49.818	514.50	1010.00	1.60	49.840
512.50	1009.50	1.69	49.754	513.50	1009.50	1.65	49.792	514.50	1009.50	1.62	49.826
512.50	1009.00	1.70	49.744	513.50	1009.00	1.66	49.788	514.50	1009.00	1.62	49.826
512.50	1008.50	1.67	49.772	513.50	1008.50	1.67	49.778	514.50	1008.50	1.61	49.832
512.50	1008.00	1.67	49.774	513.50	1008.00	1.60	49.840	514.50	1008.00	1.60	49.842
512.50	1007.50	1.64	49.804	513.50	1007.50	1.58	49.862	514.50	1007.50	1.58	49.866
512.50	1007.00	1.61	49.836	513.50	1007.00	1.58	49.866	514.50	1007.00	1.53	49.912
512.50	1006.50	1.56	49.880	513.50	1006.50	1.52	49.922	514.50	1006.50	1.51	49.932
512.50	1006.00	1.55	49.894	513.50	1006.00	1.48	49.962	514.50	1006.00	1.48	49.962
512.50	1005.50	1.52	49.926	513.50	1005.50	1.46	49.986	514.50	1005.50	1.46	49.986
512.50	1005.00	1.54	49.906	513.50	1005.00	1.50	49.948	514.50	1005.00	1.49	49.950
512.50	1004.50	1.53	49.912	513.50	1004.50	1.54	49.902	514.50	1004.50	1.53	49.914
512.50	1004.00	1.51	49.934	513.50	1004.00	1.54	49.906	514.50	1004.00	1.54	49.904
512.50	1003.50	1.53	49.914	513.50	1003.50	1.56	49.882	514.50	1003.50	1.58	49.866
512.50	1003.00	1.60	49.848	513.50	1003.00	1.64	49.808	514.50	1003.00	1.60	49.842
512.50	1002.50	1.61	49.830	513.50	1002.50	1.65	49.796	514.50	1002.50	1.63	49.812
512.50	1002.00	1.62	49.820	513.50	1002.00	1.62	49.824	514.50	1002.00	1.61	49.838
512.50	1001.50	1.63	49.818	513.50	1001.50	1.65	49.790	514.50	1001.50	1.60	49.844
512.50	1001.00	1.65	49.798	513.50	1001.00	1.66	49.786	514.50	1001.00	1.61	49.830
512.50	1000.50	1.63	49.814	513.50	1000.50	1.61	49.832	514.50	1000.50	1.60	49.848
512.50	1000.00	1.63	49.810	513.50	1000.00	1.61	49.836	514.50	1000.00	1.56	49.884

X-Grid Coordinate (m)	Y-Grid Coordinate (m)	Center Rod Reading (m)	Elevation (m)
515.00	1000.00	1.55	49.892
515.00	1000.50	1.56	49.884
515.00	1001.00	1.56	49.882
515.00	1001.50	1.57	49.878
515.00	1002.00	1.58	49.862
515.00	1002.50	1.58	49.866
515.00	1003.00	1.59	49.854
515.00	1003.50	1.56	49.886
515.00	1004.00	1.53	49.910
515.00	1004.50	1.50	49.942
515.00	1005.00	1.51	49.932
515.00	1005.50	1.52	49.922
515.00	1006.00	1.50	49.948
515.00	1006.50	1.51	49.938
515.00	1007.00	1.51	49.934
515.00	1007.50	1.52	49.920
515.00	1008.00	1.55	49.894
515.00	1008.50	1.57	49.872
515.00	1009.00	1.58	49.862
515.00	1009.50	1.61	49.832
515.00	1010.00	1.61	49.836
515.00	1010.50	1.60	49.840
515.00	1011.00	1.59	49.858
515.00	1011.50	1.59	49.854
515.00	1012.00	1.58	49.862
515.00	1012.50	1.56	49.884
515.00	1013.00	1.57	49.874
515.00	1013.50	1.54	49.908
515.00	1014.00	1.55	49.892
515.00	1014.50	1.57	49.872
515.00	1015.00	1.57	49.874

Appendix D. Example of Cesium Gradiometer Survey Raw Data

Local X-Grid Position (m)	Local Y-Grid Position (m)	Top Magnetometer Magnitude (nT)	Bottom Magnetometer Magnitude (nT)	Vertical Gradient (0.5m/nT)	Line	Clock	JulianDate
500.00	1000.00	53424.30	53419.94	8.719	0.00	12.00	84.00
500.00	1000.03	53424.41	53420.11	8.602	0.00	12.00	84.00
500.00	1000.05	53424.61	53420.28	8.656	0.00	12.00	84.00
500.00	1000.08	53424.48	53420.30	8.344	0.00	12.00	84.00
500.00	1000.11	53424.57	53420.50	8.148	0.00	12.00	84.00
500.00	1000.13	53424.54	53420.72	7.641	0.00	12.00	84.00
500.00	1000.16	53424.58	53420.92	7.312	0.00	12.00	84.00
500.00	1000.18	53424.61	53421.00	7.211	0.00	12.00	84.00
500.00	1000.21	53424.68	53421.15	7.062	0.00	12.00	84.00
500.00	1000.24	53424.71	53421.21	7.000	0.00	12.00	84.00
500.00	1000.26	53424.59	53421.27	6.656	0.00	12.00	84.00
500.00	1000.29	53424.64	53421.50	6.289	0.00	12.00	84.00
500.00	1000.32	53424.72	53421.79	5.867	0.00	12.00	84.00
500.00	1000.34	53424.74	53421.95	5.578	0.00	12.00	84.00
500.00	1000.37	53424.87	53422.39	4.961	0.00	12.00	84.00
500.00	1000.39	53424.95	53422.73	4.422	0.00	12.00	84.00
500.00	1000.42	53424.91	53423.04	3.742	0.00	12.00	84.00
500.00	1000.45	53424.87	53423.37	3.000	0.00	12.00	84.00
500.00	1000.47	53424.85	53423.60	2.508	0.00	12.00	84.00
500.00	1000.50	53424.86	53423.76	2.195	0.00	12.00	84.00
500.00	1000.53	53424.86	53424.04	1.648	0.00	12.00	84.00
500.00	1000.55	53425.04	53424.55	0.969	0.00	12.00	84.00
500.00	1000.58	53425.11	53424.93	0.359	0.00	12.00	84.00
500.00	1000.61	53424.96	53425.29	-0.648	0.00	12.00	84.00
500.00	1000.63	53424.96	53425.64	-1.352	0.00	12.00	84.00
500.00	1000.66	53424.89	53425.93	-2.086	0.00	12.00	84.00
500.00	1000.68	53424.97	53426.24	-2.531	0.00	12.00	84.00
500.00	1000.71	53424.87	53426.52	-3.297	0.00	12.00	84.00
500.00	1000.74	53425.12	53426.87	-3.508	0.00	12.00	84.00
500.00	1000.76	53424.80	53426.61	-3.617	0.00	12.00	84.00
500.00	1000.79	53424.76	53426.68	-3.828	0.00	12.00	84.00
500.00	1000.82	53424.82	53426.65	-3.664	0.00	12.00	84.00
500.00	1000.84	53424.86	53426.72	-3.711	0.00	12.00	84.00
500.00	1000.87	53424.69	53426.77	-4.172	0.00	12.00	84.00
500.00	1000.89	53424.63	53426.77	-4.281	0.00	12.00	84.00
500.00	1000.92	53424.81	53427.10	-4.570	0.00	12.00	84.00
500.00	1000.95	53424.57	53426.75	-4.367	0.00	12.00	84.00
500.00	1000.97	53424.68	53426.88	-4.406	0.00	12.00	84.00
500.00	1001.00	53424.61	53426.82	-4.430	0.00	12.00	84.00
500.00	1001.02	53424.55	53426.92	-4.727	0.00	12.00	84.00
500.00	1001.05	53424.40	53426.73	-4.664	0.00	12.00	84.00
500.00	1001.07	53424.46	53426.72	-4.523	0.00	12.00	84.00
500.00	1001.10	53424.40	53426.55	-4.289	0.00	12.00	84.00
500.00	1001.12	53424.13	53426.25	-4.227	0.00	12.00	84.00
500.00	1001.15	53423.91	53425.95	-4.070	0.00	12.00	84.00

Appendix E. GSSI's 500D settings

Antenna type	$500MHz$
Data collection mode	Continuous
Range	$100ns$
Samples per scan	512
Resolution	8 bits
Number of gain points	5
Vertical high pass filter	$62.5MHz$
Vertical low pass filter	$1000MHz$
Scans per second	32
Horizontal smoothing	4 scans
Transmit rate	$64KHz$
Depth of viewing window	Approximately $5m$
	(assuming a dielectric constant of 9)

Appendix F. Ground Penetrating Radar Raw Profiles

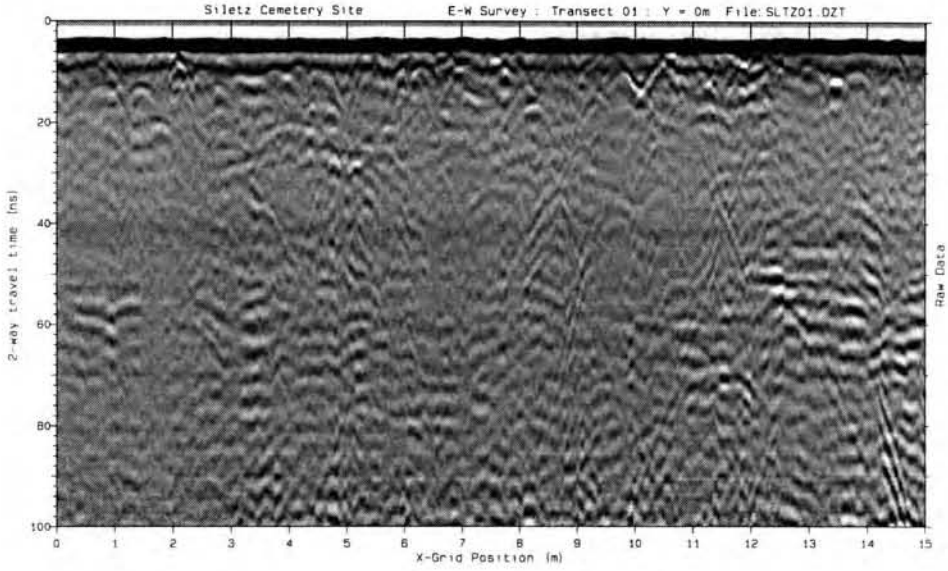

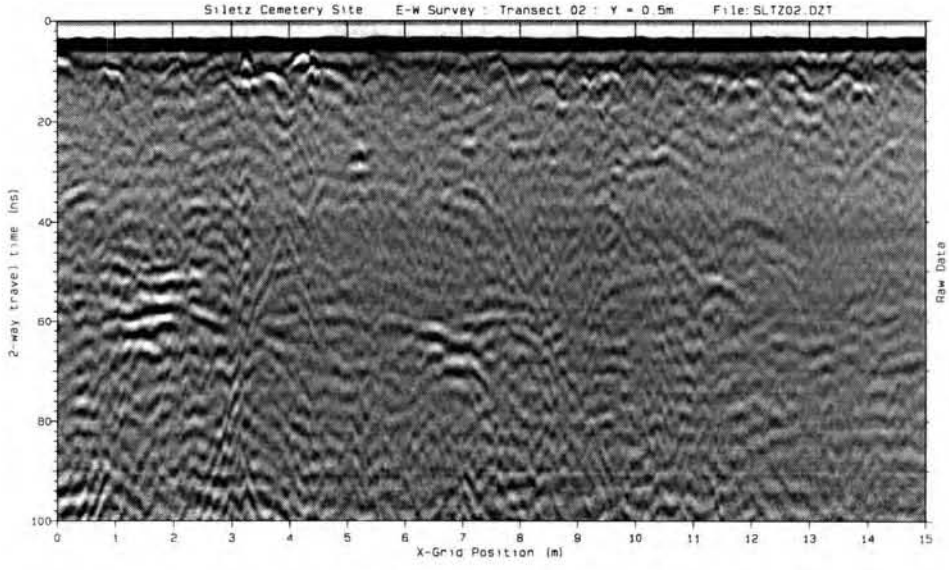

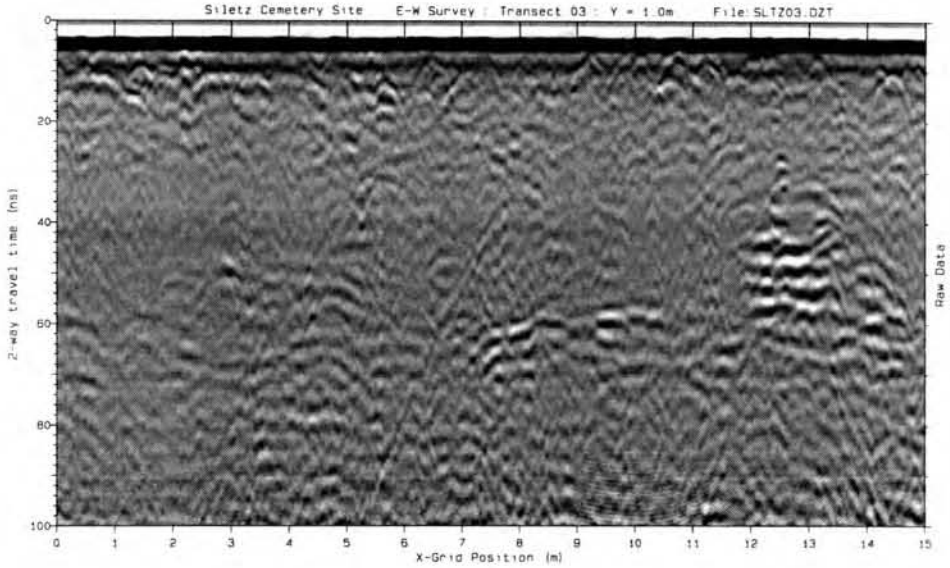
Siletz Cemetery Site E-W Survey : Transect 03 : Y = 1.0m File: SLTZ03.DZT
2-way travel time (ns)
X-Grid Position (m)
Raw Data

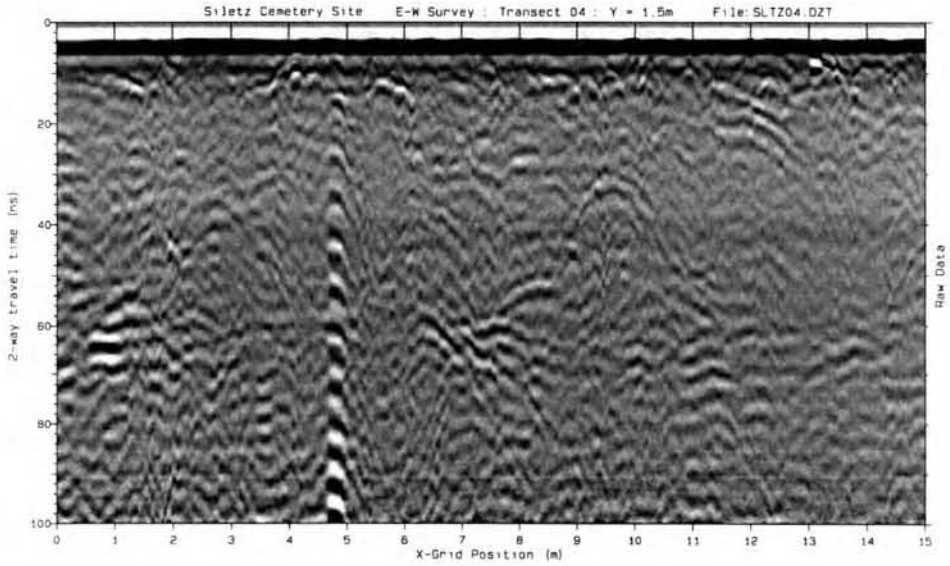
Siletz Cemetery Site E-W Survey : Transect 04 : Y = 1.5m File: SLTZ04.DZT
2-way travel time (ns)
X-Grid Position (m)
Raw Data

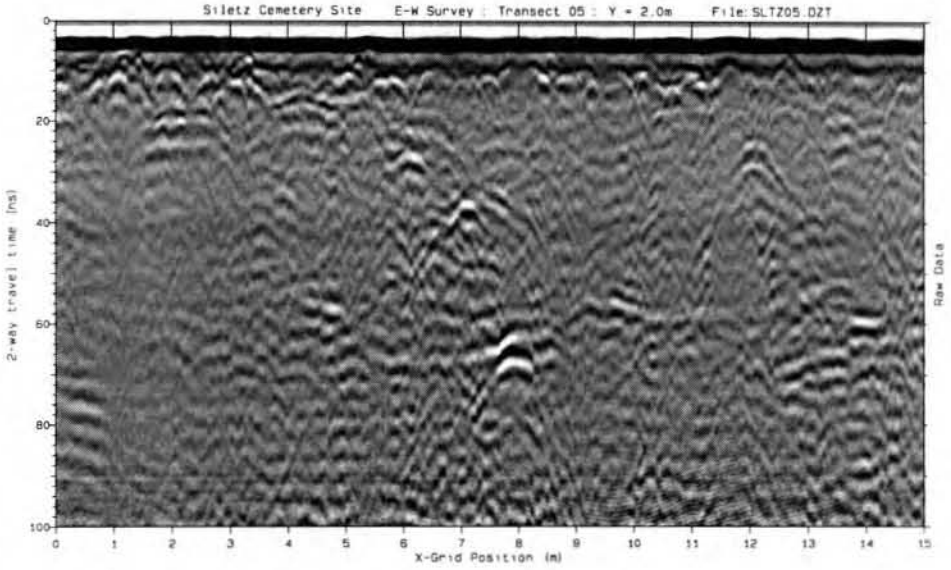
Siletz Cemetery Site E-W Survey : Transect 05 : Y = 2.0m File: SLTZ05.DZT
2-way travel time (ns)
X-Grid Position (m)
Raw Data

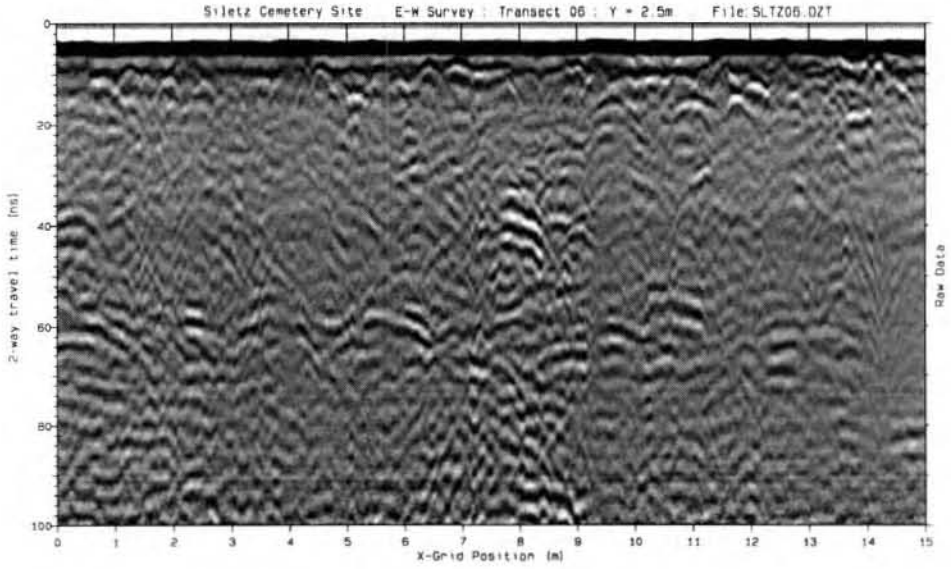
Siletz Cemetery Site E-W Survey : Transect 06 : Y = 2.5m File: SLTZ06.DZT
2-way travel time (ns)
X-Grid Position (m)
Raw Data

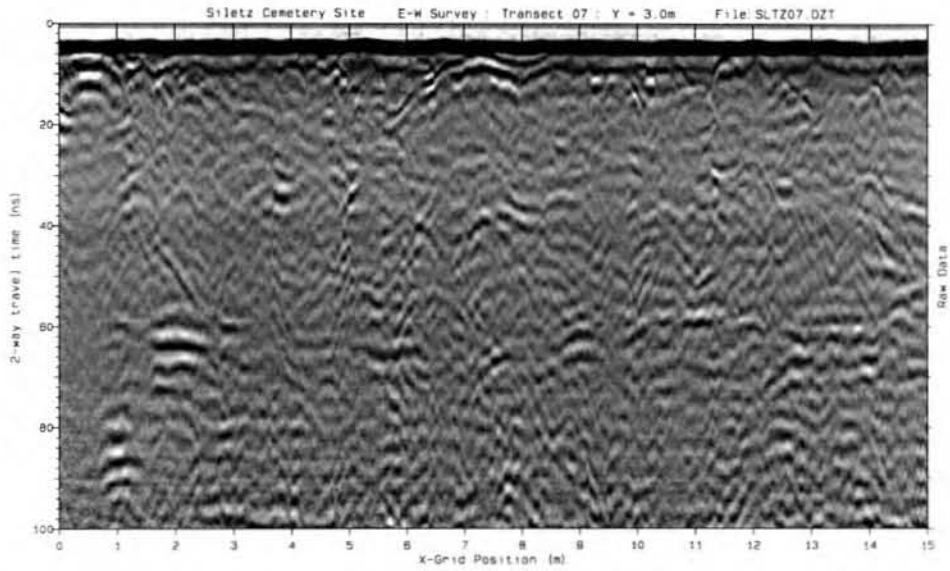
Siletz Cemetery Site E-W Survey : Transect 07 : Y = 3.0m File: SLTZ07.DZT
2-way travel time (ns)
X-Grid Position (m)
Raw Data

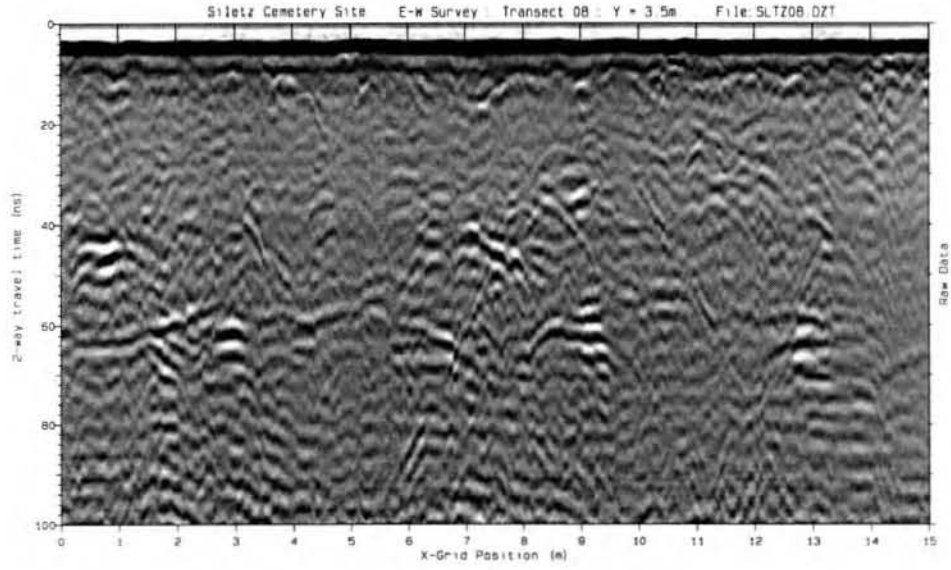
Siletz Cemetery Site E-W Survey : Transect 08 : Y = 3.5m File: SLTZ08.DZT
2-way travel time (ns)
X-Grid Position (m)
Raw Data

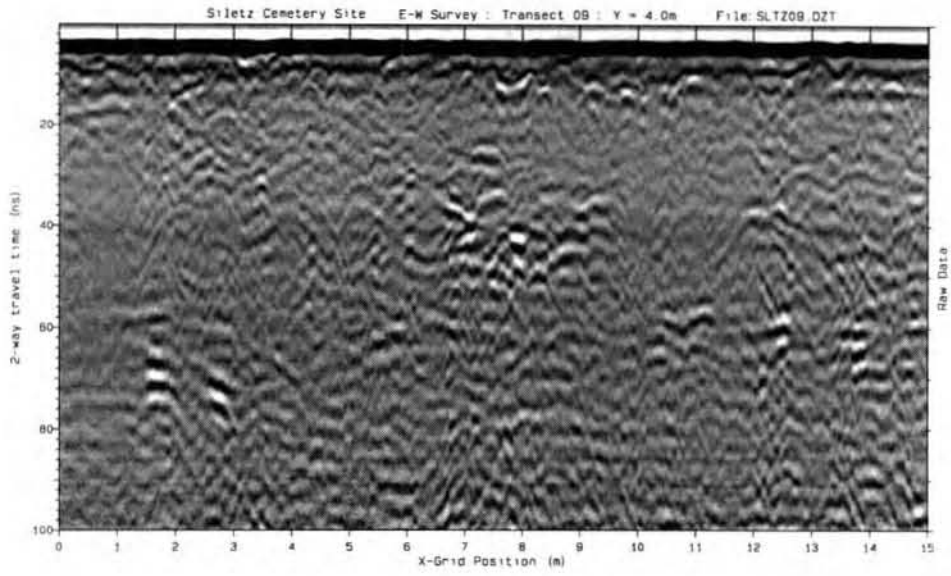
Siletz Cemetery Site E-W Survey : Transect 09 : Y = 4.0m File: SLTZ09.DZT
2-way travel time (ns)
X-Grid Position (m)
Raw Data

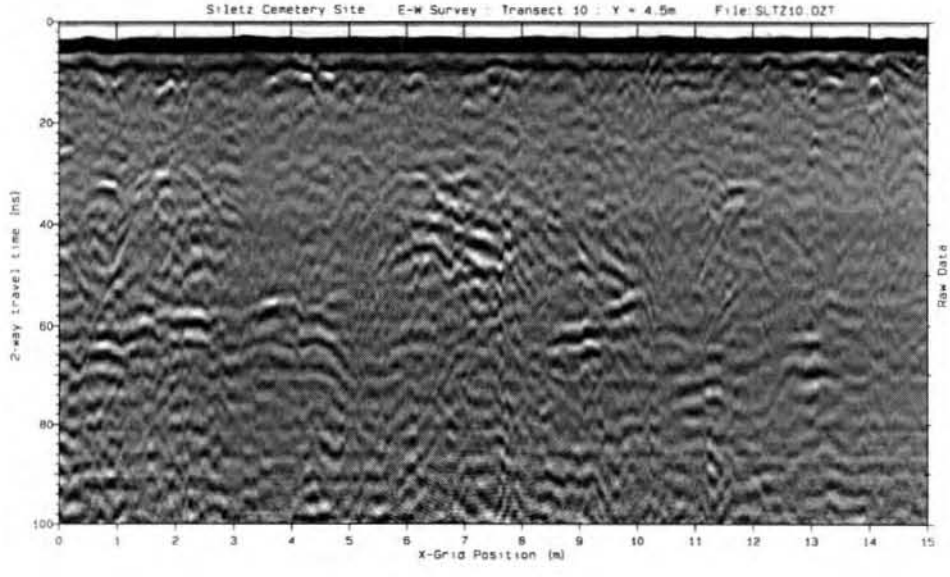
Siletz Cemetery Site E-W Survey : Transect 10 : Y = 4.5m File: SLTZ10.DZT
2-way travel time (ns)
X-Grid Position (m)
Raw Data

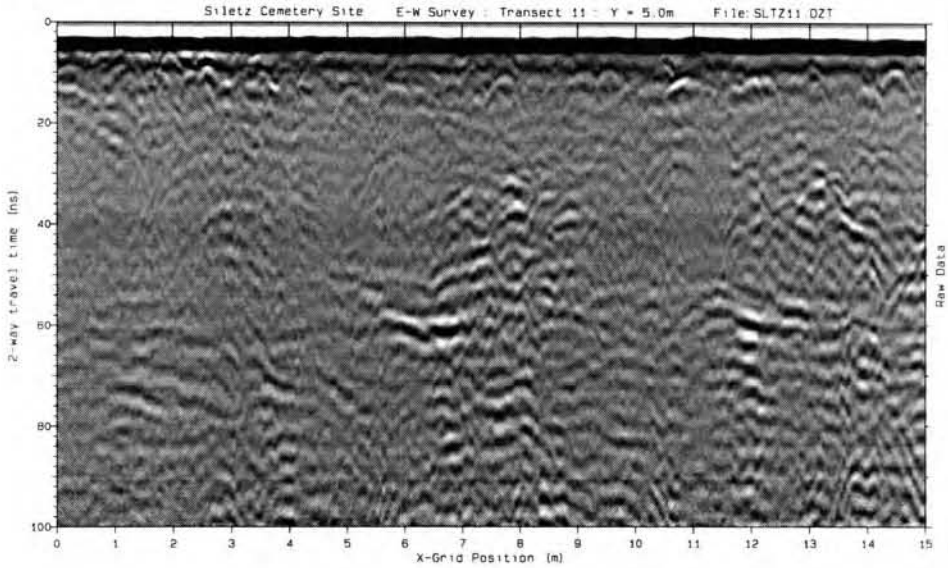
Siletz Cemetery Site E-W Survey : Transect 11 : Y = 5.0m File: SLTZ11.DZT
2-way travel time (ns)
X-Grid Position (m)
Raw Data

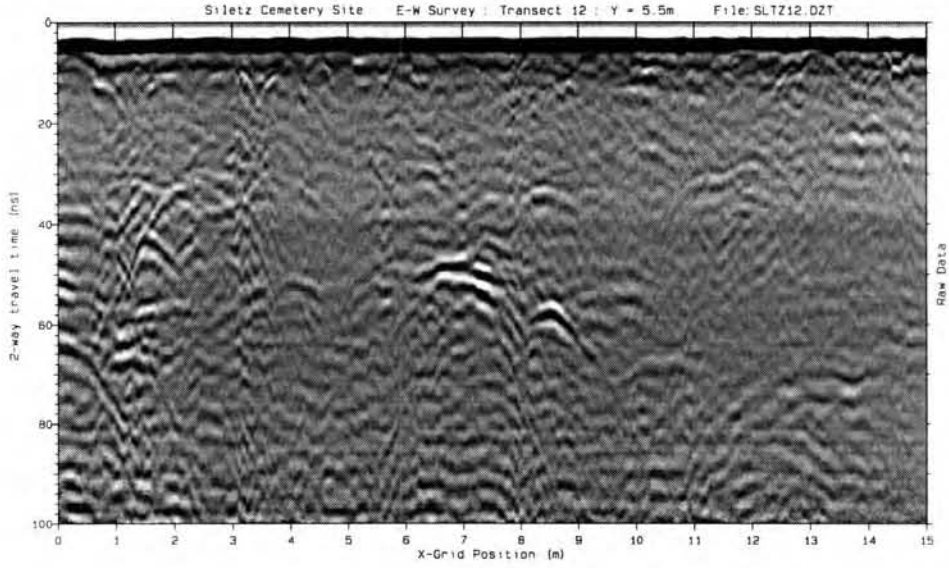
Siletz Cemetery Site E-W Survey : Transect 12 : Y = 5.5m File: SLTZ12.DZT
2-way travel time (ns)
X-Grid Position (m)
Raw Data

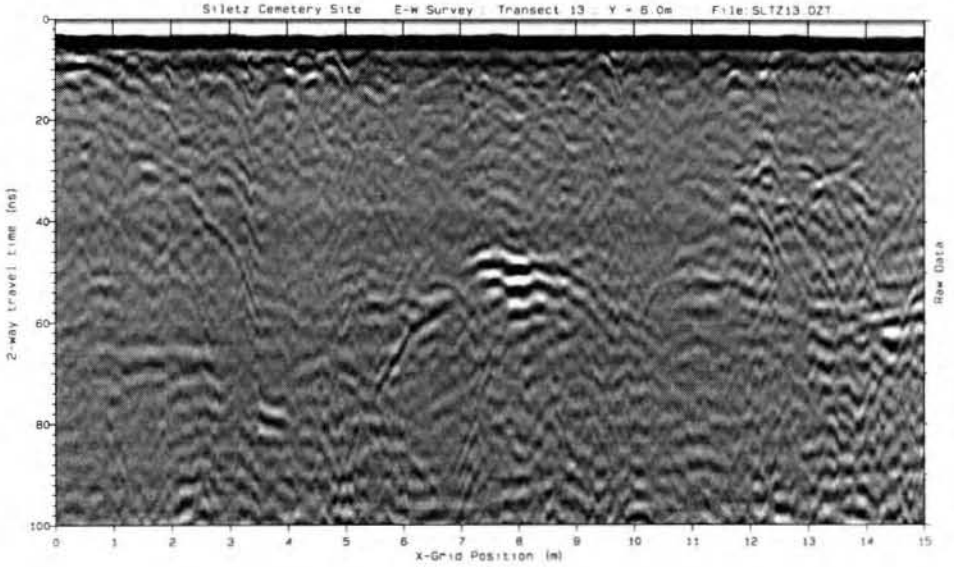
Siletz Cemetery Site E-W Survey : Transect 13 : Y = 6.0m File: SLTZ13.DZT
2-way travel time (ns)
X-Grid Position (m)
Raw Data

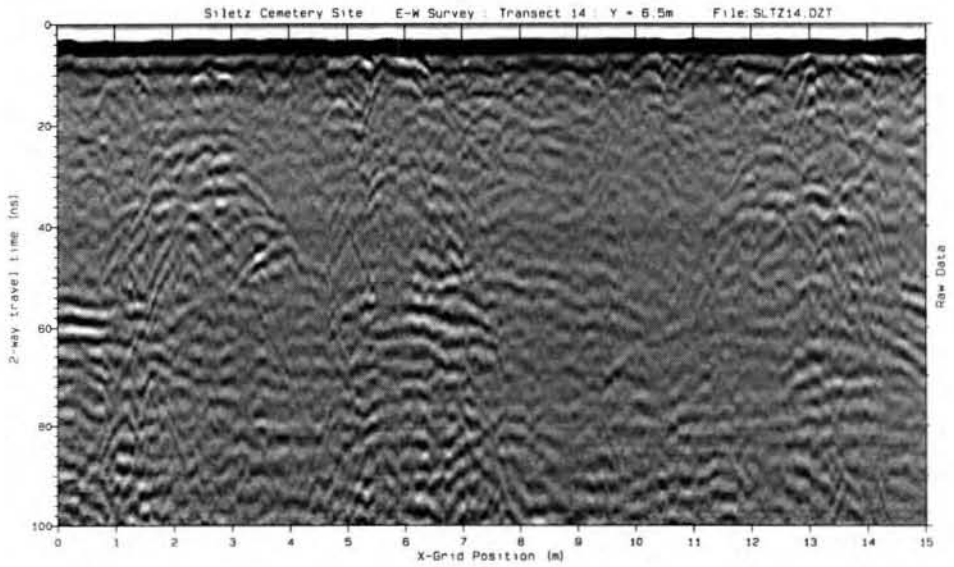
Siletz Cemetery Site E-W Survey : Transect 14 : Y = 6.5m File: SLTZ14.DZT
2-way travel time (ns)
X-Grid Position (m)
Raw Data

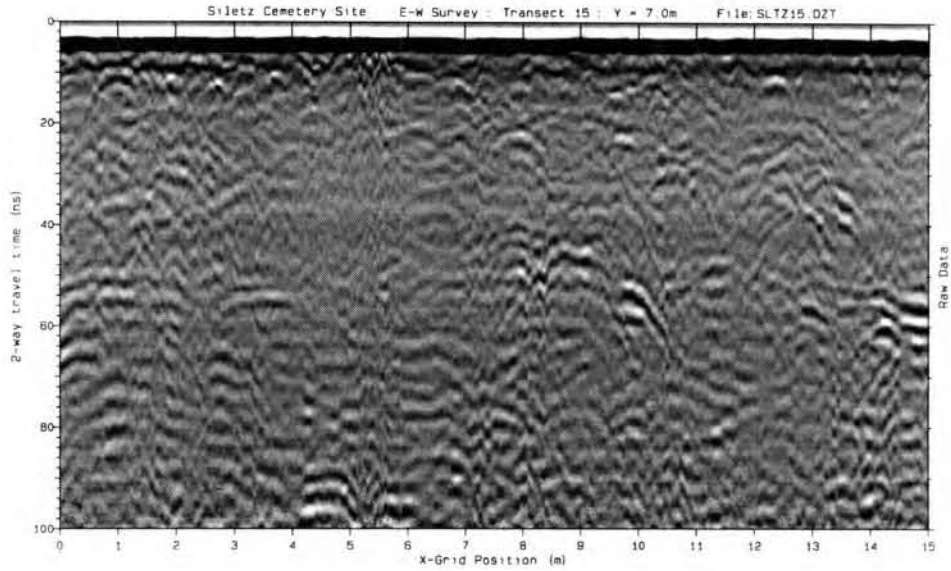
Siletz Cemetery Site E-W Survey : Transect 15 : Y = 7.0m File: SLTZ15.DZT
2-way travel time (ns)
X-Grid Position (m)
Raw Data

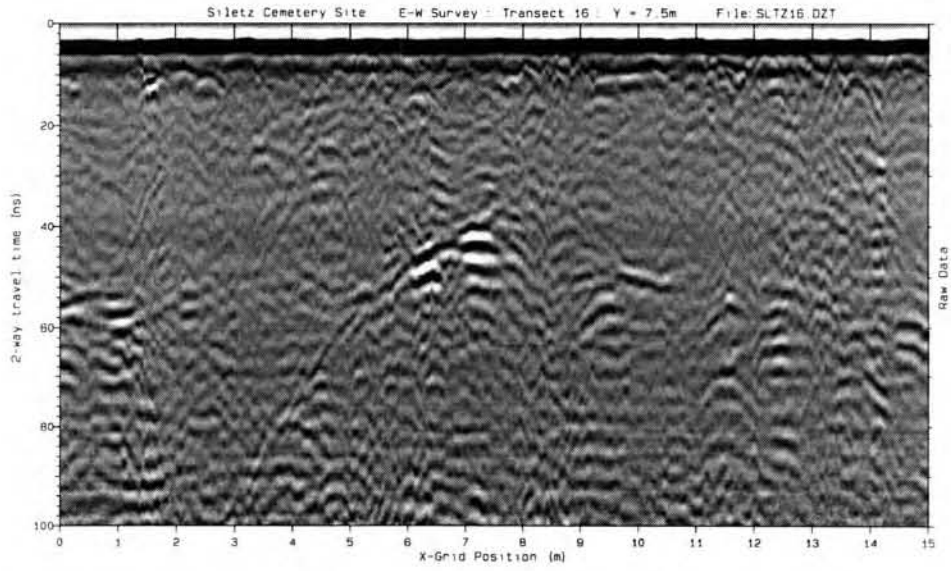
Siletz Cemetery Site E-W Survey : Transect 16 : Y = 7.5m File: SLTZ16.DZT
2-way travel time (ns)
X-Grid Position (m)
Raw Data

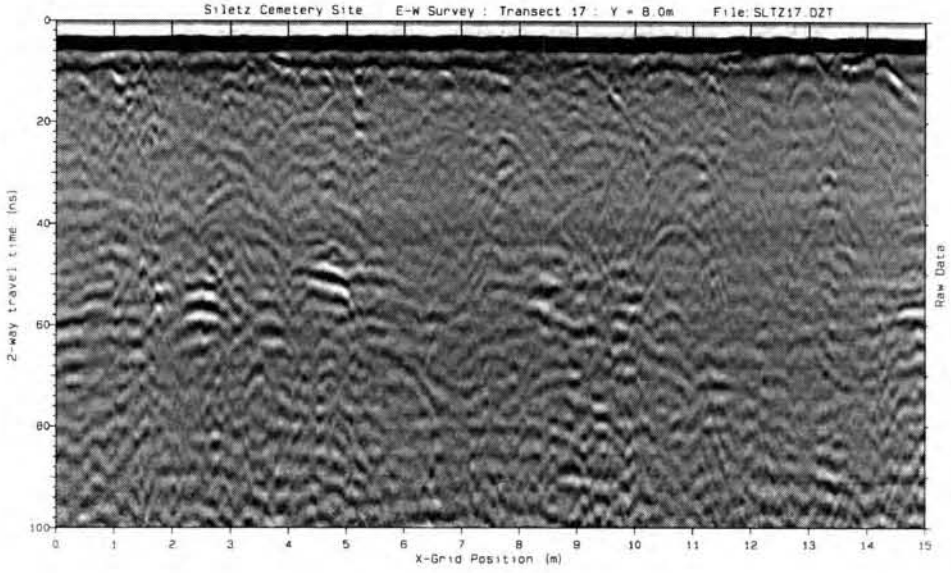
Siletz Cemetery Site E-W Survey : Transect 17 : Y = 8.0m File: SLTZ17.DZT
2-way travel time (ns)
X-Grid Position (m)
Raw Data

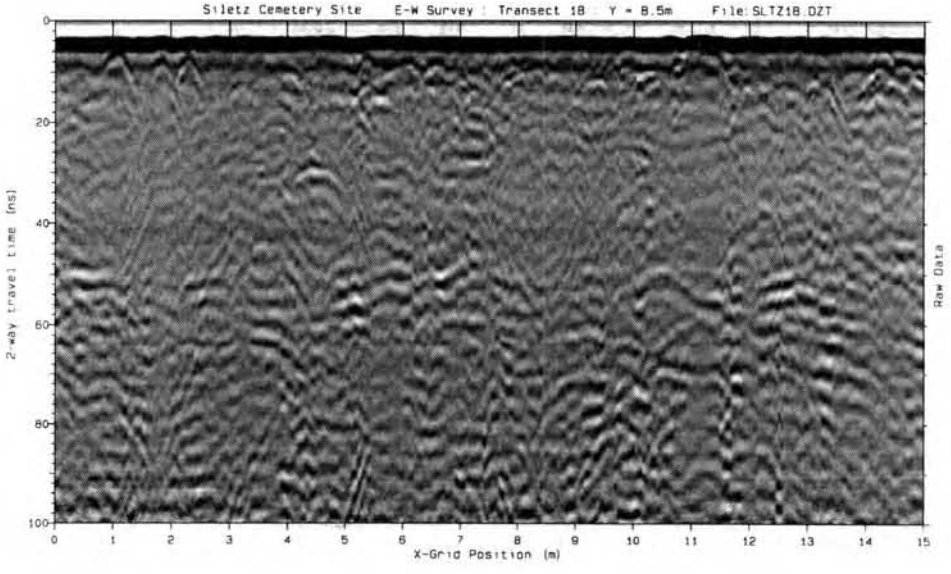
Siletz Cemetery Site E-W Survey : Transect 18 : Y = 8.5m File: SLTZ18.DZT
2-way travel time (ns)
X-Grid Position (m)
Raw Data

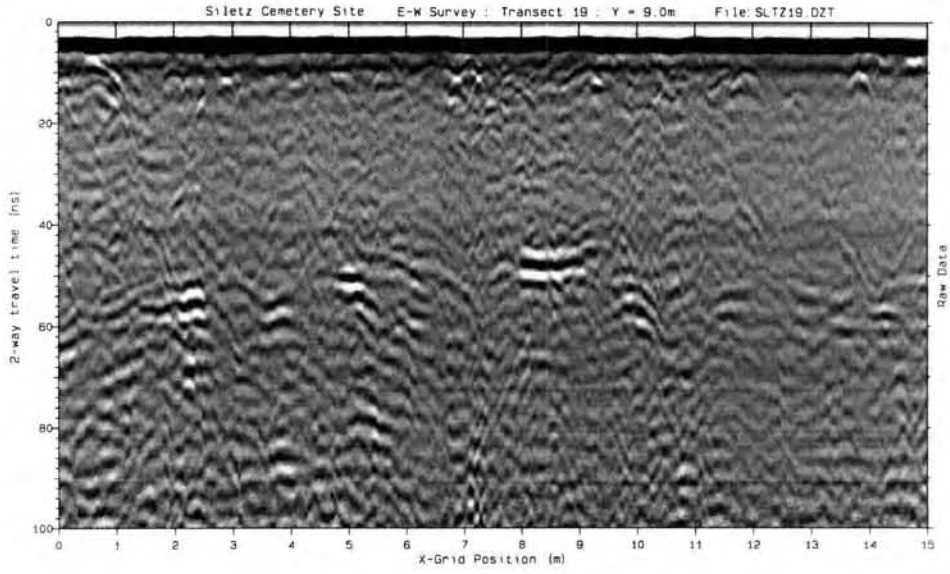
Siletz Cemetery Site E-W Survey : Transect 19 : Y = 9.0m File: SLTZ19.DZT
2-way travel time (ns)
X-Grid Position (m)
Raw Data

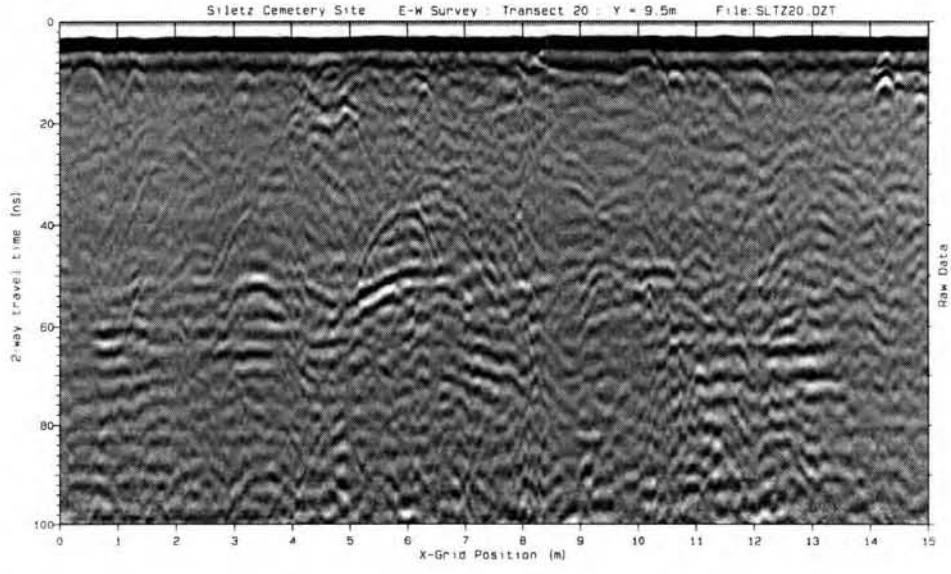
Siletz Cemetery Site E-W Survey : Transect 20 : Y = 9.5m File: SLTZ20.DZT
2-way travel time (ns)
X-Grid Position (m)
Raw Data

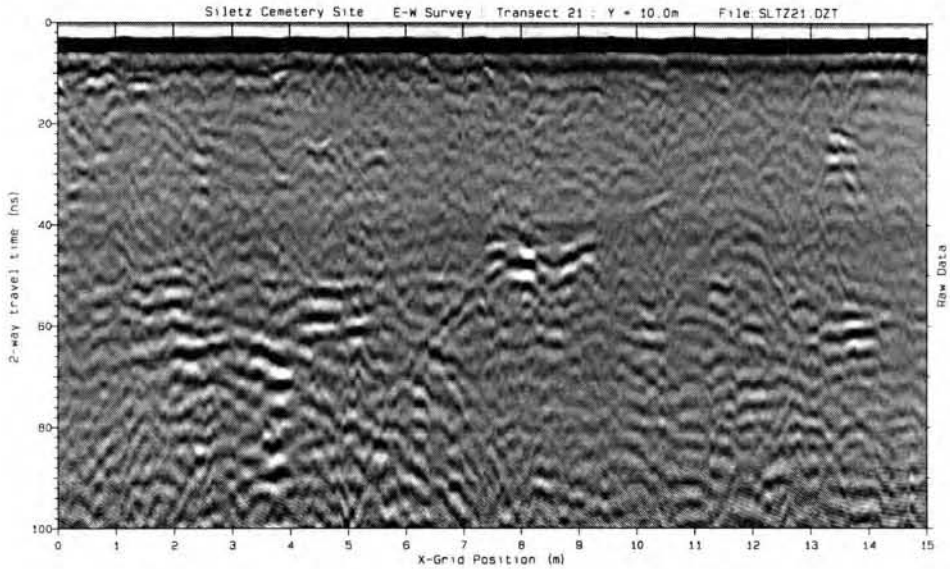
Siletz Cemetery Site E-W Survey Transect 21 : Y = 10.0m File: SLTZ21.DZT
2-way travel time (ns)
X-Grid Position (m)
Raw Data

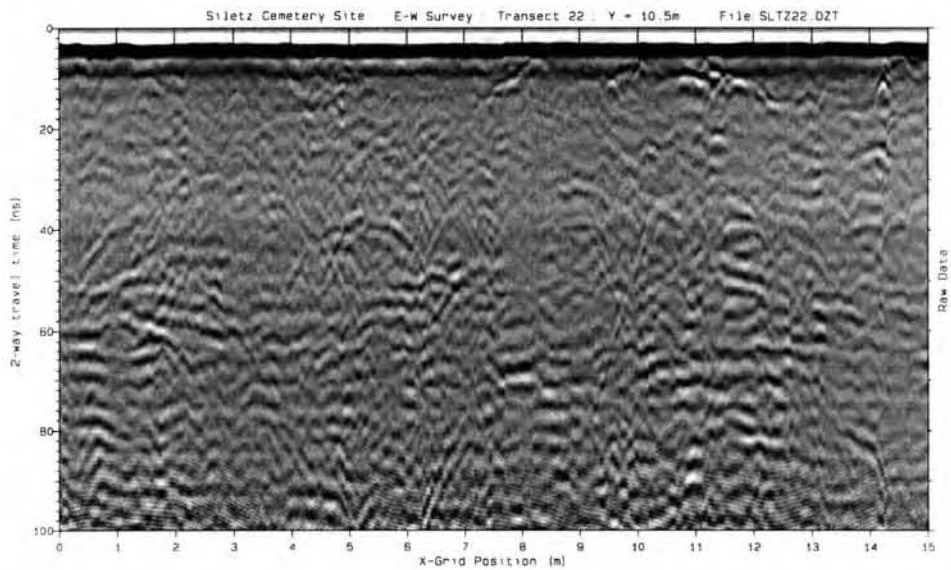
Siletz Cemetery Site E-W Survey Transect 22 : Y = 10.5m File: SLTZ22.DZT
2-way travel time (ns)
X-Grid Position (m)
Raw Data

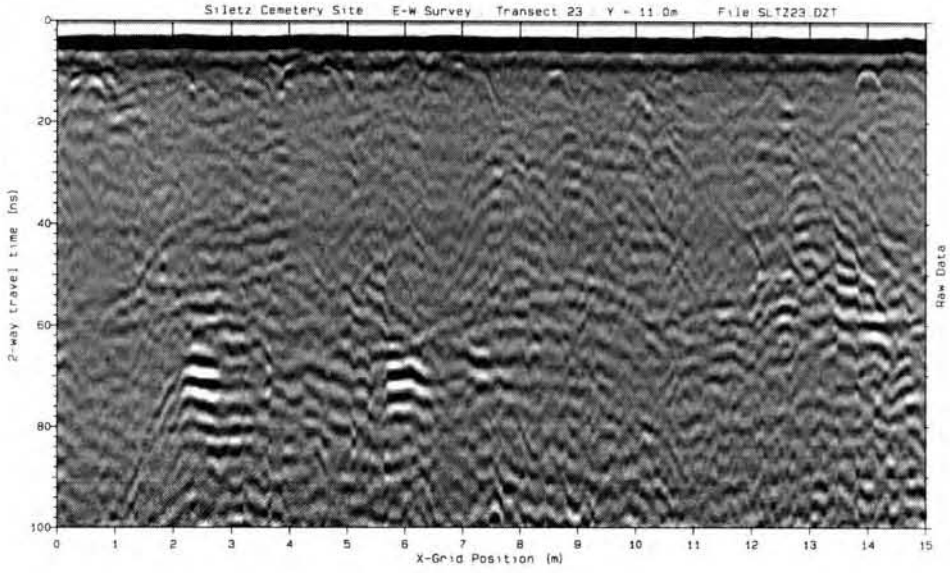
Siletz Cemetery Site E-W Survey Transect 23 Y = 11.0m File:SLTZ23.DZT
2-way travel time (ns)
X-Grid Position (m)
Raw Data

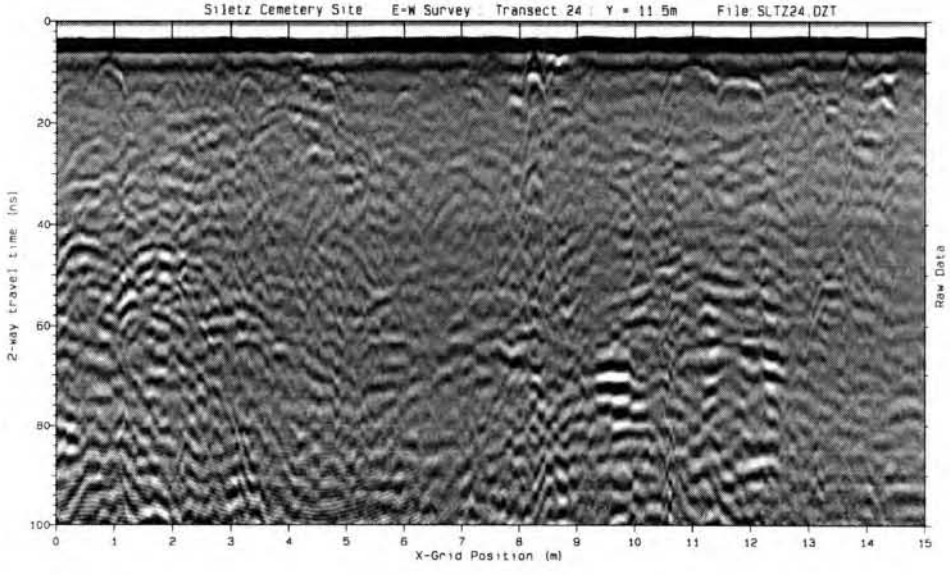
Siletz Cemetery Site E-W Survey Transect 24 Y = 11.5m File:SLTZ24.DZT
2-way travel time (ns)
X-Grid Position (m)
Raw Data

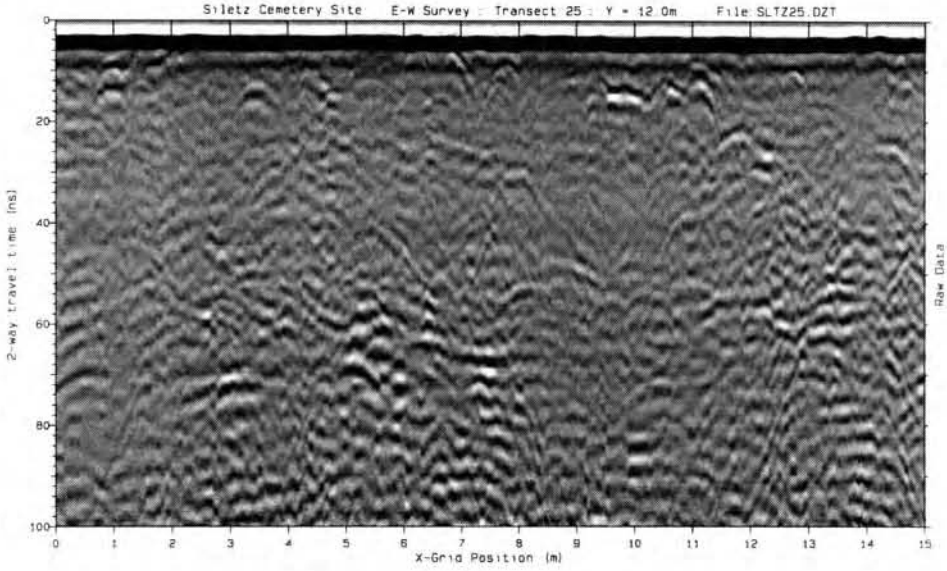
Siletz Cemetery Site E-W Survey : Transect 25 : Y = 12.0m File:SLTZ25.DZT
2-way travel time (ns)
X-Grid Position (m)
Raw Data

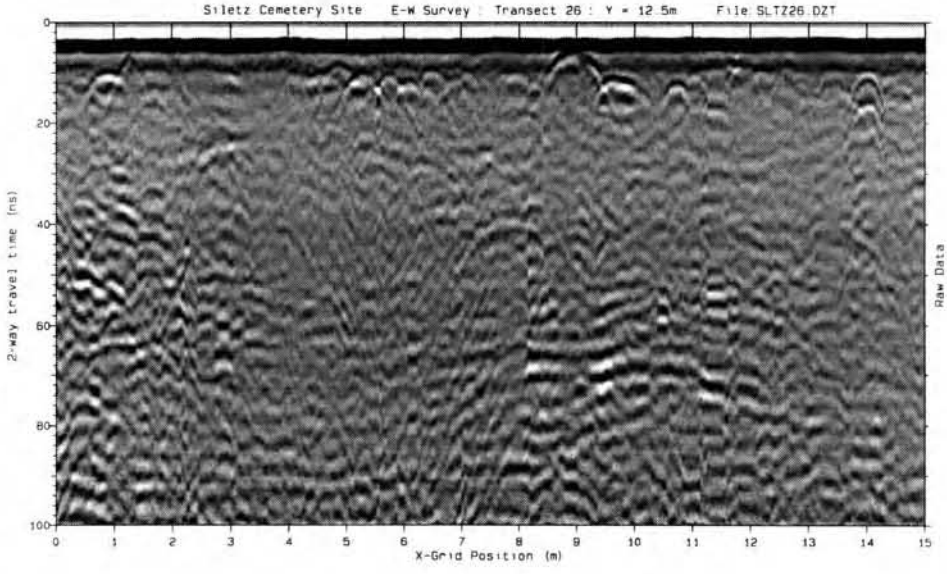
Siletz Cemetery Site E-W Survey : Transect 26 : Y = 12.5m File:SLTZ26.DZT
2-way travel time (ns)
X-Grid Position (m)
Raw Data

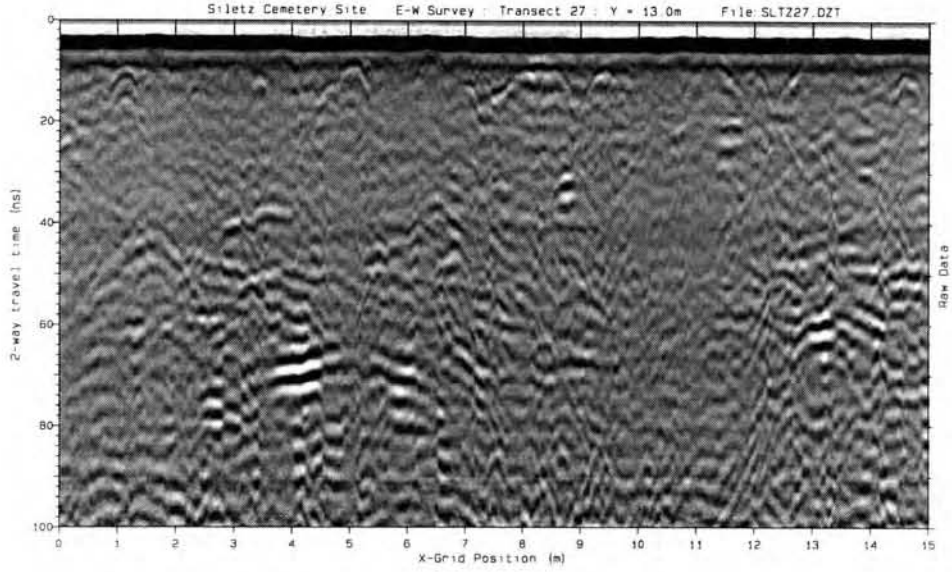
Siletz Cemetery Site E-W Survey : Transect 27 : Y = 13.0m File:SLTZ27.DZT
2-way travel time (ns)
X-Grid Position (m)
Raw Data

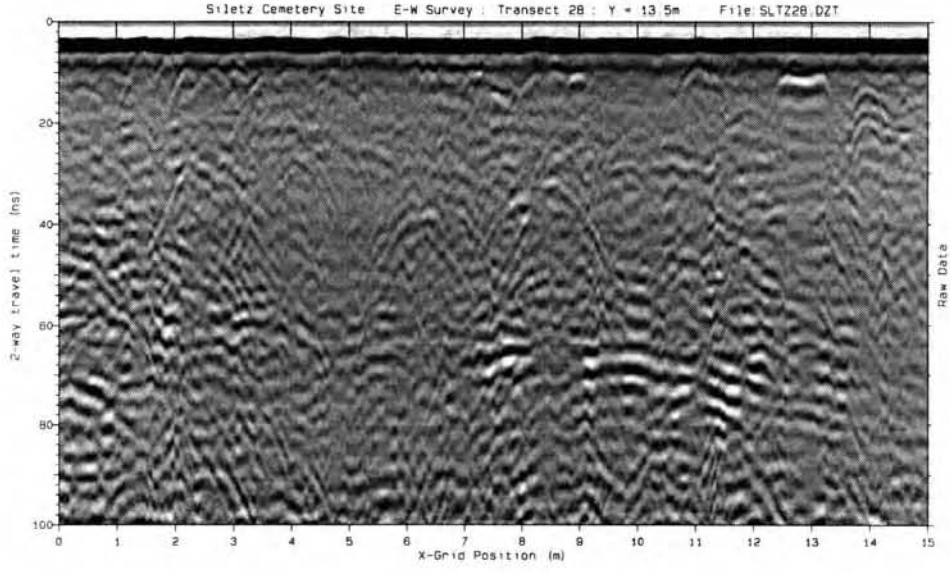
Siletz Cemetery Site E-W Survey : Transect 28 : Y = 13.5m File:SLTZ28.DZT
2-way travel time (ns)
X-Grid Position (m)
Raw Data

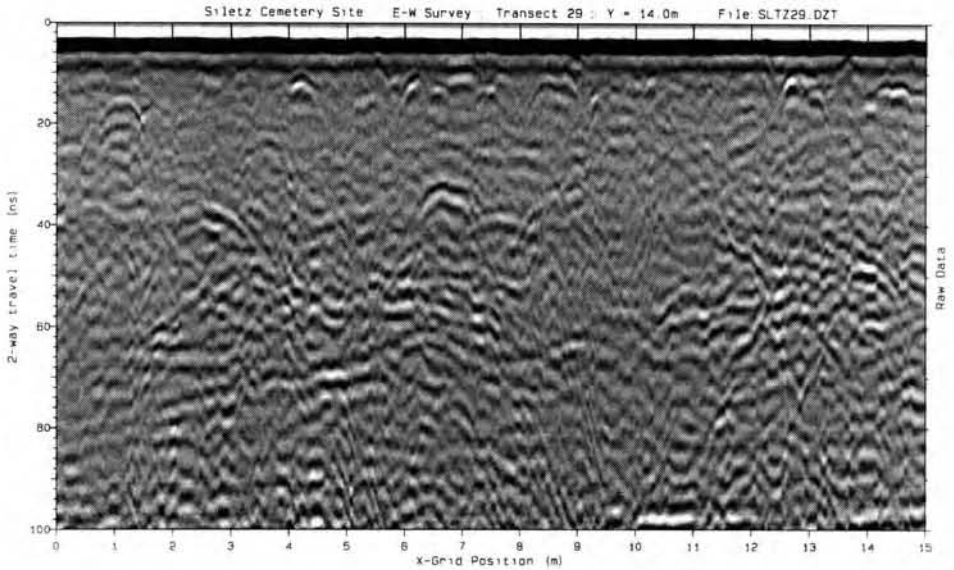
Siletz Cemetery Site E-W Survey Transect 29 Y = 14.0m File:SLTZ29.DZT
2-way travel time (ns)
X-Grid Position (m)
Raw Data

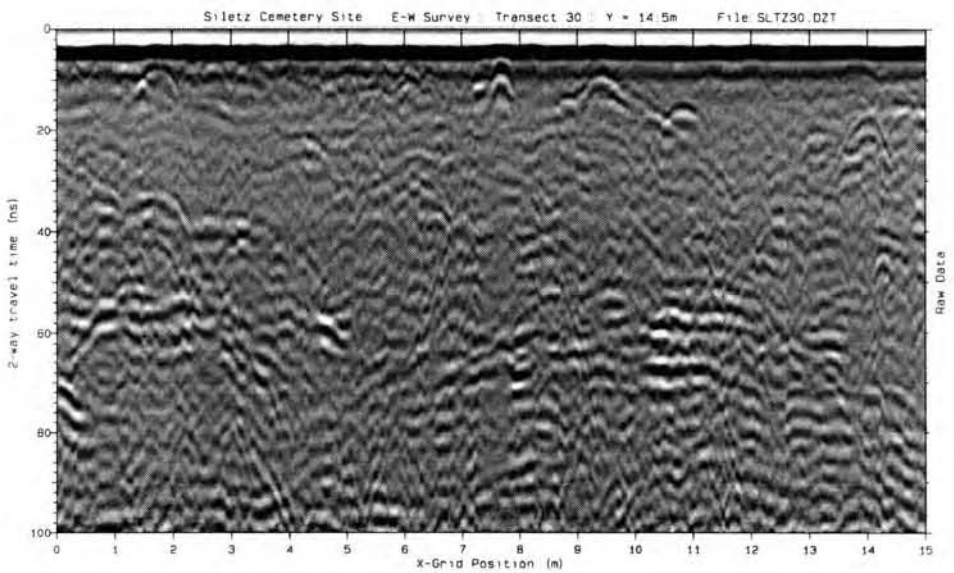
Siletz Cemetery Site E-W Survey Transect 30 Y = 14.5m File:SLTZ30.DZT
2-way travel time (ns)
X-Grid Position (m)
Raw Data

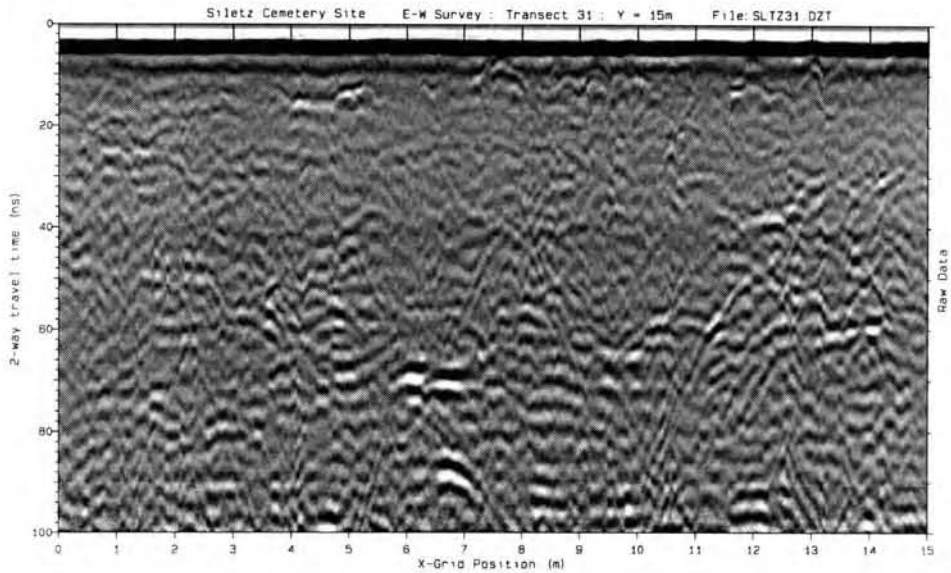
Siletz Cemetery Site E-W Survey : Transect 31 : Y = 15m File: SLTZ31.DZT
2-way travel time (ns)
X-Grid Position (m)
Raw Data

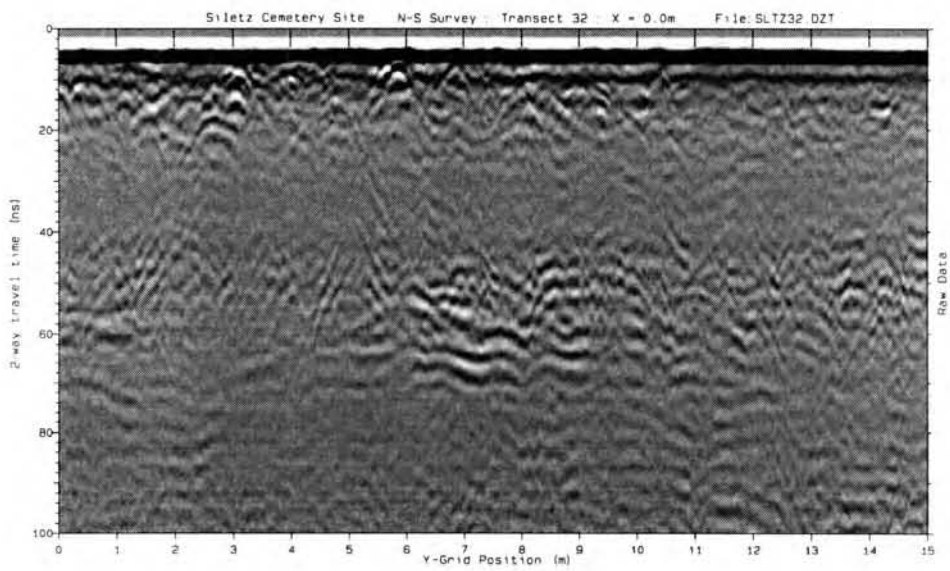
Siletz Cemetery Site N-S Survey : Transect 32 : X = 0.0m File: SLTZ32.DZT
2-way travel time (ns)
Y-Grid Position (m)
Raw Data

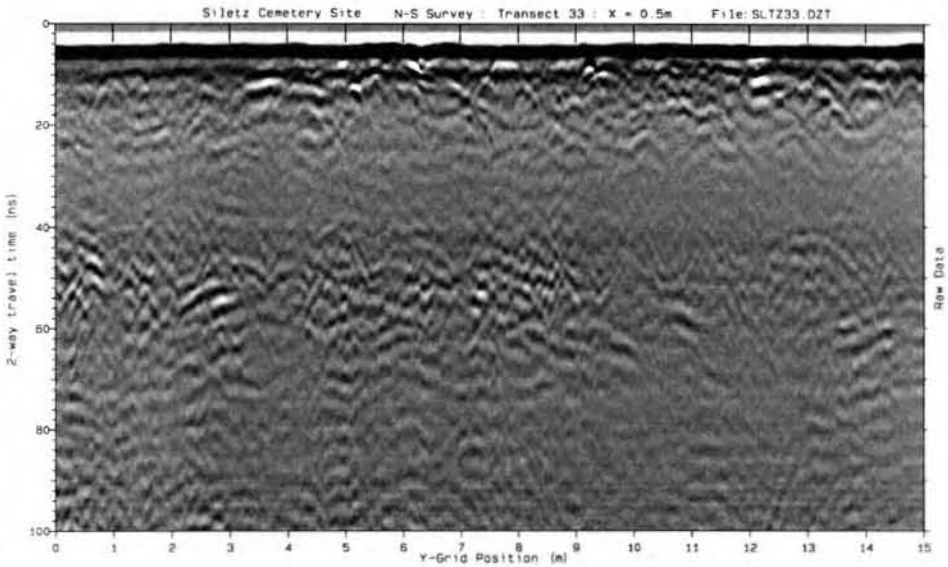
Siletz Cemetery Site N-S Survey : Transect 33 : X = 0.5m File: SLTZ33.DZT
2-way travel time (ns)
Y-Grid Position (m)
Raw Data

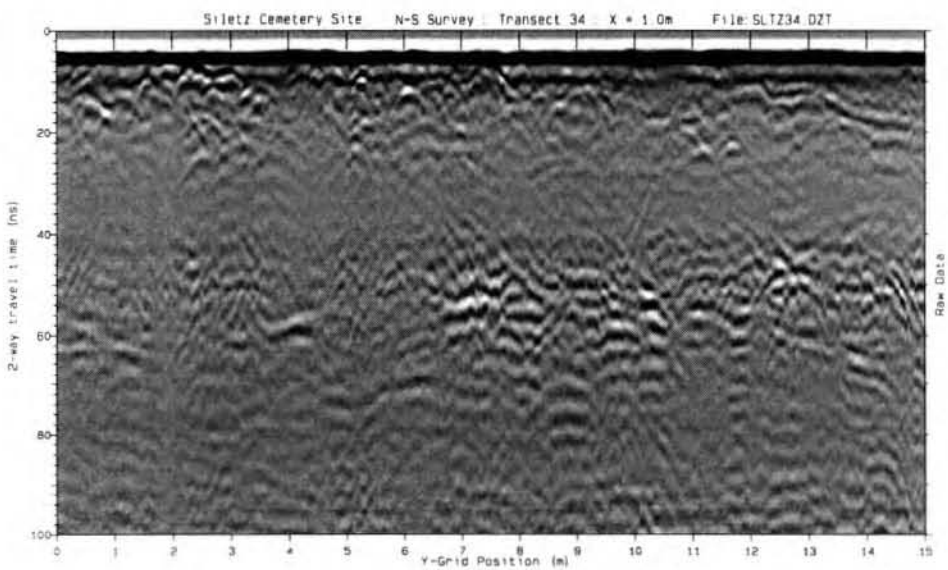
Siletz Cemetery Site N-S Survey : Transect 34 : X = 1.0m File: SLTZ34.DZT
2-way travel time (ns)
Y-Grid Position (m)
Raw Data

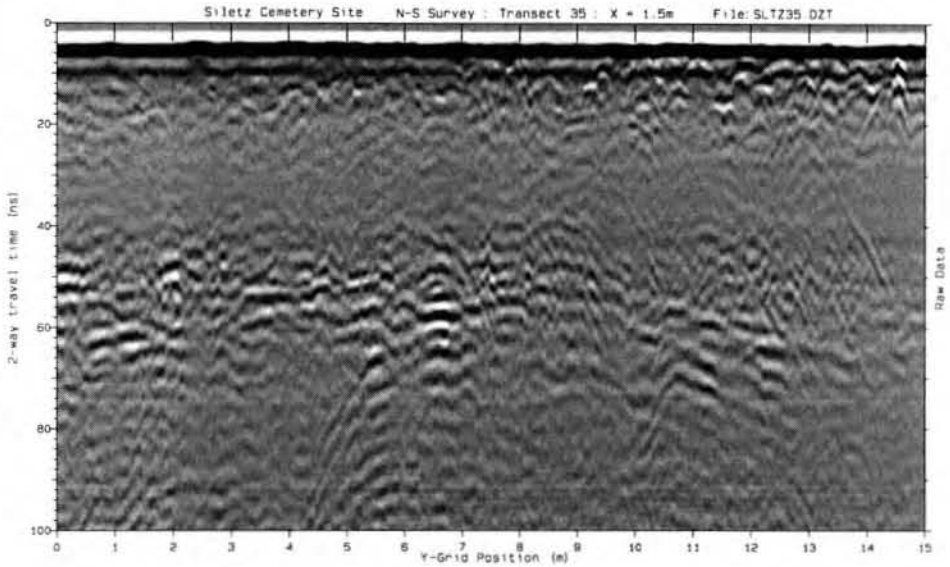
Siletz Cemetery Site N-S Survey : Transect 35 : X = 1.5m File: SLTZ35.DZT
2-way travel time (ns)
Y-Grid Position (m)
Raw Data

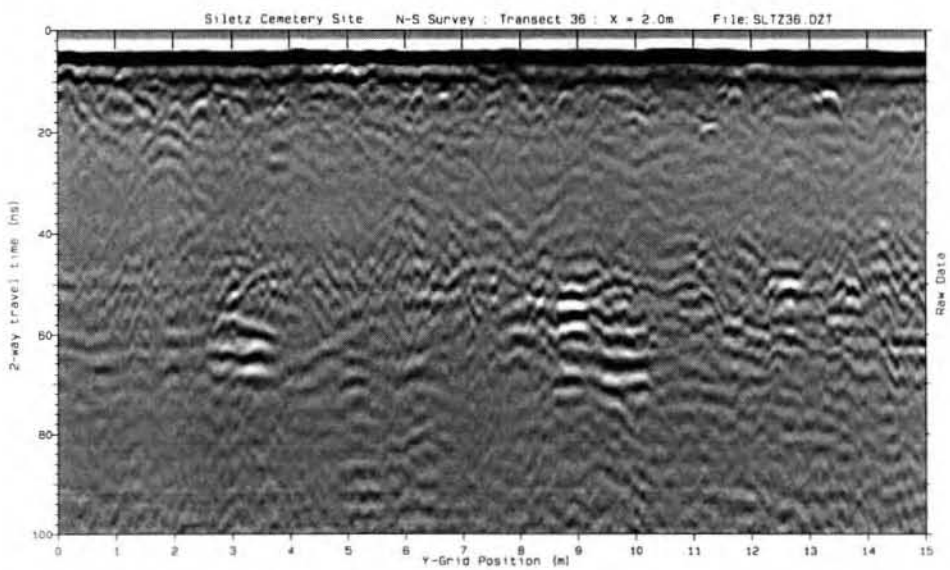
Siletz Cemetery Site N-S Survey : Transect 36 : X = 2.0m File: SLTZ36.DZT
2-way travel time (ns)
Y-Grid Position (m)
Raw Data

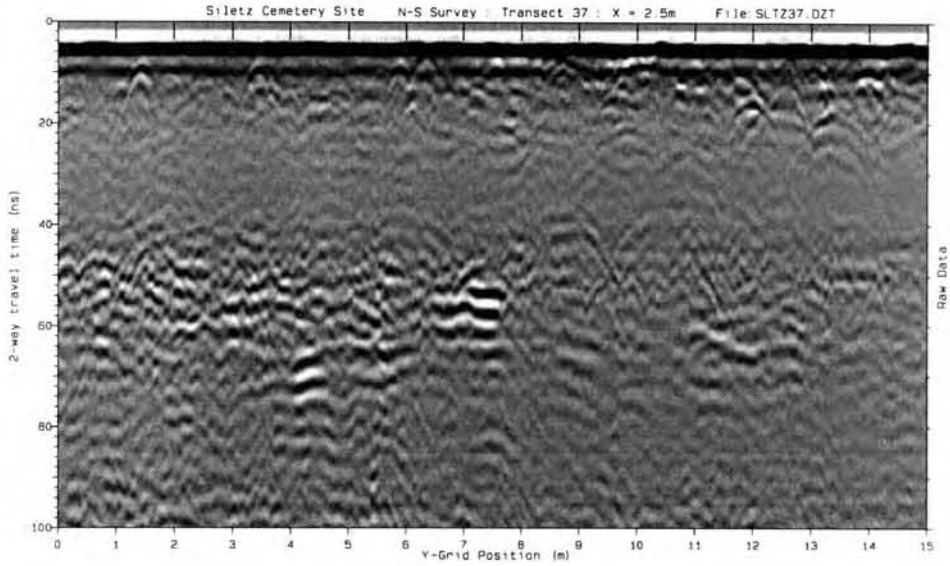
Siletz Cemetery Site N-S Survey : Transect 37 : X = 2.5m File: SLTZ37.DZT
2-way travel time (ns)
Y-Grid Position (m)
Raw Data

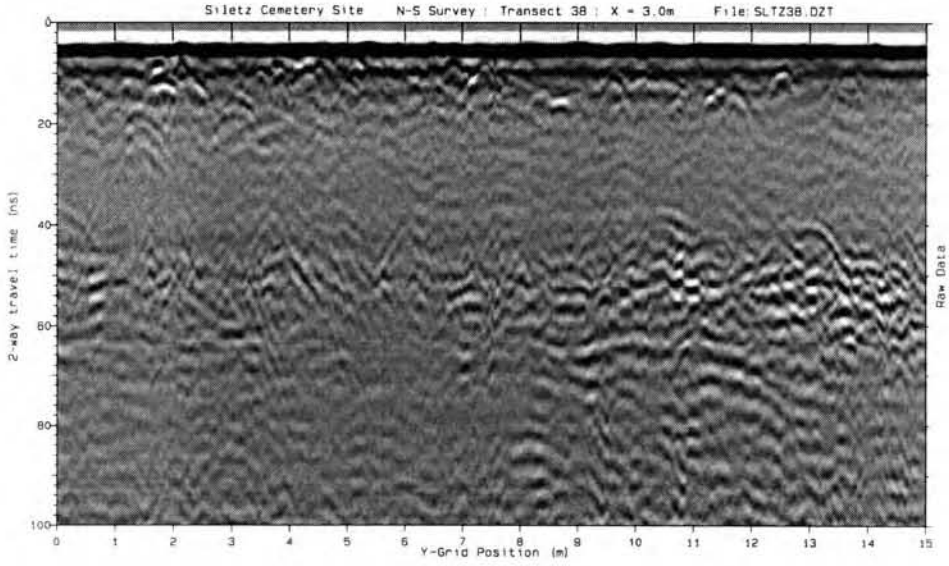
Siletz Cemetery Site N-S Survey : Transect 38 : X = 3.0m File: SLTZ38.DZT
2-way travel time (ns)
Y-Grid Position (m)
Raw Data

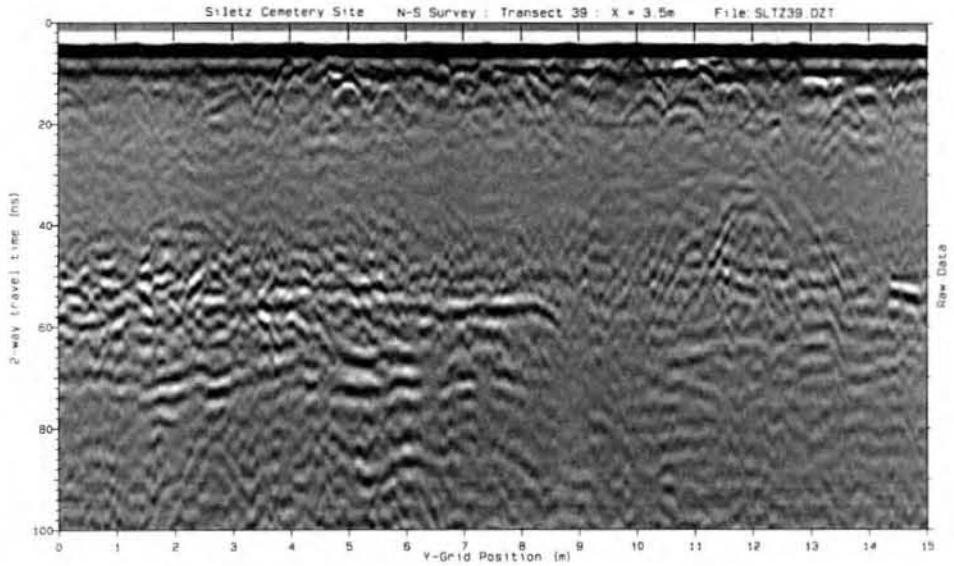
Siletz Cemetery Site N-S Survey : Transect 39 : X = 3.5m File: SLTZ39.DZT
2-way travel time (ns)
Y-Grid Position (m)
Raw Data

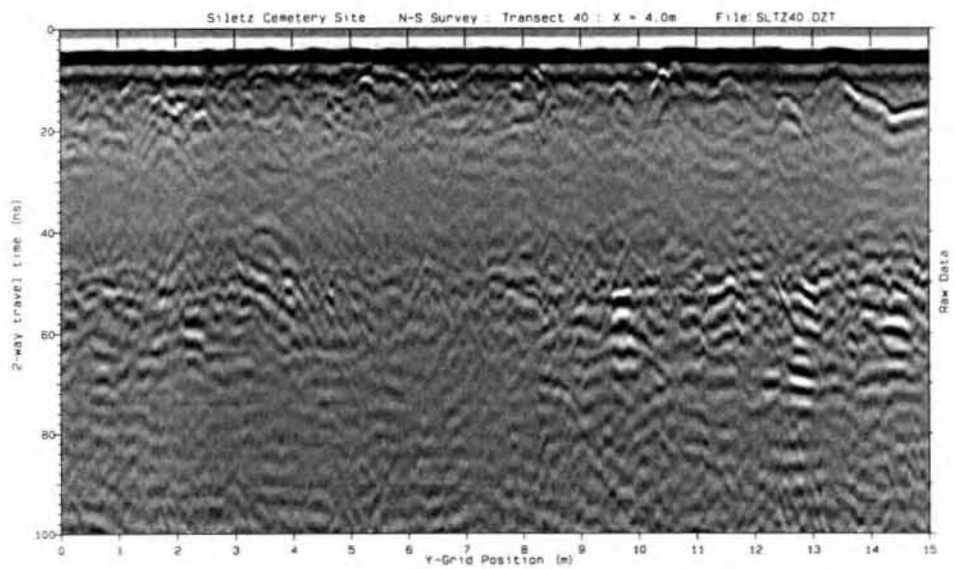
Siletz Cemetery Site N-S Survey : Transect 40 : X = 4.0m File: SLTZ40.DZT
2-way travel time (ns)
Y-Grid Position (m)
Raw Data

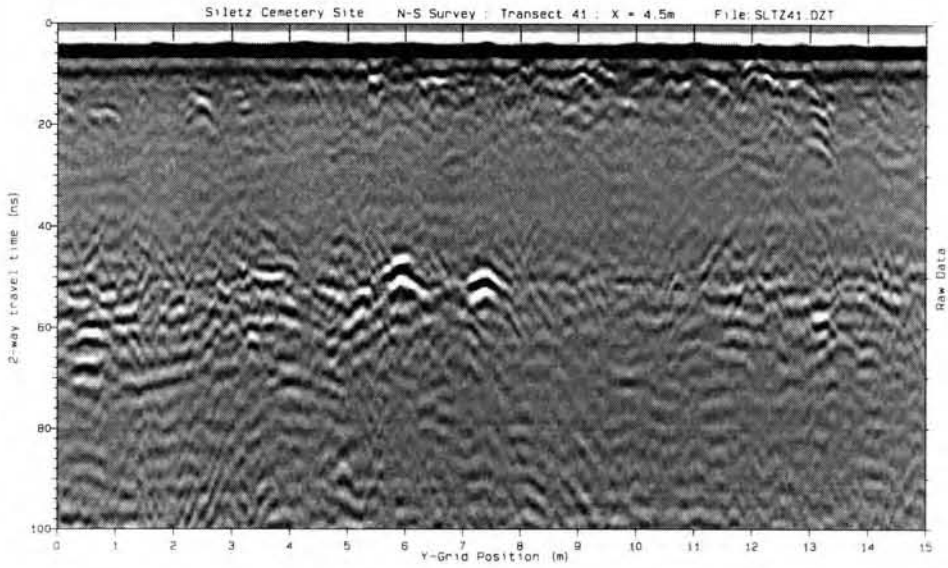
Siletz Cemetery Site N-S Survey : Transect 41 : X = 4.5m File: SLTZ41.DZT
2-way travel time (ns)
Y-Grid Position (m)
Raw Data

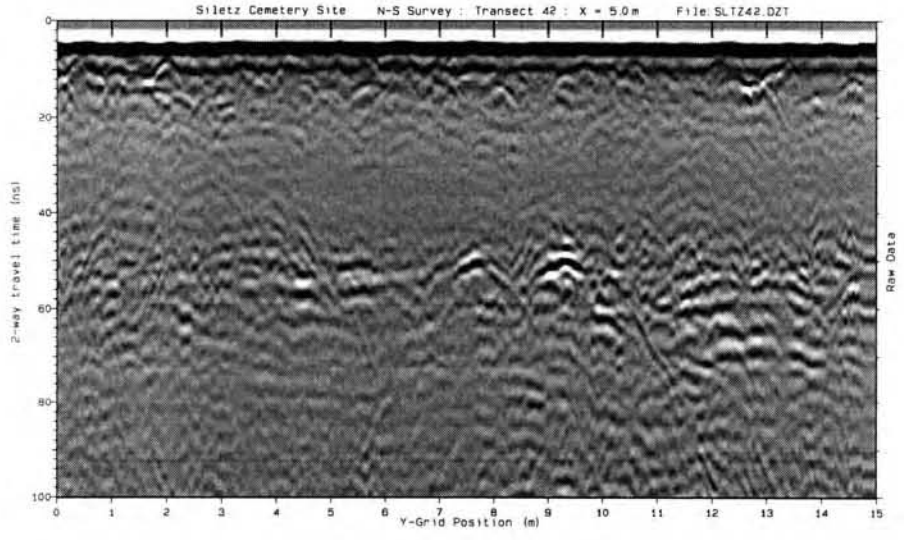
Siletz Cemetery Site N-S Survey : Transect 42 : X = 5.0m File: SLTZ42.DZT
2-way travel time (ns)
Y-Grid Position (m)
Raw Data

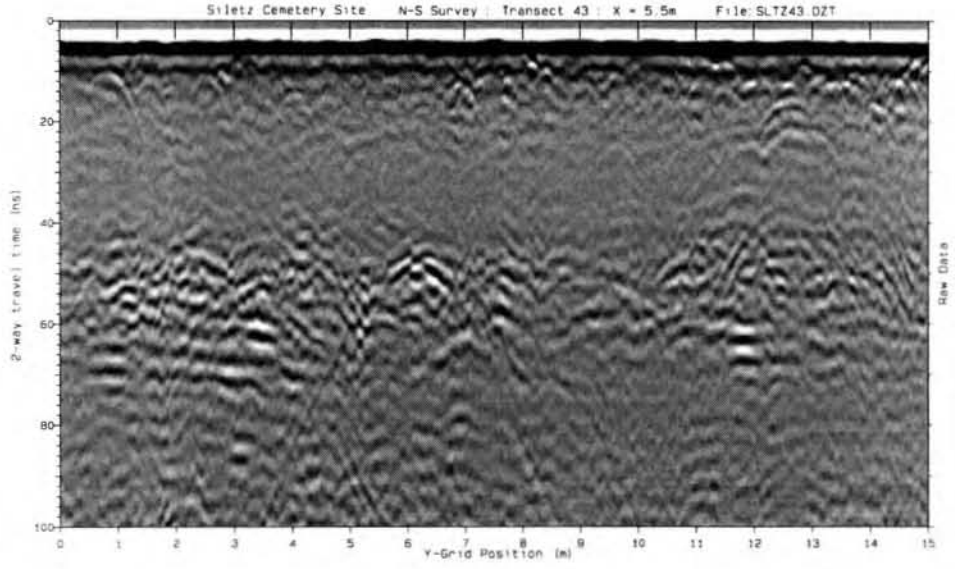
Siletz Cemetery Site N-S Survey : Transect 43 : X = 5.5m File: SLTZ43.DZT
2-way travel time (ns)
Y-Grid Position (m)
Raw Data

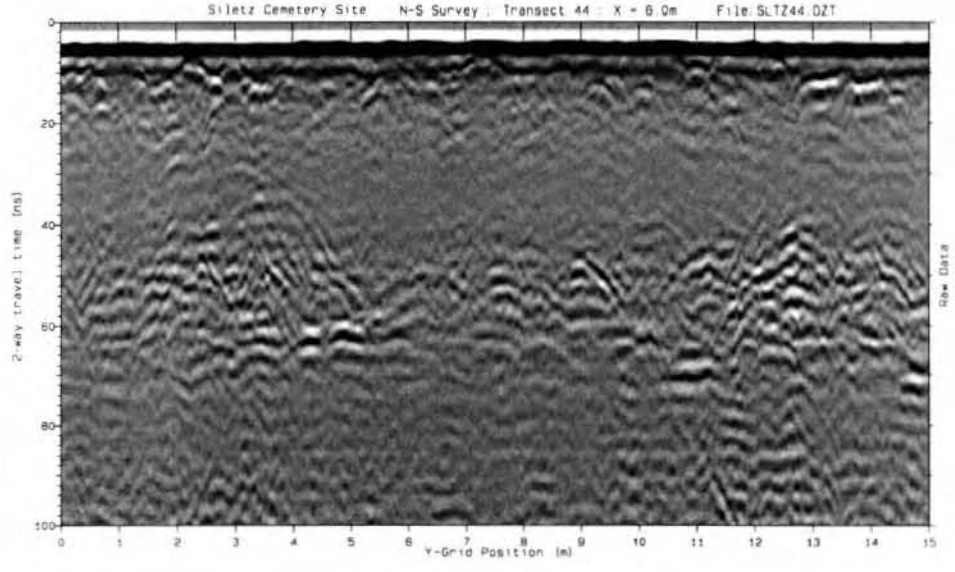
Siletz Cemetery Site N-S Survey : Transect 44 : X = 6.0m File: SLTZ44.DZT
2-way travel time (ns)
Y-Grid Position (m)
Raw Data

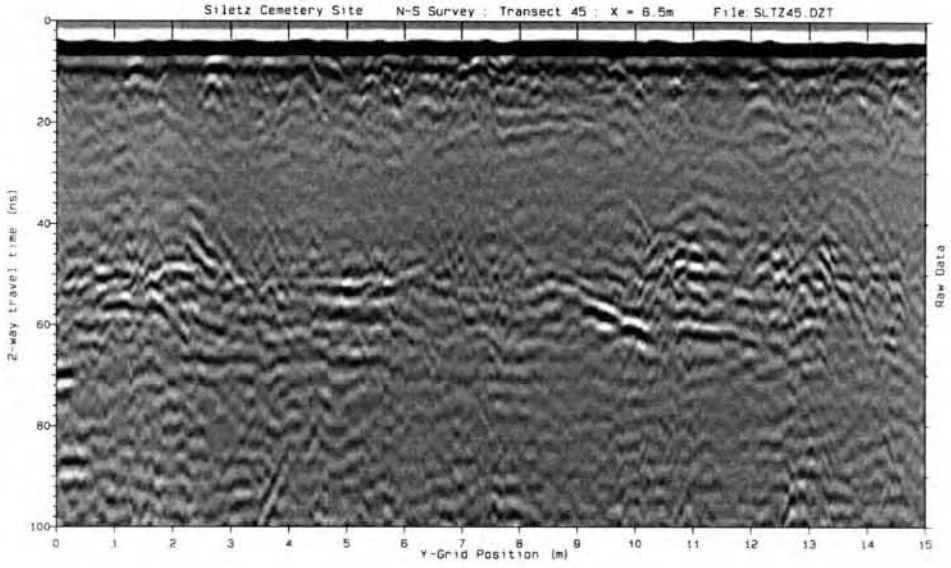
Siletz Cemetery Site N-S Survey : Transect 45 : X = 6.5m File: SLTZ45.DZT
2-way travel time (ns)
Y-Grid Position (m)
Raw Data

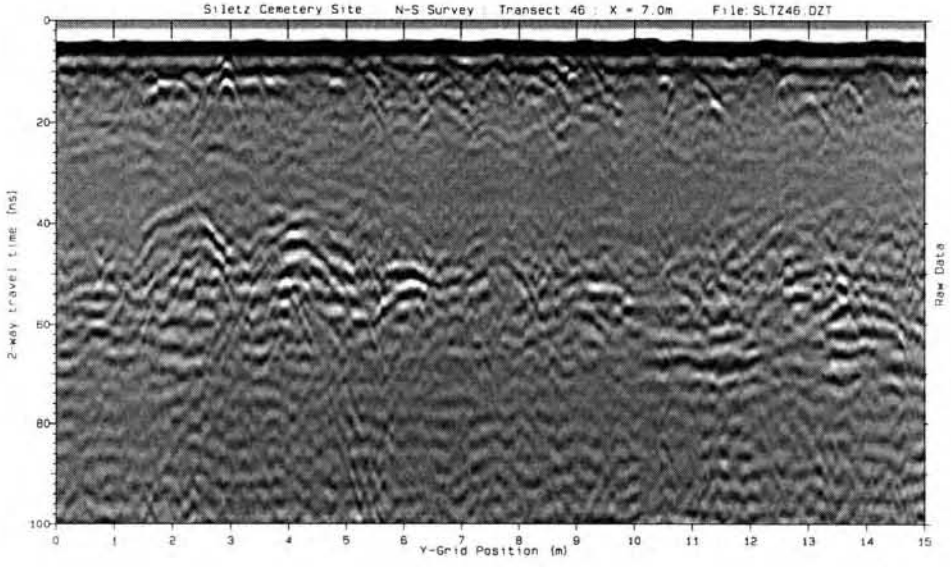
Siletz Cemetery Site N-S Survey : Transect 46 : X = 7.0m File: SLTZ46.DZT
2-way travel time (ns)
Y-Grid Position (m)
Raw Data

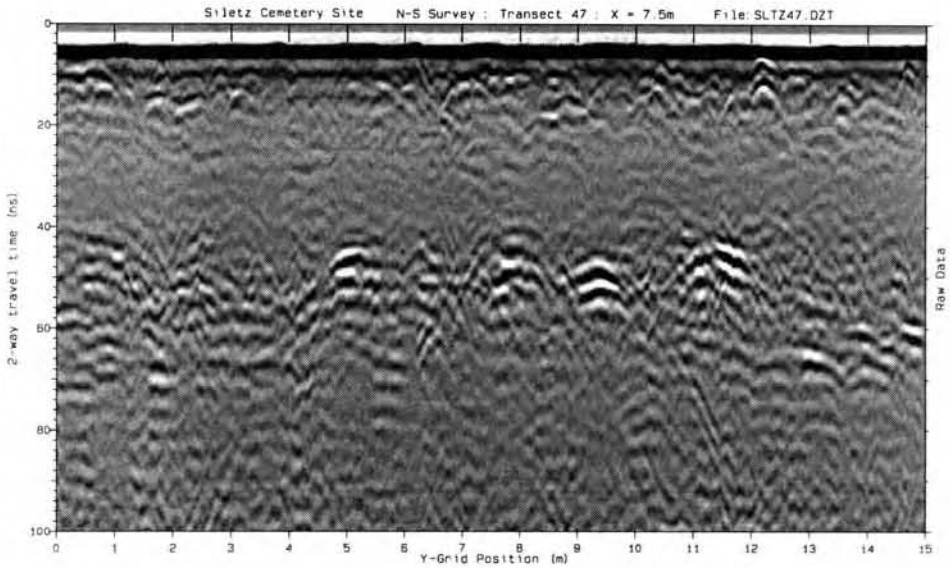
Siletz Cemetery Site N-S Survey : Transect 47 : X = 7.5m File: SLTZ47.DZT
2-way travel time (ns)
Y-Grid Position (m)
Raw Data

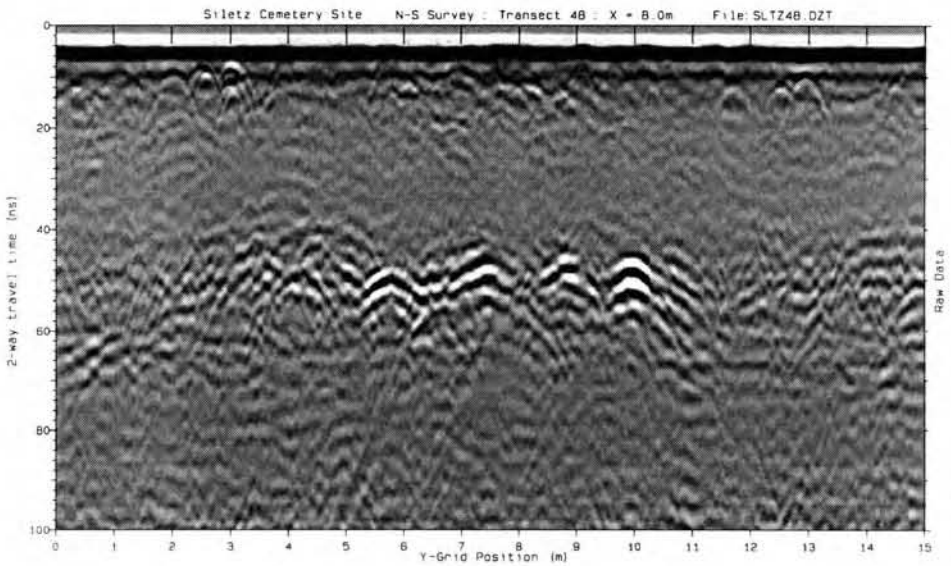
Siletz Cemetery Site N-S Survey : Transect 48 : X = 8.0m File: SLTZ48.DZT
2-way travel time (ns)
Y-Grid Position (m)
Raw Data

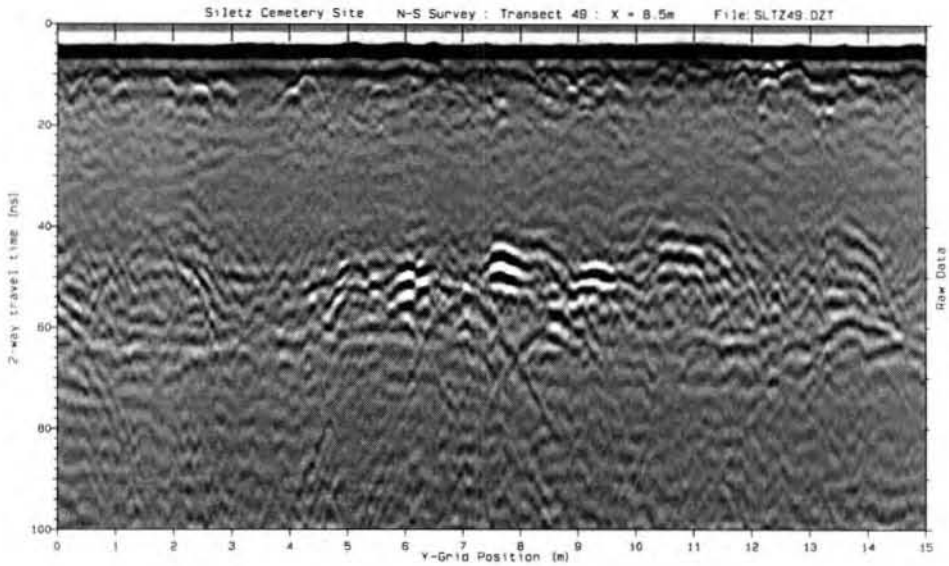
Siletz Cemetery Site N-S Survey : Transect 49 : X = 8.5m File:SLTZ49.DZT
2-way travel time (ns)
Y-Grid Position (m)
Raw Data

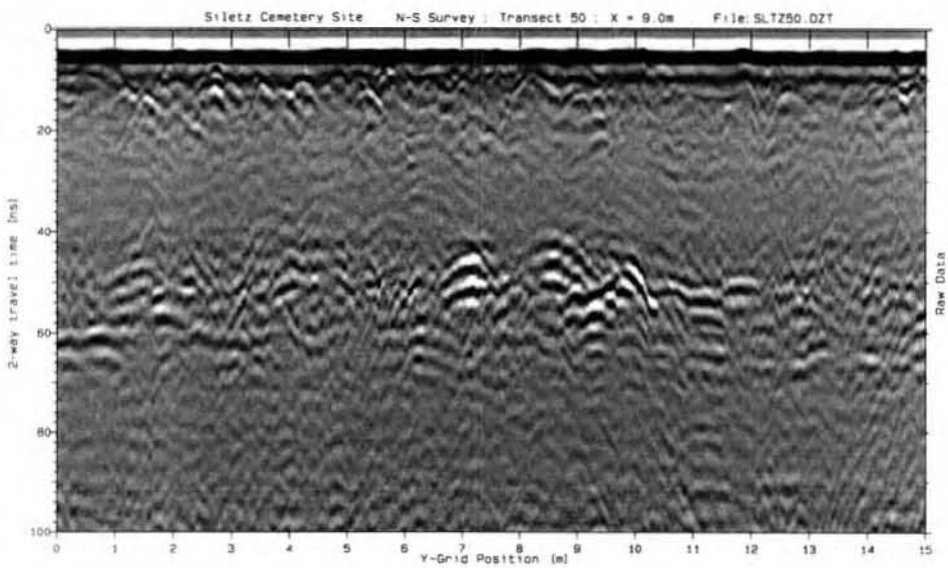
Siletz Cemetery Site N-S Survey : Transect 50 : X = 9.0m File:SLTZ50.DZT
2-way travel time (ns)
Y-Grid Position (m)
Raw Data

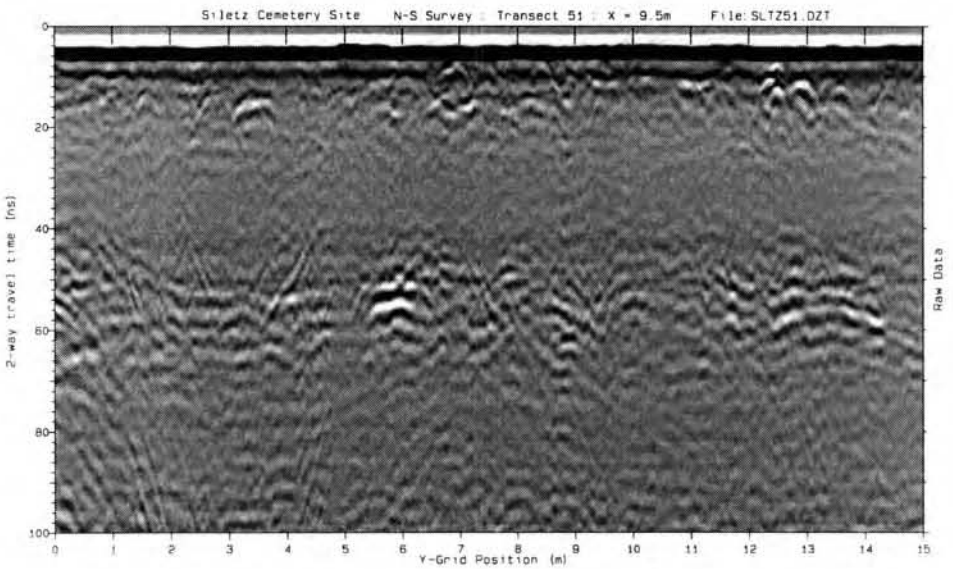
Siletz Cemetery Site N-S Survey : Transect 51 : X = 9.5m File: SLTZ51.DZT
2-way travel time (ns)
Y-Grid Position (m)
Raw Data

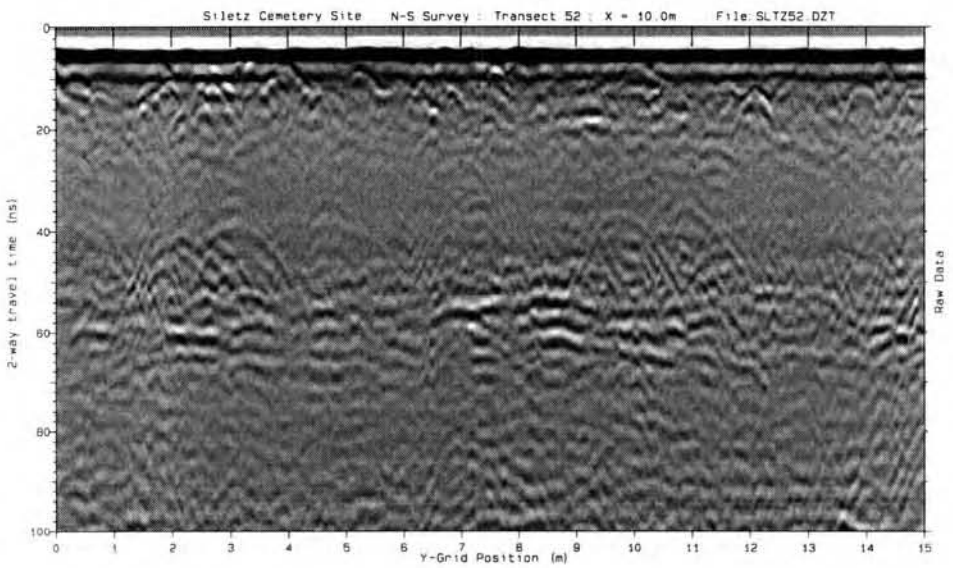
Siletz Cemetery Site N-S Survey : Transect 52 : X = 10.0m File: SLTZ52.DZT
2-way travel time (ns)
Y-Grid Position (m)
Raw Data

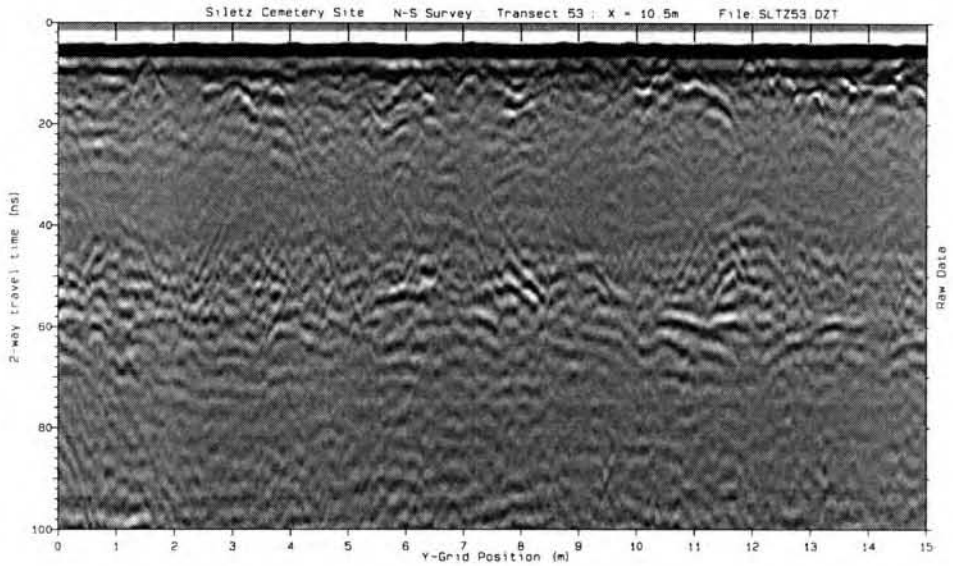
Siletz Cemetery Site N-S Survey Transect 53 : X = 10.5m File: SLTZ53.DZT
2-way travel time (ns)
Y-Grid Position (m)
Raw Data

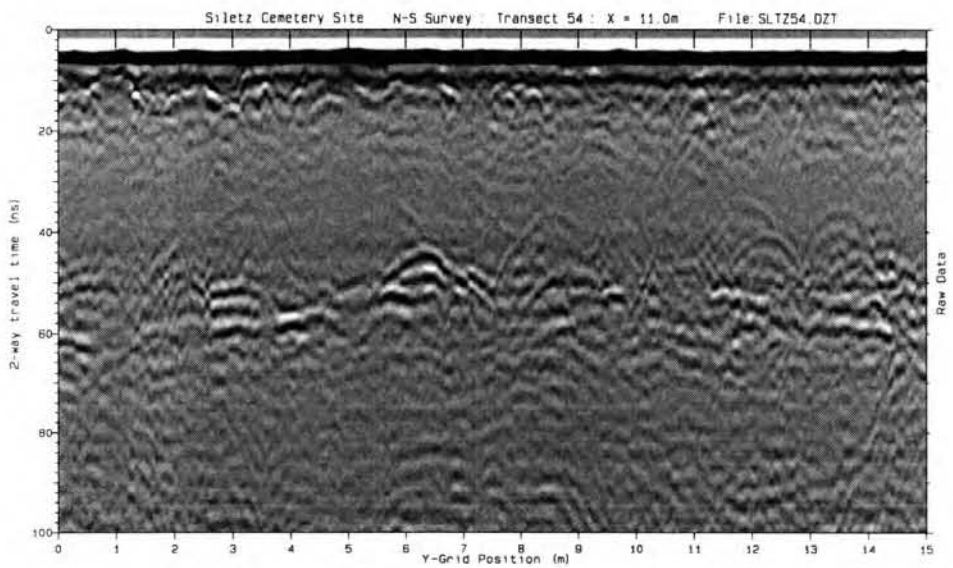
Siletz Cemetery Site N-S Survey Transect 54 : X = 11.0m File: SLTZ54.DZT
2-way travel time (ns)
Y-Grid Position (m)
Raw Data

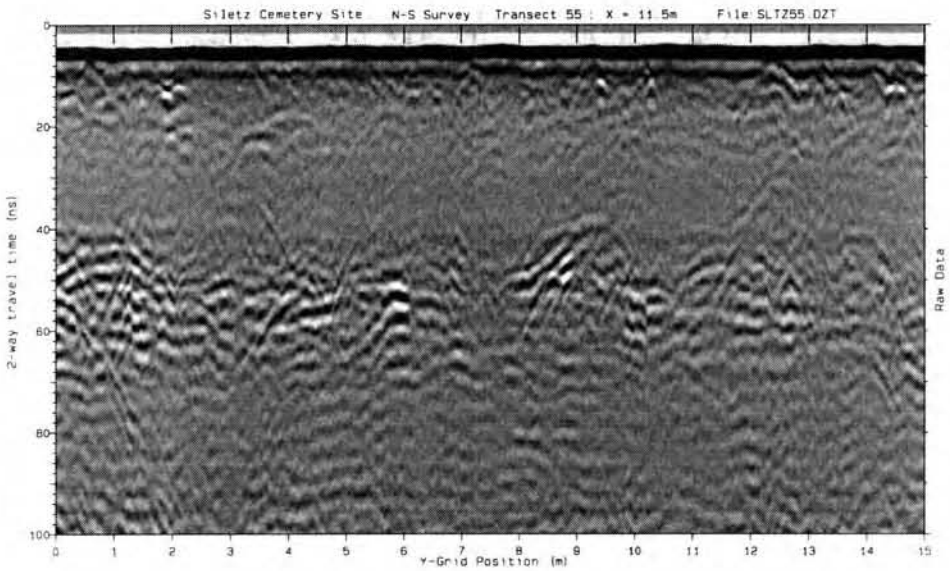
Siletz Cemetery Site N-S Survey Transect 55 : X = 11.5m File:SLTZ55.DZT
2-way travel time (ns)
Y-Grid Position (m)
Raw Data

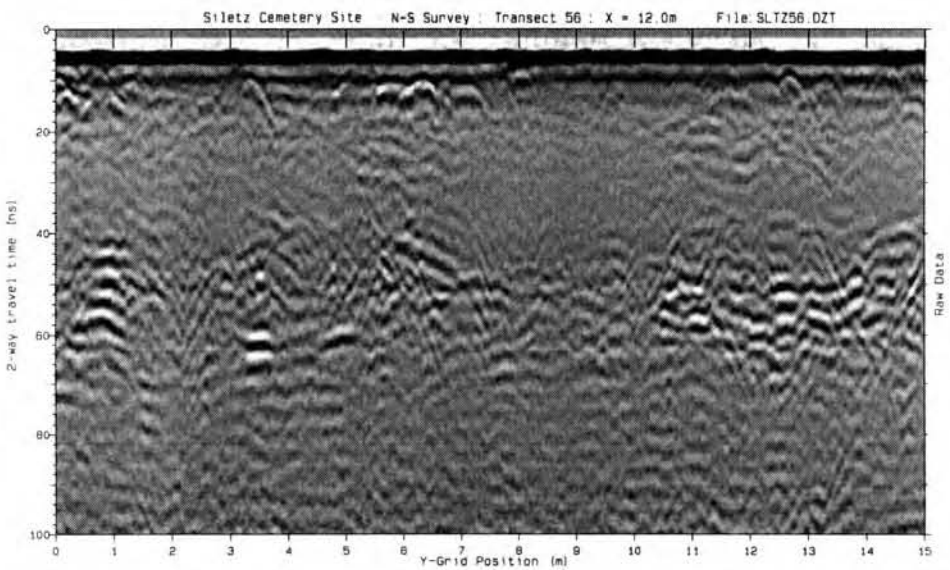
Siletz Cemetery Site N-S Survey Transect 56 : X = 12.0m File:SLTZ56.DZT
2-way travel time (ns)
Y-Grid Position (m)
Raw Data

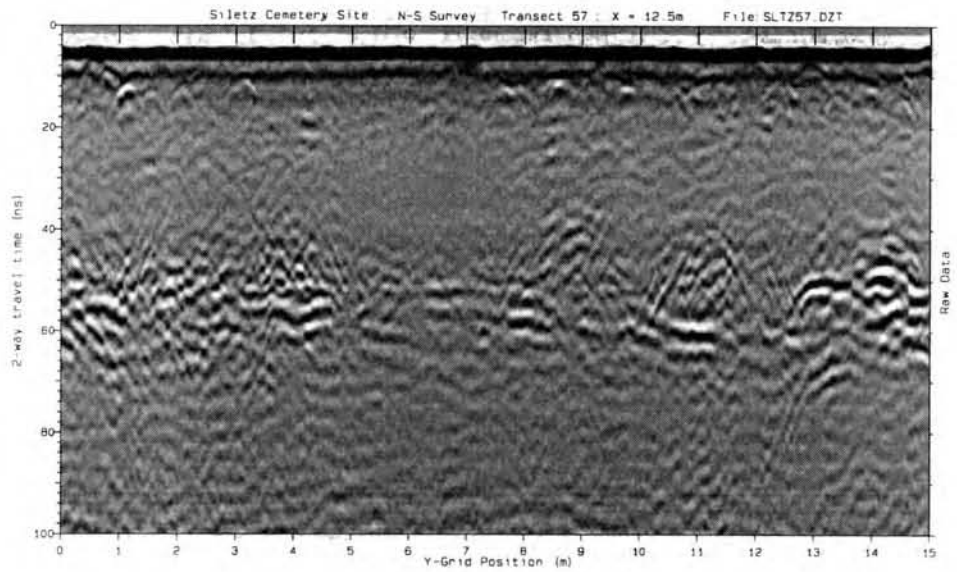
Siletz Cemetery Site N-S Survey Transect 57 : X = 12.5m File:SLTZ57.DZT
2-way travel time (ns)
Y-Grid Position (m)
Raw Data

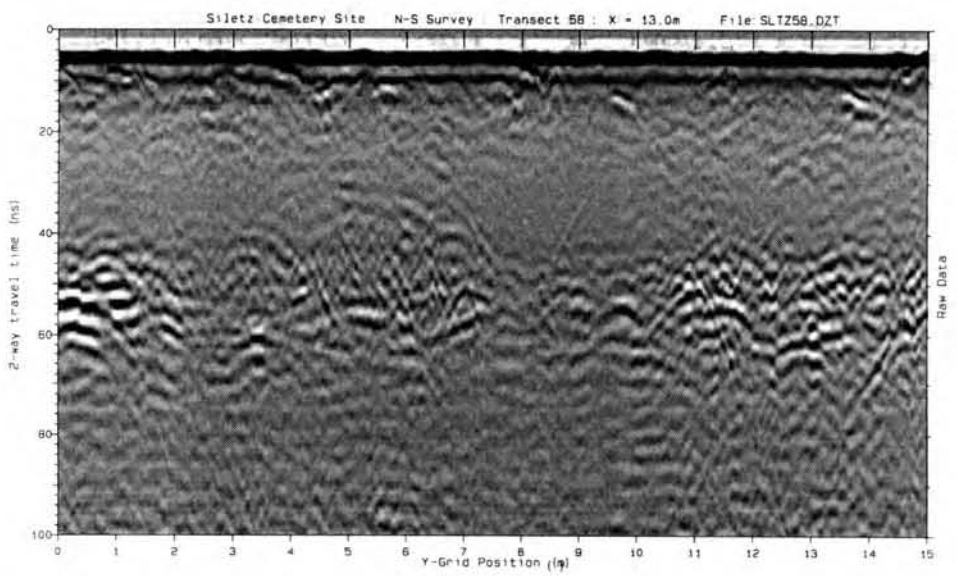
Siletz Cemetery Site N-S Survey Transect 58 : X = 13.0m File:SLTZ58.DZT
2-way travel time (ns)
Y-Grid Position (m)
Raw Data

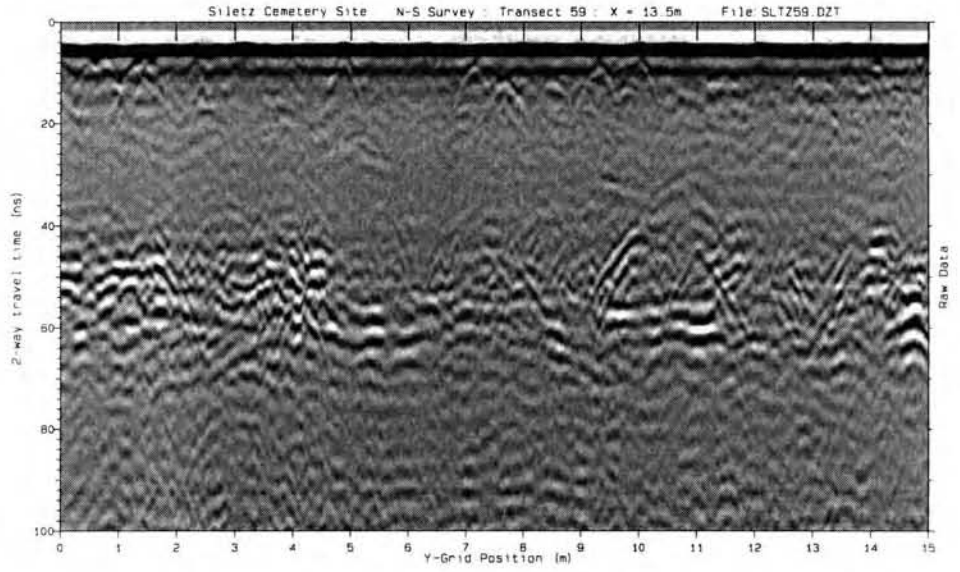
Siletz Cemetery Site N-S Survey : Transect 59 : X = 13.5m File: SLTZ59.DZT
2-way travel time (ns)
Y-Grid Position (m)
Raw Data

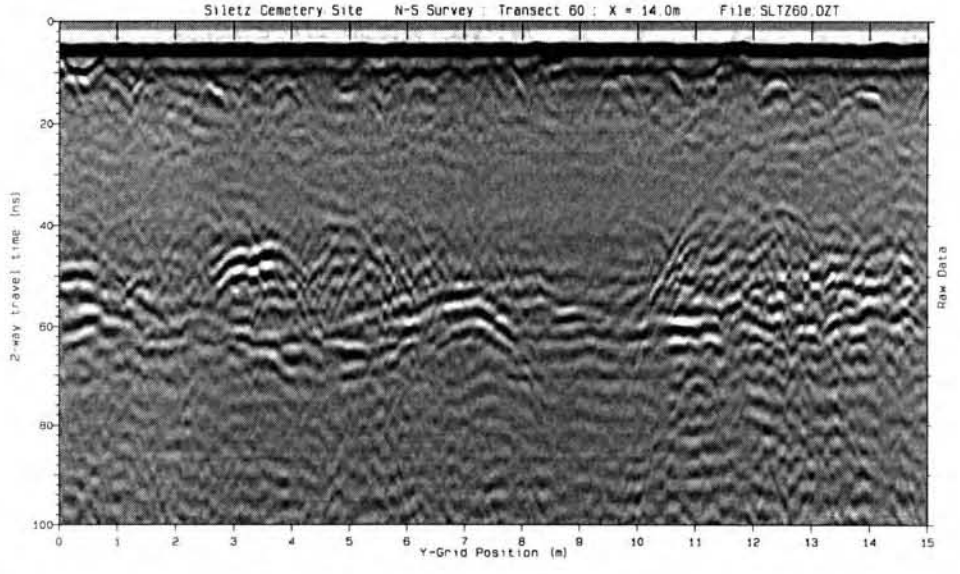
Siletz Cemetery Site N-S Survey : Transect 60 : X = 14.0m File: SLTZ60.DZT
2-way travel time (ns)
Y-Grid Position (m)
Raw Data

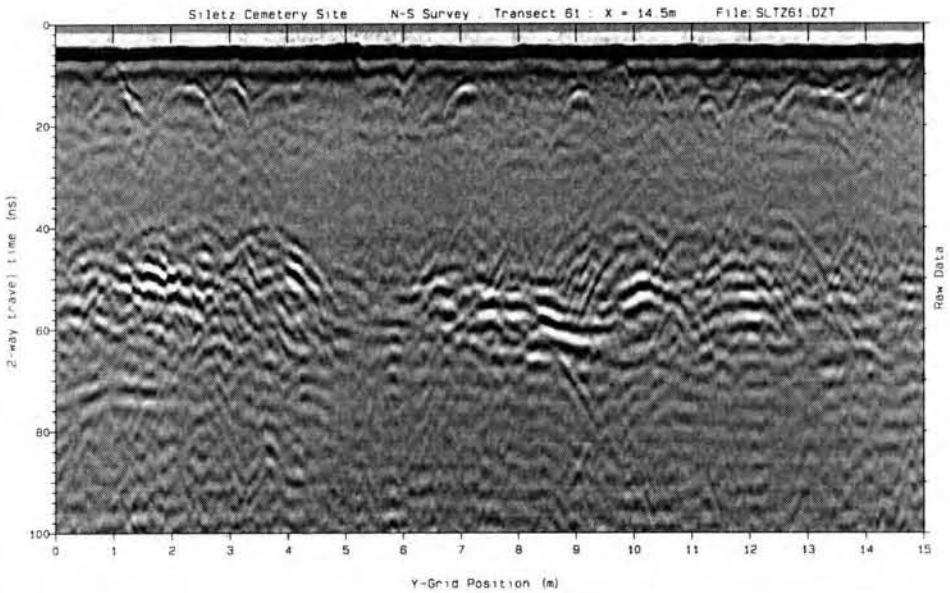
Siletz Cemetery Site N-S Survey Transect 61 : X = 14.5m File: SLTZ61.DZT
2-way travel time (ns)
Y-Grid Position (m)
Raw Data

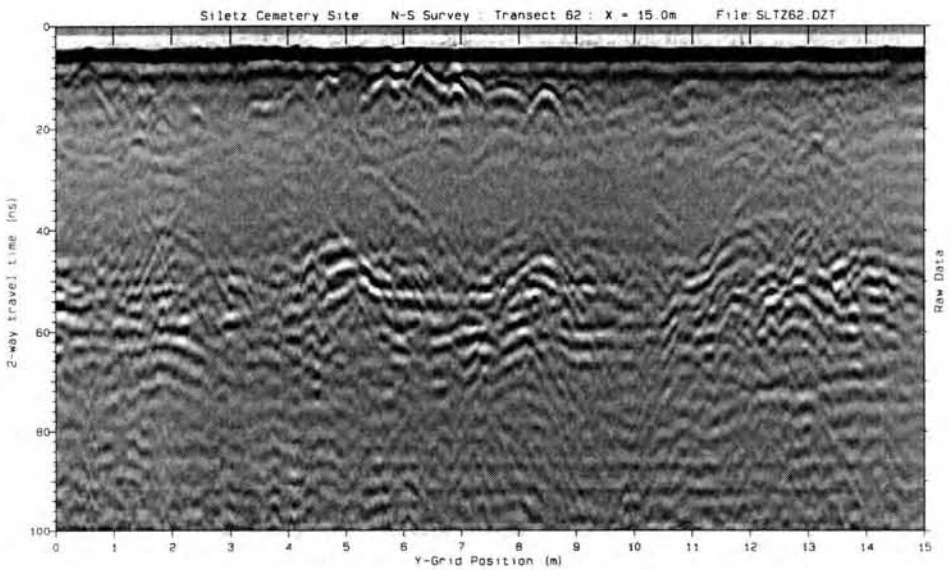
Siletz Cemetery Site N-S Survey Transect 62 : X = 15.0m File: SLTZ62.DZT
2-way travel time (ns)
Y-Grid Position (m)
Raw Data

Appendix G. Results of Different Slice Parameters

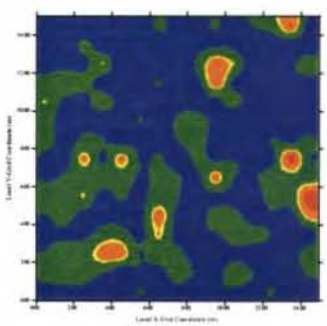

(a) X-Box Size = 0.25m, Y-Box Size = 0.75m

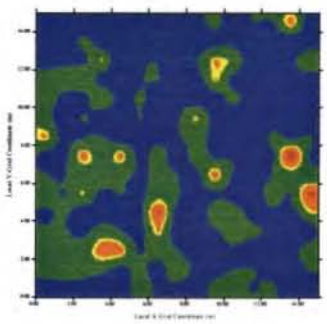

(a) X-Box Size = 0.15m, Y-Box Size = 0.75m

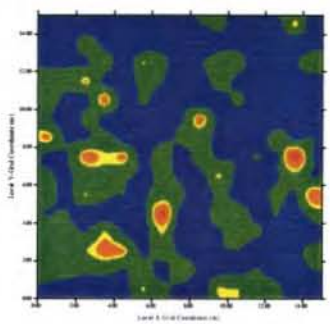

(a) X-Box Size = 0.05m, Y-Box Size = 0.75m

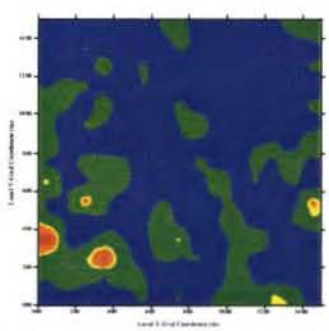

(a) X-Box Size = 0.05m, Y-Box Size =1.00m

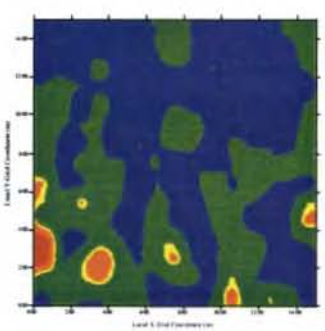

(a) X-Box Size = 0.05m, Y-Box Size = 1.25m

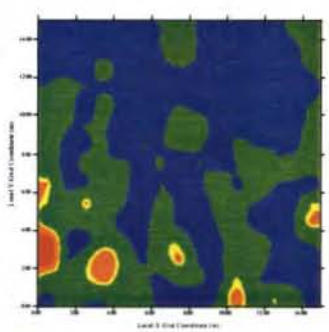

(a) X-Box Size = 0.05m, Y-Box Size =1.50m

Confederated Tribes of Siletz Indians Cemetery (SLTZ) Site

Examination of the affect of different box sizes
while conducting time slice analysis

Time slices conducted OCT-00 using GPR-Process

Map created using Golden Software's Surfer on01-NOV-00
Gridding Method: Kriging
Mapping Method: Image Plot

Grid Data: X=0.10m, Y=0.10m

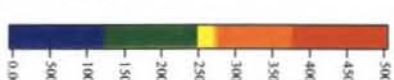

GPR Reflection Amplitude (Squared)

Magnetic North is 19 degrees 30' East
of Geographic North
Based on the 1984 USGS 7.5' Toledo North
Quadrangle-Oregon Topographic Map

~Site Location: Township 10S, Range 10W
UTM 4,952,350N, 428,240E

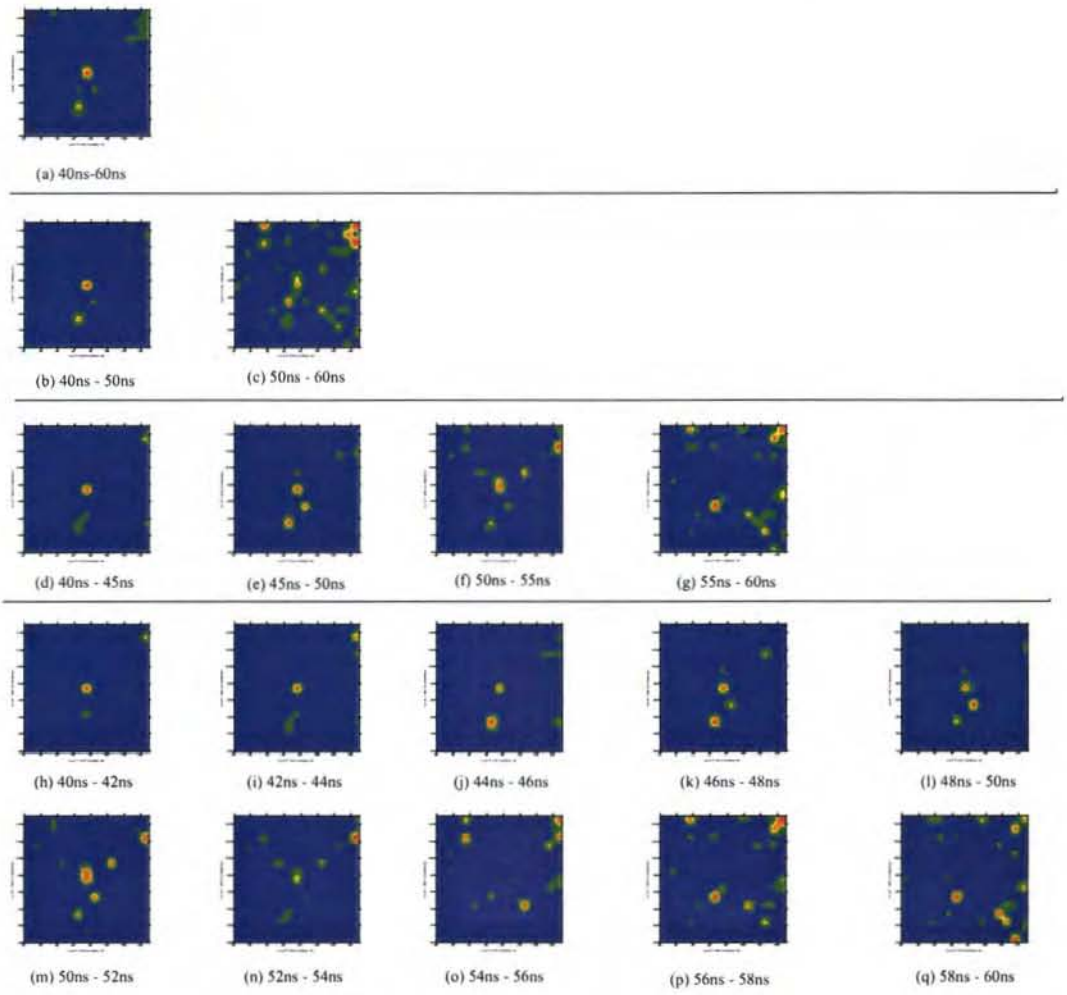

Confederated Tribes of Siletz Indians Cemetery (SLTZ) Site

Examination of the affect of different slice thicknesses around the burial level while conducting time slice analysis

Time slices conducted OCT-00 using GPR-Process

Map created using Golden Software's Surfer on01-NOV-00
Gridding Method: Kriging Grid Data: X=0.10m, Y=0.10m
Mapping Method: Image Plot

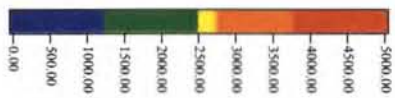

GPR Reflection Amplitude (Squared)

Magnetic North is 19 degrees 30' East of Geographic North
Based on the 1984 USGS 7.5' Toledo North Quadrangle-Oregon Topographic Map

~Site Location: Township 10S, Range 10W
UTM 4,952,350N, 428,240E